Fate of 2,4,6-trinitrotoluene (TNT) in historically contaminated aquifer sediments

Nicole Leah Fahrenfeld

Dissertation submitted to the faculty of the Virginia Polytechnic Institute and State University in partial fulfillment of the requirements for the degree of

Doctor of Philosophy
In
Civil Engineering

Amy J. Pruden (Co-Chair)
Mark A. Widdowson (Co-Chair)
Peter J. Vikesland
Madeline E. Schreiber

April 27, 2012
Blacksburg, VA

Keywords: TNT, 2,4,6-trinitrotoluene, biodegradation, desorption, mass transfer

Fate of 2,4,6-trinitrotoluene (TNT) in historically contaminated aquifer sediments

Nicole Leah Fahrenfeld

Abstract

The nitroaromatic explosive 2,4,6-trinitrotoluene is a widespread, toxic groundwater contaminant. The objective of this work was to describe TNT fate in contaminated aquifer sediments. A series of bench scale experiments and model simulations were performed to evaluate the fate of TNT in historically contaminated aquifer sediments. A TNT contaminated site on the National Priorities List, Former Nansemond Ordnance Depot (FNOD), Suffolk, VA, served as the model site for this work. To describe desorption rate in contaminated sediments, two approaches for a first order single-site desorption were evaluated. In Model 1, the driving force for desorption is mathematically related to the sorbed phase concentrations, whereas in Model 2 the rate is based on aqueous phase concentrations. Two data sets were used to evaluate the models: (1) batch draw-and-fill experiments using FNOD sediment and (2) results from a previously published report from the Louisiana Army Ammunition Plant. Both models provided adequate fit, but Model 2 was better behaved and first order parameters fell within a smaller confidence interval. Draw-and-fill experiments were observed to yield first-order mass transfer coefficients well aligned with those derived from column experiments.

The effect of organic amendments on anaerobic TNT degradation rate and microbial community structure in culture enriched from the FNOD site was studied in batch anaerobic microcosms. TNT readily degraded under all experimental conditions. A reductive pathway of TNT degradation was observed across all conditions, however, denaturing gradient gel electrophoresis (DGGE) analysis revealed distinct bacterial community compositions. In all microcosms, Gram-negative γ- or β-Proteobacteria and Gram-positive Negativicutes or Clostridia were observed. According to non-metric multidimensional scaling analysis of DGGE profiles, the microcosm communities were most similar to field site sediment corresponding to the highest TNT concentration, relative to moderately and uncontaminated sediments, suggesting that TNT contamination itself is a major driver of microbial community structure. Candidate degraders were identified and a *Pseudomonas* sp. was observed to be stimulated under all conditions, which was confirmed to rapidly degrade TNT in pure culture.

Mathematical modeling of the batch microcosm results revealed that TNT degraded 1.7 times faster in lactate amended microcosms than in ethanol amended microcosms, which degraded 3.0 times faster than natural organic matter amended microcosms. Simulation of the TNT degradation pathway included determination of branching coefficients representing whether the first reduction of nitro group occurred in the ortho or para position or whether TNT was removed from the aqueous phase (i.e. bound to dissolved organic matter). Branching coefficients were greater for initial reduction of para (17-27% initial TNT concentration) over ortho (3-9% initial TNT concentration) for all test

conditions. However, a greater degradate recovery and a different (lower para/ortho) ratio was observed for ethanol compared to lactate and un-amended conditions. Given the difference in sorption parameters between degradate isomers, these results suggest that differences in pathway branching stimulated by different electron donors are potentially relevant to long term site models. This work provides parameter values and model simulations of desorption relevant to other TNT contaminated sites, qualitative observations of how TNT-reducing bacterial community structure changes in response to electron donor addition, and quantitative comparison of the effect of electron donor addition on biodegradation rate with cultures relevant to field conditions; in addition, this work serves as a feasibility study demonstrating biodegradation as well as biostimulation potential at FNOD.

Acknowledgements

I would like to begin by expressing my appreciation to my co-advisers, Amy Pruden and Mark Widdowson, for their support and guidance during my PhD studies. Both not only provided me with amazing opportunities to contribute to work beyond that presented here, but were also patient as I pursued personal interests teaching and exploring interdisciplinary learning opportunities at Virginia Tech. The latter of which was a truly expansive experience that I am grateful to have shared with Dean DePauw, David Kinola, and my colleagues in the Global Perspectives 2010 Cohort.

Several people contributed to the feasibility and execution of this work. The work performed at the Former Nansemond Ordnance Depot would not have been possible without Jeff Zoeckler and Clarkson Meredith. Several months of analysis were possible due to support from Amy Egan who graciously shared BSE's LC. Thank you to Madeline Schreiber and Peter Vikesland for serving on my committee and Julie Petruska for her kindness, guidance, and technical assistance. Finally, I express my sincere gratitude to Jody Smiley for her invaluable analytical support and friendship.

Collaborating, learning, working, and traveling with my research groups' members had a great impact on my experience at Virginia Tech. Thank you to Mike Mobile, Lashun King, Chad McKinney, Hong Wang, Yanjun Ma, Virginia Riquelme, Jill Hong, Gargi Singh, Jen Miller, and Laurel Ackison for being top notch colleagues. I am especially appreciative of Janelle Boncal and Rachel Kistler who contributed both their time and positive energy during the lab phase of this work.

Thanks to Virginia Tech, the Via Academic Preparation Program, the Edna Bailey Sussman Foundation, and the US Army Corps of Engineers along with Versar for providing funding.

My time at Virginia Tech would not have been the same without the miles, meals, laughs I shared with my friends in the EWR program and beyond. I am incredibly lucky to have such good friends in my life. Finally, I would not be here without the love and support of my amazing parents, Marisa, and Lauren – thanks for still taking my calls!

Contents

Tables

Figures

Attribution

Each coauthor is duly credited for his or her contribution to this work, both in their sharing of ideas and technical expertise.

Amy Pruden, Ph.D. *Associate Professor of Environmental Engineering*

(Co-Principal Investigator) Department of Civil and Environmental Engineering, Virginia Polytechnic Institute and State University. Blacksburg, VA 24061

Coauthor of chapters 2,3,4

Mark Widdowson, Ph.D., P.E. *Professor of Environmental Engineering*
(Co-Principal Investigator) Department of Civil and Environmental Engineering, Virginia Polytechnic Institute and State University. Blacksburg, VA 24061

Coauthor of chapters 2,3,4

Jeffery Zoeckler M.S. *Project Engineer*
Army Corps of Engineers, Norfolk District, 803 Front Street, Norfolk, VA 23510
Jeffery Zoeckler provided historical site data for the Former Nansemond Ordnance Depot and assisted with sampling efforts and site access.

Coauthor of chapter 3

Michael Mobile *Doctoral Student*
Department of Civil and Environmental Engineering, Virginia Polytechnic Institute and State University. Blacksburg, VA 24061
Mike Mobile performed column elution modeling that complimented the batch desorption bench scale experiments and simulations performed by the author.

Coauthor of chapter 2

CHAPTER 1: Introduction

1.1 Background

Groundwater provides 50% of the world's drinking water and dependence on groundwater is only expected to increase as population grows (USGS 1995). Leaching of pollutants from contaminated sediments into drinking water aquifers, therefore, poses a threat to the sustainability of groundwater resources. Energetic compounds, or explosives, are of particular concern due to widespread contamination: 50 million acres of land in the US are estimated to have been used as military bombing and target ranges (Armstrong 1999). One important energetic compound is the priority pollutant 2,4,6-trinitrotoluene (TNT). The US Department of Defense has identified over 1200 sites contaminated with TNT (Jenkins and Walsh 1993) and it is a known contaminant at 20 of the current sites on the National Priority List (NPL) (US EPA 2011b). TNT contamination is a concern not only within the US. For example, Germany produced over 800,000 tons of TNT during World War II (Lenke et al. 2000) and now has hundreds of contaminated sites (Majcherczyk et al. 1994).

TNT pollution is of concern because TNT and its degradates have been found to be mutagenic (Alborg et al. 1988; Padda et al. 2003) toxic (Berthe-Corti et al. 1998; Simini et al. 2004), teratogenic (Saka 2004), and persistent (Won et al. 1976). The EPA considers TNT to be a possible human carcinogen based on results of epidemiological studies (Kolb et al. 1993) in addition to known human reproductive effects (Li et al. 1993). Certain degradates and co-contaminants of TNT pose health risks that are greater than TNT to some organisms (Sims and Steevens 2008). For example, 4-amino-2,6-dinitrotoluene (4ADNT) is more toxic than TNT to earthworms (Lachance et al. 2004) and 2,4-dinitrotoluene (24DNT) was shown to be more toxic to aquatic invertebrate than TNT (Sims and Steevens 2008). Such findings indicate that further degradation of TNT is necessary before health risks decrease.

1.2 TNT Fate

The fate of TNT is driven by its chemical structure. TNT is a symmetrically substituted aromatic. The highly oxidized nitro ($-NO_2$) groups exert an electron withdrawing character, resulting in an electron deficient ring that is resistant to electrophilic (oxidative) attack. Therefore, all known biotic [as reviewed by (Esteve-Nunez et al. 2001; Smets et al. 2007; Hawari et al. 2000)] and several abiotic pathways [i.e. Fe^{2+}, Fe^0, quinones, and mineral sulfides (Hofstetter et al. 1999; Dunnivant et al. 1992; Brannon et al. 1998; Elovitz and Weber 1999)] involve initial reductions. Thus, under aerobic or anaerobic conditions, the nitro group in the 2 or the 4 position is reduced to the reactive nitroso (-NO), hydroxyl amino (-NHOH), then amino ($-NH_2$) functional groups (Hawari et al. 2000; Lewis et al. 2004) (Fig. 1.1). Products of reduction contain reactive functional groups that can undergo a variety of biotic and abiotic transformations, unfortunately none of which are known to involve ring cleavage (Hawari, 2000). Thus, to date, only biotransformation pathways are known for TNT, none for TNT mineralization. Microbial biotransformation of TNT is possible through a series of successive reductions to 2,4,6-triaminotoluene (TAT) [i.e. (Daun et al. 1998)]. Denitration or deamination of TAT could lead to ring cleavage and therefore mineralization of TNT, but evidence for such phenomena lacked radiolabeling for confirmation (Boopathy et al. 1998; Boopathy and Kulpa 1992). Recently, promising stable isotope probing results indicated uptake of labeled nitrogen from TNT, however, pathway for nitrogen release and degradates remain to be reported (Gallagher et al. 2010).

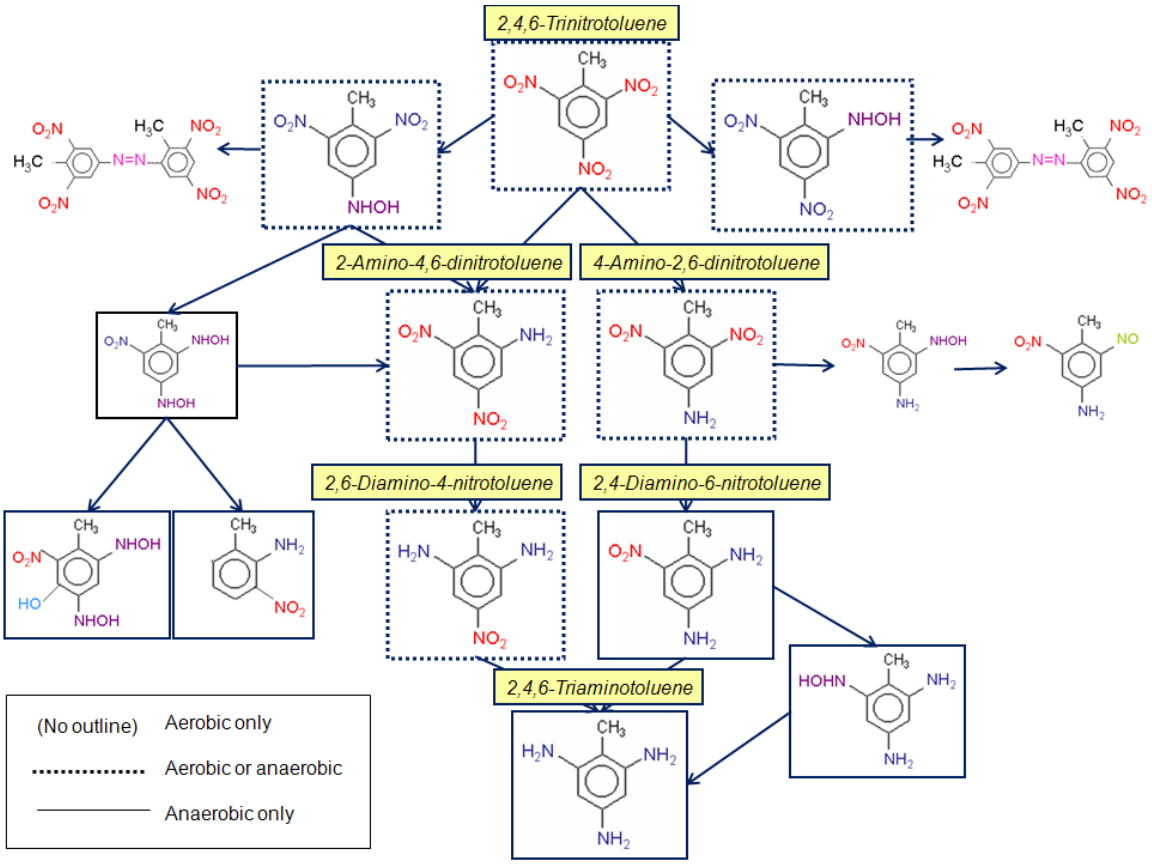

Figure 1.1 Proposed TNT degradation pathway for both aerobic and anaerobic conditions. Suspected major products are labeled with their chemical name.

Given that TNT degradation does not progress to achieve ring cleavage, and none of the known anaerobic biotransformation pathways involve loss of the methyl group, microbes must obtain carbon from another source. In addition to an external carbon source, anaerobic degradation of TNT requires addition of electron donors. Electron donor addition has been shown to increase TNT degradation rates with cultures obtained from wastewater (Daun et al. 1998; Adrian and Arnett 2007; Adrian et al. 2003), landfills (Krumholz et al. 1997), and surface soils (In et al. 2008; Fuller et al. 2004), but robust rate and pathway data have not been obtained for electron donor addition using indigenous microbial populations from contaminated anaerobic soils. To the author's knowledge, there has been only one reported field scale demonstration of TNT biostimulation. A treatability study of enhanced TNT degradation using hydrogen release compound (HRC), a polylactate polymer with a glycerol backbone designed for slow release of lactate, was performed over 11 months at the West Virginia Ordnance Works (Point Pleasant,

WV) (Downey et al, 2005; Regenesis, 2004). Injection of HRC lowered oxidation reduction potential to methanogenic conditions and after two injections, TNT levels were below the 10μg/L goal level. Rebound of TNT was seen between injections.

1.3 Former Nansemond Ordnance Depot Site History

The Former Nansemond Ordnance Depot (FNOD), Suffolk, VA, (Fig.1.2) is an NPL site that serves a model site for a boarder understanding of TNT fate. Munitions materials were improperly disposed of at the site while it was active during World Wars I and II. Ordnance was first found on 2-3-acres at the site in April 1987 (USACE 2003). A groundwater investigation found that TNT was above acceptable levels for protecting the health of children. Remedial actions including detonating unexploded ordnance including a several ton slab of crystalline TNT, as well as removal of 30,000 lbs of sediment took place between 1988 and 1992 (USACE 2003). Because no maximum contaminant level exists for TNT, contamination is defined by the EPA Region 3 Residential Soil and Tap Water regional screening levels (RSL), summarized in Table 1.1. Co-contaminants detected at the site include 1,3,5-Trinitrobenzene (TNB), 1,3-dinitrobenzene (13DNB) TNT, 24DNT, 2,6-dinitrotoluene (26DNT), 2-amino-4,6-dinitrotoluene (2ADNT), 4ANDT, nitrobenzene, o-and p- nitrotoluene, tetryl, and polyaromatic hydrocarbons, but most have not been found to exceed RSLs and those that do are not at levels as high as TNT. Thus, TNT is the primary contaminant of concern. Of the co-contaminants, only 2ADNT and 4ADNT are known degradation products of TNT. Plume maps are included in Fig. 1.2 for TNT and ADNTs.

Sampling for this study took place in May of 2009 and 2010, with direct-push technology (i.e. Geoprobe^{TM}), as detailed in Chapter 2.4.1. Sediment cores were cut, topped with rubber caps, and packed in N2 on ice for transport to the lab. Aliquots of the cores were air dried, homogenized, and extracted and analyzed via EPA Method 8330B for explosives. The samples were taken at various depths for each core and steep gradients of TNT contamination were found with depth from the sediment cores (Appendix A). Concentrations of TNT ranged from over 3000ppm to below detection. Other contaminants were found at trace levels including 24DNT, 26DNT, 2ADNT, and 4ADNT.

Table 1.1 Regional screening levels for EPA Region 3 (US EPA 2011c) and drinking water equivalent levels* (DWEL) for TNT (US EPA 2011a) and selected degradates.

Contaminant	*Residential soil (mg/kg)*[1]	*Industrial soil (mg/kg)*[1]	*Tap water (µg/L)*[1]	*DWEL (µg/L)*[2]
2,4,6-Trinitrotoluene	19	79	2.2	20
2-Amino-4,6-dinitrotoluene	150	200	30	n.a.
4-Amino2,6-dinitrotoluene	150	190	30	n.a.

* Non-cancer risk related to a possible human carcinogen [1] (US EPA 2011c) [2] (US EPA 2011a)
n.a. = none available

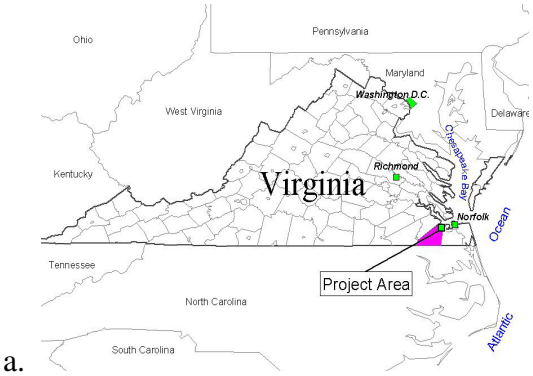

a.

b.

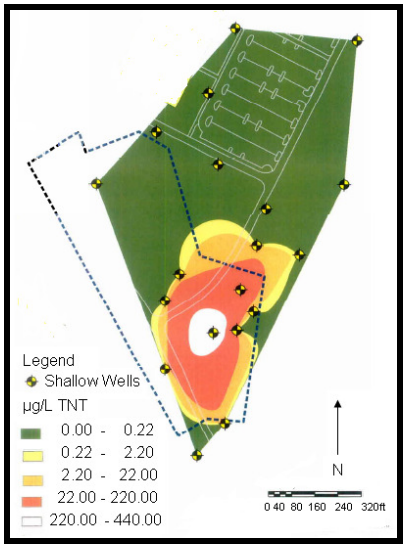

c.

Figure 1.2 a. Map showing location of FNOD. b. Aerial view of the FNOD site with the TNT operational unit highlighted. c. Contour map of TNT concentrations in groundwater defined by samples from shallow wells. Contamination in the source is 440µg/L. Groundwater flows to the north.

1.4 Research Questions

Question 1: How can we characterize bioavailability of TNT in historically contaminated sediments? The rate of TNT biodegradation is limited in aquifer systems by the bioavailability of TNT. How much of the TNT sorbed to aquifer material at FNOD is readily desorbable? And how quickly will the sorbed TNT be released? A variety of kinetic sorption models exist in the literature to describe rate limited desorption [as reviewed by (Haws et al. 2006)], but there is a lack of data describing how these apply to historically contaminated sediments as opposed to lab dosed sediments, the former of which are most relevant to field conditions and for predicting long term site remediation. The few studies done using field contaminated sediment with TNT did not model the kinetics (Sellm and Iskandar 1994; Comfort et al. 1995) or had appearance of degradates, confounding sorption phenomena (Xue et al. 1995). Kinetic parameters obtained for different experiments (batch versus column) were compared to determine if the rate parameters were at all transferrable. Comparison of kinetic parameters for FNOD sediments were made to another data set available in the literature corresponding to historically contaminated sediment with different composition.

Question 2: What is the effect of electron donor addition on TNT biodegradation rate and pathway in cultures obtained from historically contaminated aquifer sediments? It is widely known that addition of organic amendments increases the rate of reductive contaminant degradation. However, robust rate, pathway, and microbial community structure data corresponding to cultures obtained from historically contaminated aquifer sediments have not been reported. Rates and pathway data are available and have been fully modeled only for wastewater enrichment cultures (Daun et al. 1999; Daun et al. 1998; Hwang et al. 2000; Gupta 2011). Studies comparing electron donors either have not provided rate and pathway data sufficient for modeling (Adrian and Arnett 2007; Adrian et al. 2003) or modeled only TNT degradation using first order kinetics (In et al. 2008), ignoring degradate formation and degradation rates and branching. Whether electron donors affect the pathway of biodegradation is unclear: no differences were observed in the stimulated degradation pathway when comparing starch or molasses using surface soil (In et al. 2008) but some differences were seen (for example

26DANT was only observed with propylene glycol addition) using wastewater cultures (Adrian et al. 2003). Combining collection of robust rate and pathway information and mathematical modeling using bacteria enriched from historically contaminated sediment can help our understanding of the effect of electron donor addition and remedial potential at contaminated sites.

Question 3: How does a TNT-acclimated microbial community respond to electron donor addition? The effect of different amendments on the microbial community structure in TNT contaminated aquifer sediments has been uncharacterized using biomolecular techniques, despite its greater relevance to conditions in contaminated environments compared to characterization of laboratory isolates. TNT contamination is known to reduce biological activity in soils (Meyers et al. 2007; George et al. 2008; Frische and Höper 2003), cause shifts in populations towards bacteria with higher TNT tolerances (Gong et al. 2000), select for Gram-negative bacteria (Fuller and Manning 1998), and reduce soil Acidobacter community and diversity (George et al. 2009). Biomass has been shown to increase in contaminated soils during treatment as observed using phospholipid fatty acid (PFLA) analysis for soil treated with manure (Wilke et al. 2004) and in molasses fed bioslurry reactor seeded with soil from the Joliet Army Ammunition Plant (Fuller and Manning 2004). However, TNT-induced changes in community may not be consistent across different sediments (Wikström et al. 2000). While most of the above studies provide insight into microbial community shifts in terms of a toxic response to TNT, there is a general lack of molecular characterization of microbial communities associated with TNT biodegradation in aquifer sediments and their response to biostimulation.

1.5 Annotated Dissertation Outline

Chapter 1: Introduction

Chapter 2: Rate limited desorption in groundwater systems

Batch desorption results are presented and modeled using two different approaches for first order kinetic desorption. The models were applied to FNOD sediment and a historically contaminated soil for which data was taken from the literature, the Louisiana Army Ammunition Plant. First

order degradation parameters are reported as well as analysis of fit. *Question 1* is addressed in this chapter.

Chapter 3: Effect of biostimulants on 2,4,6-trinitrotoluene (TNT) degradation and bacterial community composition in contaminated aquifer sediment enrichments

The effect of ethanol, lactate, and bioavailable organic carbon on degradation rate of an enrichment culture derived from historically contaminated sediments is presented. Bacterial community structure during TNT reduction was examined across time using denaturing gradient gel electrophoresis (DGGE) providing insight into candidate degraders. Portions of this paper were included as a poster presentation at the Battelle Bioremediation Symposium, June 27, 2011 and at a platform presentation at the AEESP Education & Research Conference, July 10, 2011. It is currently under review. *Research Questions 2 and 3* are addressed in this chapter.

Chapter 4. Kinetic and pathway modeling of reductive 2,4,6-trinitrotoluene (TNT) degradation with different electron donors

The full TNT degradation pathway was modeled for each of the three electron donors explored in the study presented in Chapter 3. Rate parameter, inhibition terms, as well as pathway branching results are presented filling a gap in knowledge of the affect of biostimulants in contaminated sediments. *Research Question 2* is addressed in this chapter.

Chapter 5. Conclusions

Appendix A. ***Supplemental information for Chapter 1.*** Sediment core screening results for TNT and munitions related co-contaminants are presented as well as bioavailable iron results to help characterize current site conditions.

Appendix B. ***Supplemental information for Chapter 2.*** Batch desorption, isotherms, and remaining model fits and residuals are presented that are summarized in Chapter 2.

Appendix C. ***Supplemental information for Chapter 3.*** Proof of enrichment, gel images and band identities, proof of isolation, and characteristics of field sediment.

Appendix D. ***Supplemental information for Chapter 4.*** Sorption isotherms for TNT and degradates with and without ethanol and the qPCR primers tested with the mixed culture. Expanded modeling results to improve interpretation including full parameter tables and presentation of model residuals, are presented as well.

1.6 References

Adrian N, Arnett C (2007) Anaerobic biotransformation of explosives in aquifer slurries amended with ethanol and propylene glycol. Chemosphere 66 (10):1849-1856.

Adrian N, Arnett C, Hickey R (2003) Stimulating the anaerobic biodegradation of explosives by the addition of hydrogen or electron donors that produce hydrogen. Water Res 37 (14):3499-3507.

Alborg J, G, Einisto P, Sorsa M (1988) Mutagenic activity and metabolites in the urine of workers exposed to trinitrotoluene (TNT). British J Industr Med 45:353-358.

Armstrong D (1999) More costly cleanup on the horizon. Boston Globe, November 14, 1999,

Berthe-Corti L, Jacobi H, Kleihauer S, Witte I (1998) Cytotoxicity and mutagenicity of a 2,4,6-trinitrotoluene (TNT) and hexogen contaminated soil in S. typhimurium and mammalian cells. Chemosphere 37 (2):209-218.

Boopathy R, Gurgas M, Ullian J, Manning JF (1998) Metabolism of Explosive Compounds by Sulfate-Reducing Bacteria. Current Microbiology 37 (2):127-131.

Boopathy R, Kulpa CF (1992) Trinitrotoluene (TNT) as a sole nitrogen source for a sulfate-reducing bacteriumDesulfovibrio sp. (B strain) isolated from an anaerobic digester. Current Microbiology 25 (4):235-241.

Brannon JM, Price CB, Hayes C (1998) Abiotic transformation of TNT in montmorillonite and soil suspensions under reducing conditions. Chemosphere 36 (6):1453-1462.

Comfort SD, Shea PJ, Hundal LS, Li Z, Woodbury BL, Martin JL, Powers WL (1995) TNT transport and fate in contaminated soil. Journal of Environmental Quality 24 (6):1174-1182.

Daun G, Lenke H, Knackmuß H-J, Reuß M (1999) Experimental investigations and kinetic models for the cometabolic biological reduction of trinitrotoluene. Chemical Engineering & Technology 22 (4):308-313.

Daun G, Lenke H, Reuss M, Knackmuss HJ (1998) Biological treatment of TNT-contaminated soil. 1. Anaerobic cometabolic reduction and interaction of TNT and metabolites with soil components. Environ Sci Technol 32 (13):1956-1963.

Dunnivant FM, Schwarzenbach RP, Macalady DL (1992) Reduction of substituted nitrobenzenes in aqueous solutions containing natural organic matter. Environ Sci Technol 26 (11):2133-2141.

Elovitz MS, Weber EJ (1999) Sediment-Mediated Reduction of 2,4,6-Trinitrotoluene and Fate of the Resulting Aromatic (Poly)amines. Environ Sci Technol 33 (15):2617-2625.

Esteve-Nunez A, Caballero A, Ramos JL (2001) Biological Degradation of 2,4,6-Trinitrotoluene. Microbiology and Molecular Biology Reviews 65 (3):335-352.

Frische T, Höper H (2003) Soil microbial parameters and luminescent bacteria assays as indicators for in situ bioremediation of TNT-contaminated soils. Chemosphere 50 (3):415-427.
Fuller M, Hatzinger P, Rungmakol D, Schuster R, Steffan R (2004) Enhancing the attenuation of explosives in surface soils at military facilities: combined sorption and biodegradation. Environ Toxicol Chem 23 (2):313-324.
Fuller M, Manning J (1998) Evidence for differential effects of 2,4,6-trinitrotoluene and other munitions compounds on specific subpopulations of soil microbial communities. Environ Toxicol Chem 17 (11):2185-2195.
Fuller M, Manning J (2004) Microbiological changes during bioremediation of explosives-contaminated soils in laboratory and pilot-scale bioslurry reactors. Bioresource Technol 91 (2):123-133.
Gallagher EM, Young LY, McGuinness LM, Kerkhof LJ (2010) Detection of 2,4,6-trinitrotoluene-utilizing anaerobic bacteria by 15N and 13C incorporation. Appl Environ Microbiol 76 (5):1695-1698.
George I, Eyers L, Stenuit B, Agathos S (2008) Effect of 2,4,6-trinitrotoluene on soil bacterial communities. J Ind Microbiol Biotechnol 35 (4):225-236.
George I, Liles M, Hartmann M, Ludwig W, Goodman R, Agathos S (2009) Changes in soil Acidobacteria communities after 2,4,6-trinitrotoluene contamination. FEMS Microbiol Lett 296 (2):159-166.
Gong P, Gasparrini P, Rho D, Hawari J, Thiboutot S, Ampleman G, Sunahara G (2000) An in situ respirometric technique to measure pollution-induced microbial community tolerance in soils contaminated with 2,4,6-trinitrotoluene. Ecotoxicol Environ Safety 47 (1):96-103.
Gupta A (2011) Mathematical modeling of reductive transformation kinetics of branched degradation pathways of groundwater contaminants (Masters Thesis). Virginia Tech, Blacksburg, VA
Hawari J, Beaudet S, Halasz A, Thiboutot S, Ampleman G (2000) Microbial degradation of explosives: biotransformation versus mineralization. Appl Microbiol Biotechnol 54 (5):605-618.
Haws NW, Ball WP, Bouwer EJ (2006) Modeling and interpreting bioavailability of organic contaminant mixtures in subsurface environments. Journal of Contaminant Hydrology 82 (3–4):255-292.
Hofstetter TB, Heijman CG, Haderlein SB, Holliger C, Schwarzenbach RP (1999) Complete Reduction of TNT and Other (Poly)nitroaromatic Compounds under Iron-Reducing Subsurface Conditions. Environ Sci Technol 33 (9):1479-1487.
Hwang P, Chow T, Adrian NR (2000) Transformation of Trinitrotoluene to triaminotoluene by mixed cultures incubated under methanogenic conditions Environ Toxicol Chem 19 (4):836-841.
In B-H, Park J-S, Namkoong W, Hwang E-Y, Kim J-D (2008) Effect of co-substrate on anaerobic slurry phase bioremediation of TNT-contaminated soil. Korean Journal of Chemical Engineering 25 (1):102-107.
Jenkins T, Walsh M (1993) Field screening methods for munitions residues in soils, Seminar on technologies for remediating sites contaminated with explosive and radioactive wastes. Office of Research and Development, Washington, DC (1993) EPA/625/K-93/001 .

Kolb G, Becker N, Scheller S, Zugmaier G, Pralle H, Wahrendorf J, Havemann K (1993) Increased risk of acute myelogenous leukemia (AML) and chronic myelogenous leukemia (CML) in a county of Hesse, Germany. Soz Praventivmed 38 (4):190-195.

Krumholz LR, Li J, Clarkson WW, Wilber GG, Suflita JM (1997) Transformations of TNT and related aminotoluenes in groundwater aquifer slurries under different electron-accepting conditions. Journal of Industrial Microbiology and Biotechnology 18 (2):161-169.

Lachance B, Renoux AY, Sarrazin M, Hawari J, Sunahara GI (2004) Toxicity and bioaccumulation of reduced TNT metabolites in the earthworm Eisenia andrei exposed to amended forest soil. Chemosphere 55 (10):1339-1348.

Lenke H, Achtnich C, Daun G, Knackmuss HJ (2000) Bioremediation of TNT contaminated soil. In: Wise DJ, Trantolo DJ, Cichon EJ, Inyang HI, Stottmeister U (eds) Bioremediation of contaminated soils. Marcel Dekker, New York.

Lewis TA, Newcombe DA, Crawford RL (2004) Bioremediation of soils contaminated with explosives. J Environ Manage 70 (4):291-307.

Li Y, Jiang QG, Yao SQ, Liu W, Tian GJ, Cui JW (1993) Effects of exposure to trinitrotoluene on male reproduction. Biomedical and environmental sciences : BES 6 (2):154-160.

Majcherczyk A, Zeddel A, Huttermann A (1994) Biodegradation of TNT (2,4,6-trinitrotoluene) in contaminated soil samples by white-rot fungi. In: Hinchee RE, Anderson DB, Metting Jr. FB, Sayles GD (eds) Applied Biotechnology for Site Remediation. CRC, US.

Meyers S, Deng S, Basta N, Clarkson W, Wilber G (2007) Long-term explosive contamination in soil: Effects on soil microbial community and bioremediation. Soil Sed Contam 16 (1):61-77.

Padda RS, Wang C, Hughes JB, Kutty R, Bennett GN (2003) Mutagnicity of nitroaromatic degradation compounds. Environ Toxicol Chem 22 (10):2293-2297.

Saka M (2004) Developmental toxicity of p,p'-dichlorodiphenyl tricholorethane, 2,4,6-trinitrotoluene, ther metabolites and benzo(a)pyrene in Xenopus laevis embryos. Environ Toxicol Chem 23 (4):1065-1073.

Sellm HM, Iskandar IK (1994) Sorption-Desorption and Transport of TNT and RDX in Soils. U.S. Army Corps of Engineers Cold Regions Research & Engineering Laboratory. Report 944-7.

Simini M, Checkai RT, Kuperman RG, Phillips CT, Kolakowski JE, Kurnas CW (2004) Assessing TNT toxicity on soils with contrasting characteristics using soil invertebrate toxicity tests. Paper presented at the Proceedings for the Army Science Conference (24th) Held on 29 November - 2 December 2005, Orlando, Florida,

Sims JG, Steevens JA (2008) The role of metabolism in the toxicity of 2,4,6-trinitrotoluene and its degradation products to the aquatic amphipod Hyalella azteca. Ecotoxicology and Environmental Safety 70 (1):38-46.

Smets B, Yin H, Esteve-Nuñez A (2007) TNT biotransformation: when chemistry confronts mineralization. Appl Microbiol Biotechnol 76 (2):267-277.

US EPA (2011a) 2011 Edition of the drinking water standards and health advisories. http://water.epa.gov/action/advisories/drinking/upload/dwstandards2011.pdf. Accessed 4/5/2012

US EPA (2011b) National Priorities List. http://www.epa.gov/superfund/sites/npl/. Accessed 11/5/2011

US EPA (2011c) Regional screening levels summary. http://www.epa.gov/reg3hwmd/risk/human/rb-concentration_table/. Accessed 4/30/2012

USACE (2003) FNOD Fact Sheets. http://www.nao.usace.army.mil/Library/Factsheets/FNOD/. Accessed 7/5/2011

USGS (1995) USGS Groundwater Studies. http://water.usgs.gov/wid/html/GW.html. Accessed 7/10/2011

Wikström P, Andersson A, Nygren Y, Sjöström J, Forsman M (2000) Influence of TNT transformation on microbial community structure in four different lake microcosms. J Appl Microbiol 89 (2):302-308.

Wilke B, Gattinger A, Fröhlich E, Zelles L, Gong P (2004) Phospholipid fatty acid composition of a 2,4,6-trinitrotoluene contaminated soil and an uncontaminated soil as affected by a humification remediation process. Soil Biology Biochem 36 (4):725-729.

Won WD, DiSalvo LH, Ng J (1976) Toxicity and mutagenicity of 2,4,-6-trinitrotoluene and its microbial metabolites. Appl Environ Microbiol 31 (4):576-580.

Xue SK, Iskandar IK, Selim HM (1995) Adsorption-Desorption of 2, 4, 6-Trinitrotoluene and Hexahydro-1, 3, 5-Trinitro-1, 3, 5-Triazine in Soils. Soil Science 160 (5):317-327.

CHAPTER 2: An Evaluation of First-Order Models for Desorption of Weathered Hydrophobic Chemicals in Groundwater

In preparation for submission

2.1 Authors

Mark Widdowson, Nicole Fahrenfeld, Michael Mobile, Amy Pruden

2.2 Abstract

Kinetic desorption models were employed to simulate the elution of TNT from contaminated soil in batch and column experiments. Two first-order, single-site desorption models were primarily used in this study: an often-cited model in which the driving force for desorption is based on sorbed phase concentrations (Model 1) and a variation in which the rate is based aqueous phase concentrations (Model 2). Simulations were conducted using a numerical transport model (SEAM3D) combined with a parameter optimization code (PEST). Results showed Model 2 produced more accurate simulations relative to Model 1 including a stronger performance in matching the tailing of concentration data over time. Although neither model adequately captured both the initial transient response and the subsequent tailing period observed in the elution column experiments, both models were superior to the dual-domain and non-linear equilibrium models. Using only the tailing data, both models provided adequate representation of the experimental data but the sorbed mass was over-estimated. Sensitivity analyses showed that the Freundlich exponent most influenced the results of both Models 1 and 2. The utility of draw-and-fill experiments was demonstrated based on ability to fit data. Conducting draw-and-fill experiments with shorter than 24hr sampling intervals is recommended.

2.3 Introduction

Desorption refers to mechanisms by which sorbed compounds are released to the aqueous phase from sorbents such as sediment over time. In the case of contaminated groundwater and soil systems, desorption is known to control the bioavailability of compounds subject to microbial transformations, which in turn can impact the long-term persistence of contaminant plumes

under both natural conditions and scenarios designed to enhance or accelerate remediation. Desorption can also a primary mass transfer mechanism in contaminant source zones, particularly in the absence of appreciable volumes of a non-aqueous phase liquid (NAPL) in which dissolution is the not a dominant form of mass release to the aqueous phase. At such sites, soil and aquifer sediment are often exposed to contamination over decades, and desorption may be the rate-limiting step in the depletion of source-zone mass over time under natural or induced hydraulic gradients. Depending on site-specific conditions (e.g., the source zone mass and dimensions), desorption rates in source zones influence the efficacy of a variety of engineered remediation technologies in the pursuit of site-specific cleanup goals and may ultimately control dissipation of contaminant plumes over time (Chapelle et al. 2003).

Mathematical expressions for the combined process of sorption-desorption coupled to solute transport in porous media encompass a range of conceptualizations and assumptions including multiple sorption sites (e.g., instantaneous and kinetic), multiple kinetic desorption rates (e.g., rapid, slow and very slow), mass transfer between mobile and immobile regions (i.e., dual domain), and mass transfer within immobile regions (e.g., intraparticle diffusion) (Haws et al. 2006). When applied to flow-through experiments, kinetic-based models perform better relative to equilibrium-based sorption isotherm models in replicating the slow decline in concentration over time (often referred to as tailing) resulting from slow desorption as soil columns are flushed with clean water (Fesch et al. 1998). The question of which kinetic model is appropriate for capturing tailing breakthrough curves (BTCs) has been a topic of research with implications for remediation at larger scales. One potential concern with the kinetic approach is that with greater model complexity, more model parameters and concentration variables are required (Limousin et al. 2007). Thus, parameterization of desorption phenomena poses a significant challenge given the inherently complex behavior of hydrophobic organic contaminants combined with the heterogeneity of aquifer and soil systems observed at field sites.

One of the simplest rate-limited models for desorption is the first-order model which describes the rate of mass transfer in terms of concentration differences between the mobile aqueous phase and a single-site sorbed phase (Brusseau et al. 1989). Initial development of the first-order model focused on the application of simplified analytical and numerical models to sorption-

desorption of hydrophobic agricultural chemicals transported through soil columns (Oddson et al. 1970; Lindstrom and Boersma 1971; Van Genuchten et al. 1974). A distinct difference between the first-order model and other kinetic models is the former ignores the contribution of contaminants diffusing from intraparticle porewater into a mobile aqueous domain. One result is that the first-order mass transfer rate constant (i.e., the constant of proportionality between the aqueous-sorbed phase concentration difference and the rate of desorption) must often vary with time to account for variable desorption phenomena (Young and Ball 1995). However, given the concern for model parameterization, this very weakness is also a potential strength. Other than sorption equilibrium parameters, the mass transfer coefficient is the only required parameter for the single-site, first-order model. Not without criticism, the first-order model has been effectively used to simulate contaminant concentrations in controlled experiments (e.g., Dontsova et al. 2009). In addition, the first-order model may be adequate when experimental conditions are not favorable for intraparticle diffusion to be a dominant mechanism (e.g., relatively low porewater velocity) (Roberts et al. 1987).

Two relevant observations from past research related to the first-order desorption model are (i) model structure is based on reversible mass transfer between phases, and (ii) model validation using previously uncontaminated porous media is typical whereas the use of weathered contaminated soil is rare. Regarding mathematical representation, Van Genuchten et al. (1974) formulated an expression for the first-order model to include both forward and backward kinetic rates for sorption and desorption, respectively. The driving force for sorption-desorption in this model is based on the concentration of the sorbed phase (Ball et al. 1991). In contrast, mass transfer between domains in dual domain models is driven by aqueous phase concentrations (Young and Ball 1995). This approach is similar to the commonly-used first-order model for mass transfer from a NAPL source to the aqueous phase (Imhoff et al. 1994, and others). In an alternative first-order model, the rate of desorption is expressed in terms of the aqueous phase concentration with the limiting condition being aqueous-phase equilibrium determined by the sorbed-phase contaminant concentration (Zheng and Wang 1999). Werner et al. (2012)employed this form of the first-order model in the analysis of desorption experimental data, but the analysis was limited to the linear sorption isotherm.

As a means for data interpretation, the classic first-order model has been applied to flow-through column experiments using organic chemicals representing a range of hydrophobicity: picloram (Van Genuchten et al. 1974); fenuron and monuron (Spurlock et al. 1995); 1,3-dinitrobenzene, p-methylphenol and p-sec-butylphenol (Fesch et al. 1998); trichloroethene (Johnson et al. 2003); 2,4,6-trinitrotoluene (TNT) and hexahydro-1,3,5-trinitro-1,3,5-triazine (RDX) (Dontsova et al. 2006); toluene, benzotriazole, quinaldine, and quinoline (Bi et al. 2009); dimethyl phthalate, diethyl phthalate and di-n-propyl phthalate (Maraqa et al. 2011); benzene, chlorobenzene, o-xylene, ethylbenzene, naphthalene, and phenanthrene (Werner et al. 2012). While not a comprehensive list of studies, a common feature of the cited experiments is the introduction of a sustained pulse of solution containing a reactive solute into a flow-through column containing clean sediment. With this approach, the observed BTC includes both the increase in concentration at the point of observation (i.e., "fronting") and tailing behavior as desorption progresses. Depending on experimental conditions, the extent of contact between the solute and media is known to influence the degree to which the physical model replicates the response observed with weathered soil columns. Thus, starting with a conceptual model of contaminant mass desorbing from source zone sediment, a useful exercise would be the application of desorption models to BTC data derived from elution experiments where the starting conditions are designed to mimic the contaminated field site. In this case, simulation of the initial fronting phase (i.e., contaminant transport with sorption) is not relevant due to the presence of contaminant mass in both sorbed and aqueous phases.

The purpose of this paper is to investigate two first-order models for simulating desorption and transport of TNT using weathered site samples. The motivation for this study is the need for an evaluation of the strengths and weaknesses of the first-order, single-site desorption model for to simulating the elution of TNT from weathered sediment in a contaminated source-zone. In addition to the classic first-order sorption-desorption model, we specifically propose an alternative model in which the driving force for desorption is based on aqueous phase concentrations. In this model, the non-linear Freundlich model is adopted for calculating the aqueous equilibrium concentration. An emphasis of this study is model parameter specification, which is addressed by employing a combination of independent sorption-desorption experiments and optimization techniques to minimize error and reduce model uncertainty. Model simulations

and comparisons utilize data derived from TNT desorption experiments from two sites including a previously-published column elution study.

2.4 Materials and Methods

2.4.1 Site description and sampling

Two different sites contaminated with 2,4,6-trinitrotoluene (TNT) were used for this study. Experimental research was conducted using samples collected at the Former Nansemond Ordnance Depot (FNOD), located in the Atlantic Coastal Plain Physiographic Province of Virginia, USA. The site is underlain by a surficial aquifer comprised of a mixture of clays, clayey sands, silty sands, and sand. TNT contamination is the result of the storage and processing of ammunition between 1917 and 1949. The maximum TNT concentration in contaminated sediment (3,406 mg/kg) was observed in a sample collected in the former source area at a depth corresponding with the local water table. A TNT groundwater plume emanates from the source zone where the maximum aqueous TNT concentration is 440 μg/L. Data from a second site come from previously published work (Sellm and Iskandar 1994; Pennington and Patrick 1990) in which equilibrium sorption isotherms experiments and laboratory batch and column desorption experiments were performed using TNT-contaminated soil collected from the Louisiana Army Ammunition Plant (LAAP). LAAP site samples were described as fine-silty, Kolin soil (Sellm and Iskandar 1994).

At the FNOD site, aquifer sediment cores were collected in an uncontaminated area of the site, in the source zone adjacent to a monitoring well where the historical maximum TNT concentration was observed, and in a location downgradient of the source within the TNT plume. Cores were collected intact with direct push technology (Geoprobe^{TM}) using 5-cm-diameter polyacetate sleeves. Downhole soil sampling equipment was properly decontaminated before and after each use. Immediately prior to inserting the split spoon into the auger, all parts of the spoon were cleaned and sterilized. Upon removal from the sampling barrel, sleeve-covered cores were cut into 25-50-cm lengths, capped with rubber stoppers, wrapped in plastic to reduce contact with oxygen, packed in a N_2 atmosphere, transported on ice, and then stored at 4°C until use. Sieve

analysis of the FNOD samples using standard methods indicate the samples were best characterized as a loamy-sand (Fahrenfeld et al. submitted for publication).

2.4.2 Sorption/Desorption experiments

2.4.2.1 Batch sorption experiments

Uncontaminated sediment samples were air dried to constant mass, sieved (2 mm), and homogenized prior to use. Aliquots were treated and analyzed via EPA Method 8330B for explosives to ensure sediment was not contaminated. Sorption isotherms for the FNOD sediment were prepared by spiking varying concentrations of TNT (Accustandard, New Haven, CT) into glass vials containing 0.5 g of upgradient FNOD sediment and 1.5 mL Ultrapure (18 mΩ) distilled deionized water, and then capped with Teflon-lined septa. Following 48 hr equilibration-mixing, end-to-end on a shaker table, vials were centrifuged at 2500 rpm, and the decanted supernatant was analyzed for explosives. Sorption parameters for the LAAP soil were obtained from the literature (Pennington and Patrick 1990).

Analysis for TNT and other munitions compounds in the aqueous and solid phases was performed following EPA Method 8330 on a liquid chromatograph with photodiode array detection (Shimatdzu Prominence) using a C8 column (Restek). A methanol water mobile phase was used with a gradient method based on (Lenke et al. 1998), previously detailed (Fahrenfeld et al.)

2.4.2.2 Draw-and-fill desorption experiments

The procedure for the draw-and-fill experiment was adapted from the successive dilution method described by Amacher et al. (1988) and Sellm and Iskandar (1994) to generate kinetic desorption data. A slurry consisting of 2-8 g of wet homogenized site sediment and 25 mL of 0.005M $Ca(NO_3)_2$ were combined in glass vials that were then mixed end-to-end on a shaker table, in triplicate for each sample. The ionic strength of this solution (0.013M) is well below that used a salting-out method (Miyares and Jenkins 1991), and within the range of typical groundwaters (0.01-0.02M). Uncontaminated sand (VWR), matrix spikes, and blanks were prepared in triplicate and treated and analyzed in parallel with experimental samples. After 24 hrs, vials were centrifuged

and the decanted supernatant was treated, as described above. Fresh salt solution was added to the vials and the process was repeated until explosives were below detection. Draw-and-fill batch desorption tests were performed using contaminated site sediment collected from the TNT plume and source with samples corresponding to varying depths within the source zone. Aliquots of sediment, in triplicate, were reserved for analysis before the experiment to determine the initial TNT concentration. Once the aqueous phase TNT concentrations were below detection in the draw-and-fill experiments, the sediment was air dried and analyzed for TNT.

2.5 Mathematical Models

Two first-order kinetic models were investigated using experimental data from draw-and-fill experiments and laboratory columns. Both models assume a single sorption site where aqueous concentrations are subject to equilibrium constraints using non-linear sorption isotherms. For the purpose of comparison with the first-order kinetic models, alternative models are also presented: 1) sorption modeled using an instantaneous equilibrium isotherm (Freundlich) and 2) dual-domain model with sorption in both the mobile and immobile phases modeled using an instantaneous linear isotherm. The governing equations and variables for these alternative models are present in the Supplemental Information.

2.5.1 General equation of transport

The general form of the mass balance equation in the mobile aqueous phase for one-dimensional transport of a reactive (sorption-desorption) solute that is not subject to biodegradation or biogeochemical transformation is given as

$$\frac{\partial C}{\partial t} = -v_x \frac{\partial C}{\partial x} + D_x \frac{\partial^2 C}{\partial x^2} - \frac{\rho_b}{\theta} \frac{\partial \overline{C}}{\partial t} \quad (1)$$

where C is the mobile aqueous phase concentration of a solute [M L^{-3}]; $\overline{C}$ is the solid phase concentration [M M^{-1}]; x is distance along the column [L]; t is time [T]; v_x is the average linear pore water velocity [L T^{-1}]; D_x is the hydrodynamic dispersion coefficient [L^2 T^{-1}]; θ is mobile domain porosity [-]; and ρ_b is the bulk density of the porous medium [M L^{-3}].

The Freundlich sorption isotherm is commonly used to represent the behavior of hydrophobic compounds in soil and groundwater systems, particularly TNT (Pennington and Patrick, 1990). The equilibrium expression takes the form:

$$\overline{C} = K_f C^N \tag{2}$$

where K_f is the Freundlich constant [M^{1-N} M^{-1} L^{3N}]; and N is the Freundlich exponent [-]. As shown below, this relationship is also able to limit the rate of first-order kinetic desorption in areas of a domain where equilibrium conditions exist.

2.5.2 Kinetic model for sorption: Model 1

Early work described the development of first-order kinetic sorption models based on the concentration gradient between the solid contaminant concentration and the equilibrium limit (by (Oddson et al. 1970; Lindstrom and Boersma 1971; Van Genuchten et al. 1974). In this case, the driving force for desorption is the difference between the solid phase concentration and the sorbed concentration at equilibrium with the aqueous phase ($K_f C^N$):

$$\frac{d\overline{C}}{dt} = \alpha\left(K_f C^N - \overline{C}\right) \tag{3}$$

where α is the first-order mass transfer coefficient [T^{-1}].

2.5.3 Kinetic model for sorption: Model 2

An alternative approach to Model 1 describes the rate of mass transfer between the solid and aqueous phases in terms of the concentration difference between the aqueous concentration in equilibrium with the sorbed contaminant concentration phase (C_{eq}) using Eq. (2) and the aqueous concentration:

$$\rho_b \frac{d\overline{C}}{dt} = \beta\left(C - C_{eq}\right)\theta \tag{4}$$

where β is the first-order mass transfer coefficient [T^{-1}] for Model 2 and $C_{eq} = \left(\overline{C}/K_f\right)^{\frac{1}{N}}$. This model is formulated based on a similar first-order model for the rate of mass transfer from a non-aqueous phase liquid (NAPL) to the aqueous phase (e.g., Mukherji et al. 1997, and others) in

which C_{eq} is determined by the molar composition of the NAPL and calculated using Raoult's Law. Using Eq. (4), the overall resistance to mass transfer is controlled by aqueous-phase resistance (Seagren et al. 1999). Similar models have been employed for studies of desorption for the special case of N = 1.0 (Werner et al. 2012).

2.5.4 Solution methods

2.5.4.1 Simulation of draw-and-fill experiments

Simulation of draw-and-fill experiments using samples from both the LAAP and FNOD sites required solution of Eq. (1) combined with either Eq. (3) or (4) (i.e., Models 1 and 2, respectively). A finite difference time-stepping solution was employed by adopting a mixed implicit-explicit scheme to solve the system of non-linear ordinary differential equations. At time = 0, the initial concentration of the aqueous phase was set to 0, and the solution was stopped at time = 24 hr. The aqueous concentration was reset to 0 to simulate the experimental procedure of removal of the liquid phase from vials (i.e., draw) and replacement with liquid (i.e., fill). The solution procedure was repeated for each 24-hr cycle. Model-specific first-order mass transfer coefficients (α and β) were determined by optimizing the mass balance error (M_{error}) which was calculated using

$$M_{error} = \frac{\Delta M_{sim} - \Delta M_{obs}}{\Delta M_{obs}} x100\% \quad (5)$$

where ΔM_{sim} is the cumulative TNT mass removed during desorption experiment calculated using the product of simulated aqueous concentrations (C_{sim}) and fluid volumes (V_{aq}) (i.e., $\sum C_{sim} V_{aq}$); and ΔM_{obs} is the observed cumulative TNT mass removed based on the observed aqueous concentrations (C_{obs}). The latter was verified by calculating the difference between the initial and final sorbed mass determined by the product of the sediment mass and the measured initial and final sorbed phase TNT concentrations, respectively.

Additionally, the cumulative root-mean-square error (*RMSE*) in the concentration of aqueous phase was evaluated according to the following expression:

$$RMSE = \sqrt{\frac{\sum (C_{obs} - C_{sim})^2}{n}} \quad (6)$$

where n is the number of observations.

2.5.4.2 Simulation of column experiments

Solution of equations for transport and desorption of TNT was accomplished using the solute transport code *SEAM3D* (Waddil and Widdowson 2000) with a modified form of the *MT3DMS* Reaction Package (Zheng and Wang 1999). *SEAM3D/MT3DMS* enables a coupled solution of Eq. (1) and Eq. (3) but only for the case in which $N = 1.0$. For this study, the code was modified for the non-linear case (i.e., Model 2 with Freundlich sorption isotherm) and also to solve Eq. (1) coupled to Eq. (2) (i.e., Model 1). *SEAM3D/MT3DMS* was also employed to simulate the column experiments using the alternative sorption models described in the Appendix. An automated parameter estimation utility, *PEST* (Doherty 2005), was employed to determine an optimized solution by varying the mass transfer coefficient parameters corresponding to Models 1 and 2 (α and β, respectively). Additional optimization scenarios were conducted in which the sorption coefficients for the Freundlich isotherm (K_f and N) and the initial concentration of sorbed mass were estimated as unique parameters for Models 1 and 2 for the purpose of evaluating model sensitivity to each source-specific parameter.

Aqueous phase TNT concentration data collected during the column elution experiments were used to generate cumulative objective functions for each optimization scenario based on the sum of the squared concentration residuals. Parameter optimization was performed until the value of the objective function was minimized. Dimensionless weighting factors were used in the form of multipliers to scale the influence of each observation point on the objective function for the purpose of evaluating parameter sensitivities. *RMSE* values representing the relative quality of each calibration were calculated from the optimized results.

2.6 Results and Discussion

2.6.1 Sorption/Desorption experiments

2.6.1.1 Sorption isotherm

Experimental data from the FNOD sediment trials were fit used to fit linear, Langmuir, and Freundlich isotherms. The latter was observed to provide the best fit based on statistical goodness-of-fit (R^2=0.99) resulting in K_f = 16.1 and N = 0.57. These results fell slightly outside the ranges reported by Pennington and Patrick (1990) for the surface soils collected at 13 army ammunition plants ($5.3 \leq K_f \leq 16$ and $0.62 \leq N \leq 0.71$). However, variation in sorption parameters was expected based on the range of sediment characteristics including texture and fraction of organic carbon. FNOD sediment was characterized as a sandy loam (81% sand, 7% silt, 12% clay) while the surface soils including the LAAP (50% sand, 39% silt, 11% clay) reported by Pennington and Patrick (1990) represented a range compositions. Sorption of TNT has been previously observed to increase with increased organic content (Yamamoto et al. 2004; Larson et al. 2008; Dontsova et al. 2009), percent fines (Larson et al. 2008), surface area (Larson et al. 2008), and iron content (Dontsova et al. 2009). A weak correlation was reported (R^2=0.47) with clay content of soils (Pennington and Patrick 1990), and it is known that the composition of the clay minerals and their relative degree of saturation affects sorption parameters (Haderlein et al. 1996), as well. Given the long-term exposure of sediment to TNT at both sites, the nature and rate of contaminated desorption was the primary research interest.

2.6.1.2 FNOD draw-and-fill experiments and simulation

Sorbed TNT concentrations from the FNOD site ranged from 8 to 12 mg/kg in the plume samples and from 194 to 698 mg/kg in the source zone samples. As shown in Fig. 2.1 for the three source zone samples, TNT was below detection (20µg/L) in the aqueous phase within 10 to 20 dilution intervals for the FNOD sediments tested. After the experiment was deconstructed, only trace amounts of TNT (5.3 ± 0.9 mg/kg) were extractable from all sediments using acetonitrile, independent of the initial TNT concentration. No other munitions compounds were detected during the desorption experiment, providing evidence that degradation of TNT did not occur during the experiment. Heavily contaminated samples initially contained trace

concentrations of other munitions compounds, that were below detection during the desorption experiment. The mean experimental mass balance error ranged from 4.3% to 6.6% for the source-zone samples. Mass balance errors associated the experimental procedure may result from the possible removal of colloidal material during early sampling due to low centrifuge speeds ('solids' effect as described by several researchers (e.g., Huang et al. 1998)). Any sediment losses during sampling would increase the initial observed aqueous phase concentrations and thereby introduce a systematic error by reducing aqueous phase concentrations for subsequent sampling events.

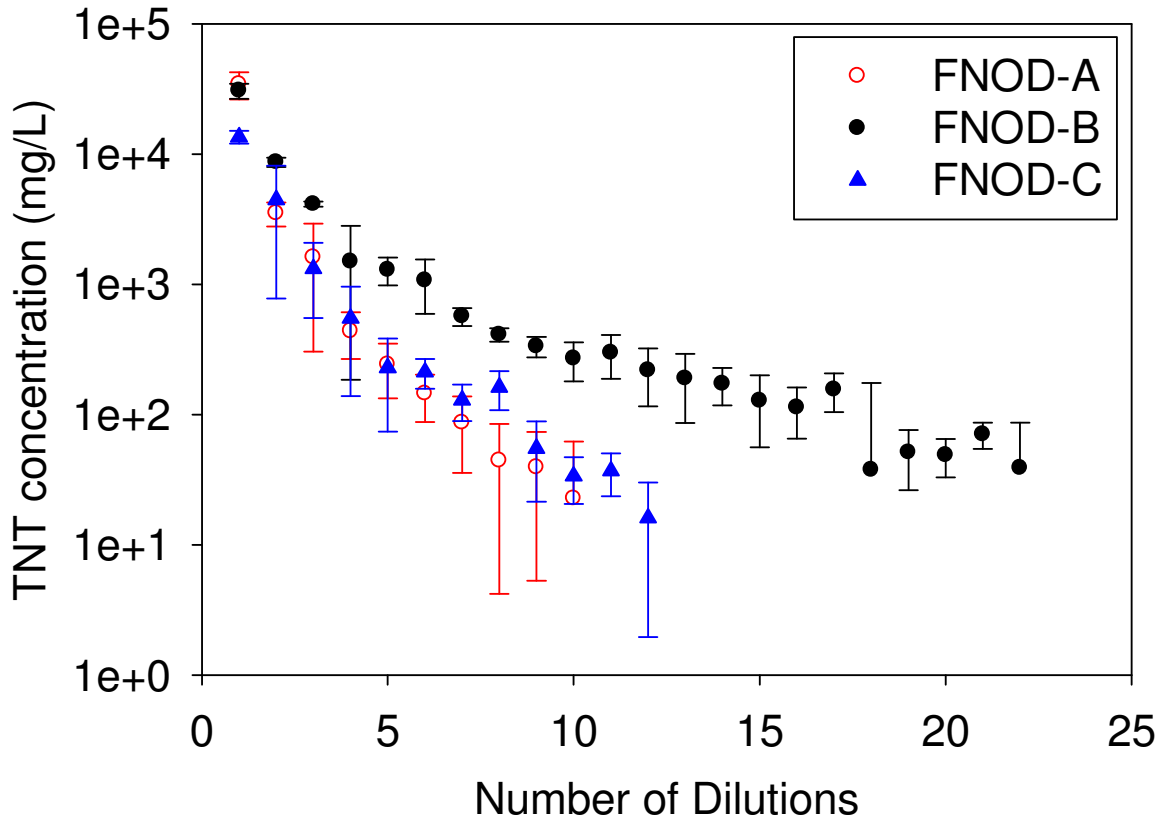

Figure 2.1 Draw-and-fill concentration data for FNOD sediment samples.

A representation of model optimization is shown in Figs. 2.2a and 2.2b for Models 1 and 2, respectively for one of the source zone samples (FNOD-C, starting concentration = 221 mg/kg). Both the RMSE and mass balance error are shown for a range of first order mass transfer coefficients. RMSE decreased in value for increased values of the first order mass transfer

coefficients for both models. As shown in Fig. 2.2, threshold values for the mass transfer coefficients were reached after which only incremental decreases in RMSE were achieved by increasing mass transfer coefficient because the RMSE exhibited asymptotic behavior. As a result, using RMSE for model optimization yields exceedingly large confidence intervals for the mass transfer coefficients in most cases. However, the mass balance error (Eq. 5) was more sensitive to changes in the mass transfer coefficient, and minima were achieved in the asymptotic portion of the RMSE for both models. Minimizing mass balance error resulted in heavy weighting of the higher concentration (early sampling) data relative to the lower concentration (late sampling event) data. However, the mass balance error minimum fell near the threshold RMSE for Model 2 and was lower than the threshold RMSE for Model 1. This suggests that optimizing to mass balance error was an appropriate strategy for determining a unique and optimized mass transfer coefficient. Thus, the model was optimized using mass balance error for each draw-and-fill experiment.

Plots of observed aqueous phase concentration versus simulated aqueous phase concentration for FNOD-C are shown in Figs. 2.3a and 2.3b. For Model 1, high concentration data was underestimated and low concentration data were overestimated. In contrast, Model 2 showed a superior performance relative to Model 1 as indicated by the pattern of the observed vs simulated concentrations relative to the 1-1 line for the full range of data and by a relatively low RMSE (0.39) compared to Model 1 (2.36).

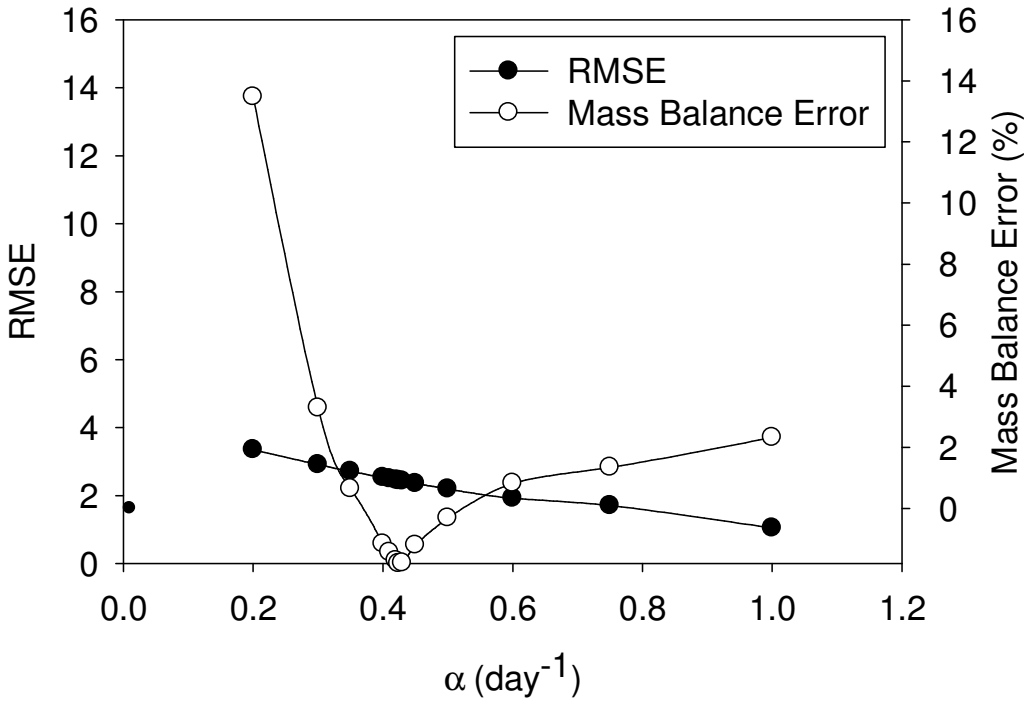

a.

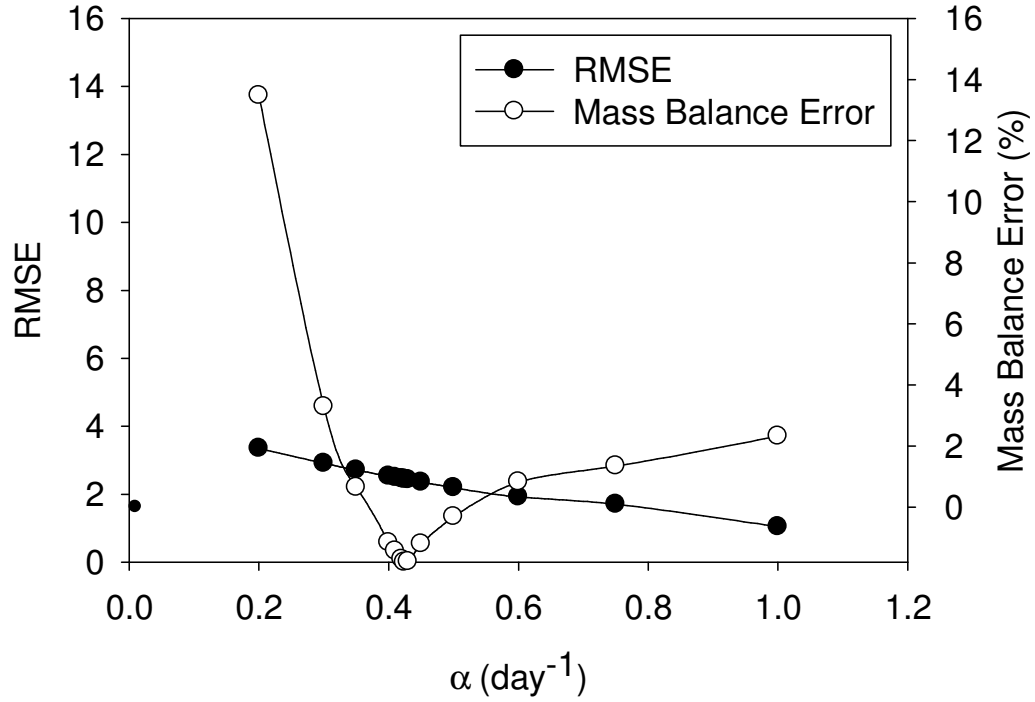

b.

Figure 2.2 RMSE and Mass balance error with changes in mass transfer coefficient values for a. Model 1 and b. Model 2.

A summary of modeling results are included in Table 1 for the draw-and-fill experiments using FNOD sample. For Model 1, the mass balance error did not reach a minimum for both FNOD-A and B, and rather like the RMSE, asymptotically approached zero. Therefore, no mass transfer coefficients were reported for these experiments. Using Model 2, mass transfer coefficients were determined by reducing the mass balance error. The mass transfer coefficient (β) varied with the initial sorbed phase concentration from 0.34, corresponding to the most heavily contaminated sample, to 0.90, for the least heavily contaminated sample. However, too few samples were analyzed to determine a trend. The exhibited variation in β was possibly due to inherent differences in availability and type of sorption site available on the different sediment samples, which could have caused the difference in sorbed concentration among the sample. Because the sediment was derived from the same core, a more likely explanation may be the inherent variability in mass transfer rather than due to differences in sediment characteristics.

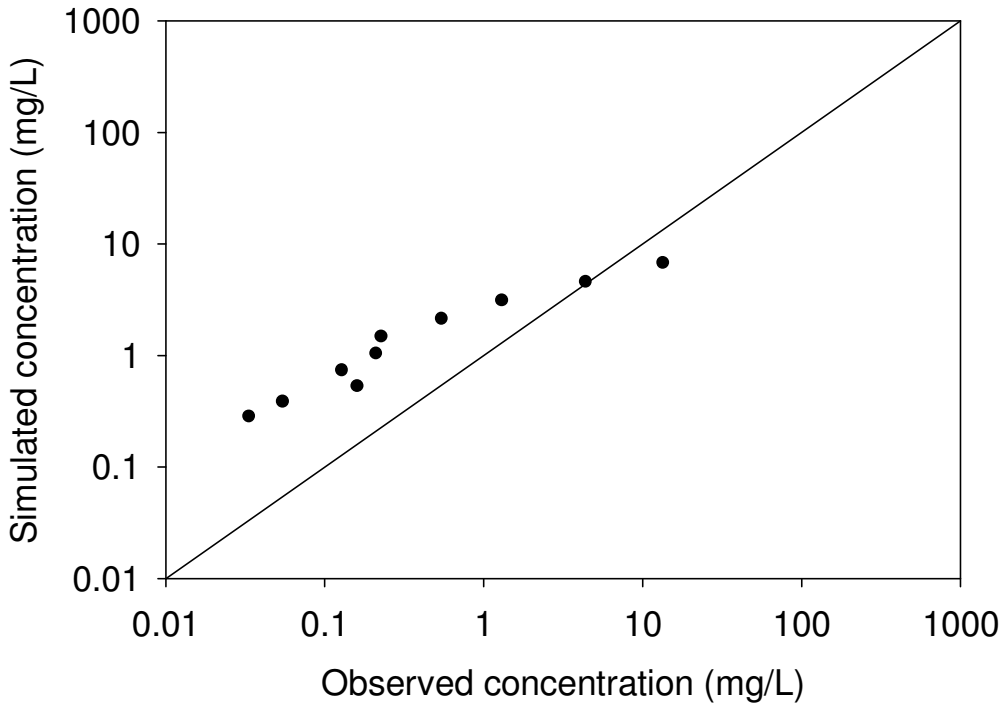

a.

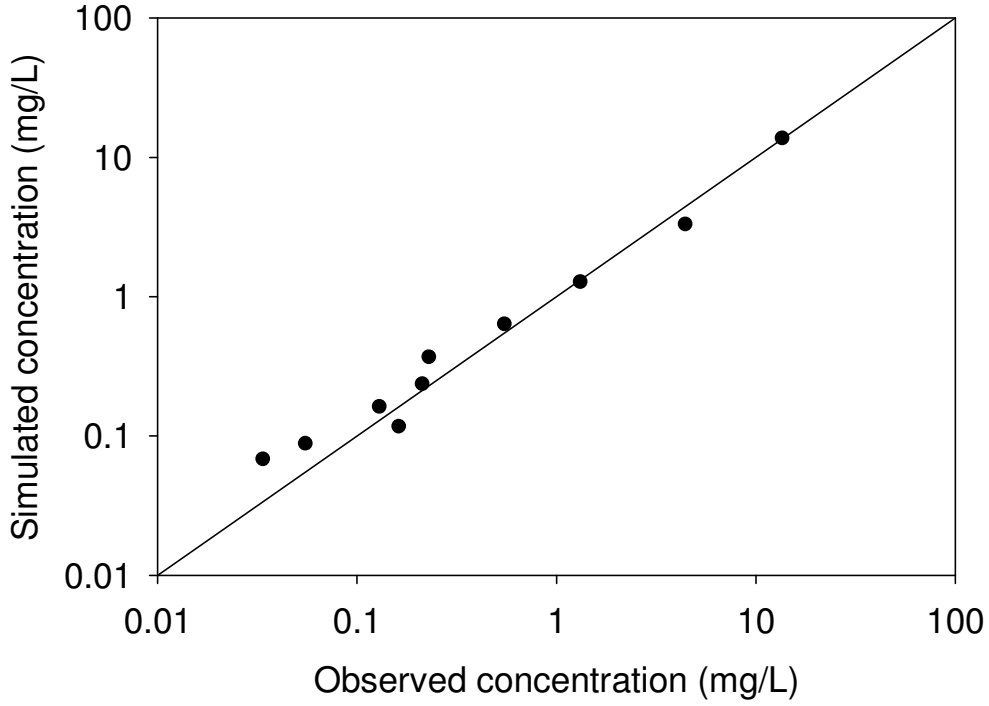

b.

Figure 2.3 Comparison of simulated and observed aqueous concentration for FNOD-C using a. Model 1 and b. Model 2.

Table 2.1 Model 1 and 2 parameters and estimation of fit for FNOD sediments.

	FNOD		
Parameter	A	B	C
Initial Concentration (mg kg^{-1})	698	194	221
Model 1			
α (d^{-1})	ND	ND	0.45
Aqueous RMSE	ND	ND	2.36
Absolute Mass Balance Error	ND	ND	0.54%
Model 2			
β (d^{-1})	0.34	0.90	0.70
Aqueous RMSE	0.42	1.72	0.39
Absolute Mass Balance Error	2.7%	8.2%	0.18%

ND = not determined

2.6.1.3 Simulation of LAAP draw-and-fill experiments

Simulation of the draw-and-fill experiments described in (Sellm and Iskandar 1994) using the LAAP sample A for both Models 1 and 2 are shown in Fig. 2.4a and 2.4b, respectively. Modeling results are summarized in Table 2.2. Sellm and Iskandar (1994) reported initial sorbed phase concentrations for the LAAP samples as 171 and 76 mg/kg for samples A and B, respectively. In these experiments, only 55% and 63% of the sorbed TNT was released to the aqueous phase, respectively. However, because the final post-experimental sorbed TNT concentrations were not reported, a closed mass balance could not be evaluated. As a result, the initial TNT concentrations in the simulations were based on the mass of desorbed TNT and not using the reported background sorbed TNT concentrations.

Similar to the results for the FNOD draw-and-fill experiments, Model 1 underestimated high concentration data and overestimated low concentration data for LAAP-A. Model 2 overestimated all concentration data. Using RMSE as a comparison, Model 2 achieved a better fit to the data. But, neither model fits mid-concentration data well. One potential reason for this was the uncertainty presented by the open mass balance in these experiments. A significantly better fit was achieved using the assumption that all but 4 mg/kg TNT are released from the sediment than using the reported initial concentrations. The results for LAAP-B (not shown) are listed in Table 2 and exhibited the same trend. Using Model 1, a slightly greater mass transfer

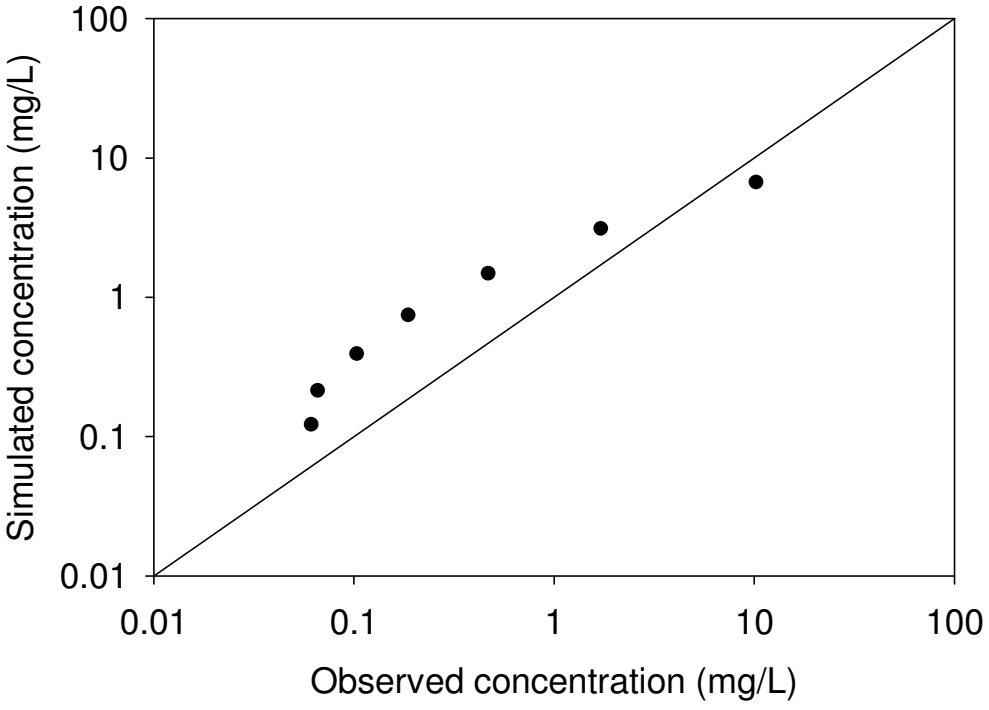

a.

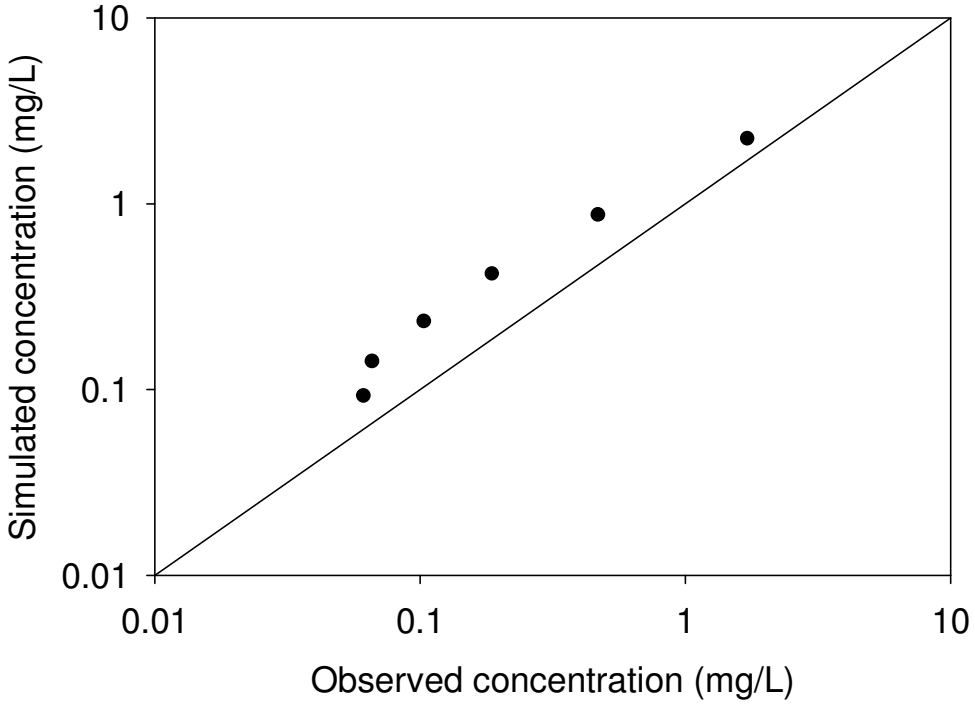

b.

Figure 2.4 Comparison of simulated and observed aqueous concentration for LAAP-A (Sellm and Iskandar 1994) using Model 1 and 2.

coefficient was found for the more heavily contaminated sample. The opposite was observed using Model 2.

Table 2.2 Model 1 and 2 parameters for LAAP sediments.

	LAAP	
Parameter	A	B
Initial Concentration (mg kg^{-1})	109[1]	46[1]
Model 1		
α	0.65	0.70
Aqueous RMSE	1.41	0.85
Absolute Mass Balance Error	0.0%	0.0%
Model 2		
β (d^{-1})	0.34	0.24
Aqueous RMSE	0.58	0.55
Absolute Mass Balance Error	0.0%	0.0%

[1]Reported initial concentrations for LAAP-A and LAAP-B were 171 and 76mg/kg, respectively

2.6.1.4 Comparison of results

Based on RMSE, Model 2 performed better than Model 1 for both sample sites. Model 1 was able to be optimized for three out of five sediment samples. Mass transfer coefficients for Model 1 (α) varied from 0.45-0.70 d^{-1} across both sites. Model 2 was optimized for all sediment samples and resulting β values ranged from 0.24-0.90 across both sites. Given the different sediment characteristics, comparing model results between the two test sites was challenging despite the fact that both sites are contaminated with TNT. FNOD samples were weathered aquifer sediment (loamy-sand) dating back >70 years while LAAP were surface soil samples (soil horizon not reported, fine silt) with no description of contamination history at the sampling locations. The variation in sediment characteristics was reflected in the sorption parameters: K_f = 16.1 and 6.09, N = 0.57 and 0.67, for FNOD and LAAP, respectively. Smaller ranges in both α and β were observed at LAAP than FNOD. However, given the small range of first order rate parameters observed for both models across test sites, it was apparent that the desorption mass transfer rate parameters were not as sensitive to differences in sediment characteristics as the equilibrium sorption parameters. A larger range of β values were observed for FNOD than at

LAAP, however, data was available for a larger range of initial starting TNT concentration for FNOD than at LAAP or more site variability in sorption. Given the small data set, comparison is not possible.

The utility of draw-and-fill experiments for determination of mass transfer coefficients was demonstrated in this work. It is recommended that the draw-and-fill experiments include smaller sampling intervals to be used to achieve first order desorption fits. For the FNOD sediment, while comparison to sorption isotherm reveals that sediment was not at sorption equilibrium (defined by 48-hr sorption isotherm), after 24 hours the aqueous phase concentration was sufficiently close to the asymptotic region of the Freundlich curve to make finding a unique model solution challenging, as discussed above.

One benefit of the draw-and-fill approach was that mass transfer rate parameters can be obtained without concern as to whether sediment samples with different contaminant concentrations also have different proprieties, like fraction of organic matter, that influence sorption. Therefore, despite the potential errors introduced by the draw-and-fill approach discussed earlier, the experiment potentially reduces sample-to-sample variability. Further, the ability to use weathered sediment samples rather than lab spiked samples in this study has the benefit that equilibrium can be presumed, whereas lab treated samples may not have reached true sorption equilibrium before desorption experiments begin (Huang et al. 1998). Rate parameters obtained from weathered sediment may be more directly applicable to expected field conditions.

2.6.2 Simulation of elution results

The aqueous phase elution curves obtained from the PEST-facilitated parameter calibration process are presented in Fig. 2.5a for Column A and Fig. 2.5b for Column B. The observed aqueous concentrations achieved early peaks in both columns and displayed tailing behavior as mass was depleted and as the concentration gradient between the sorbed and aqueous phases was reduced. Both versions of the first-order model accurately reproduced the observed peak aqueous phase concentrations that occurred after system equilibration. However, as highlighted in Fig. 2.5b, deviations are evident between the models for both columns after aqueous concentrations begin to display tailing (after day 10 of the experiment). While both models

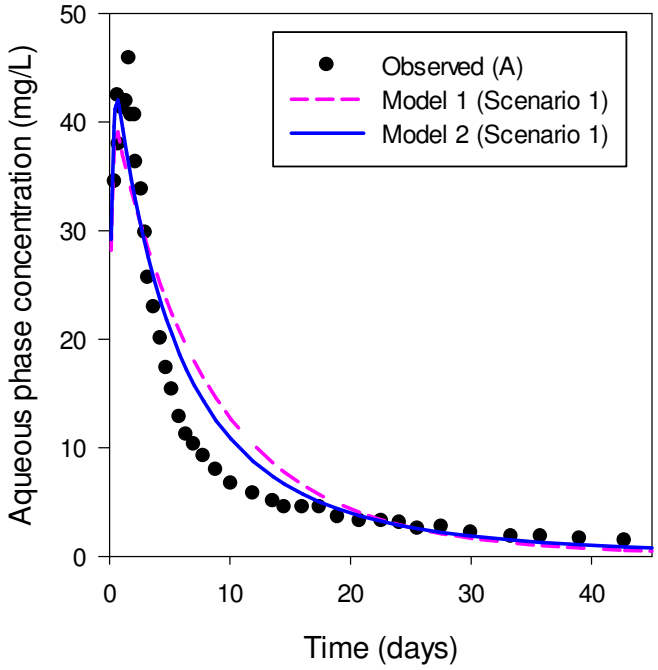

a.

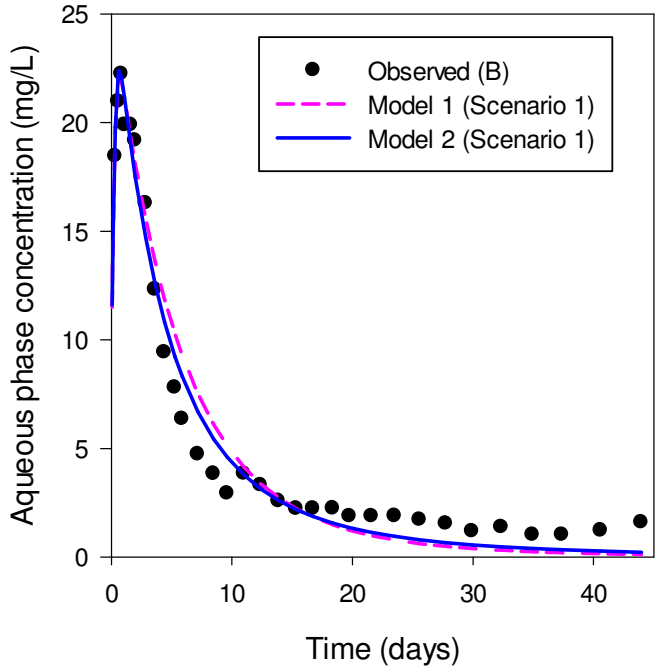

b.

Figure 2.5 Simulation of column experiments of weathered TNT-contaminated soil (Sellm and Iskandar 1994) using Models 1 and 2 for a. Column A and b. Column B. Scenario 1 is a one-parameter fit (mass transfer coefficient).

under-predicted the lower range of concentrations, Model 2 performed better in terms of minimizing concentration residuals and matching the observed data during concentration tailing.

This finding is consistent with the draw-and-fill simulation results for the FNOD and LAAP datasets which display under-predictions at low relative aqueous concentration (i.e., late time).

Elution profiles produced using the instantaneous equilibrium mass transfer model are shown in Figs. 2.6b and 2.6b for Columns A and B, respectively. The results reflect the inability of the model to capture the early peak displayed by the observed aqueous phase concentration data from both column experiments without artificial adjustment to the initial condition in the sorbed phase. Furthermore, the simulated results deviate from the data observed during concentration tailing verifying previous assertions that equilibrium-based models struggle to explain non-linear sorption/desorption behavior associated with lower energy sites (Haws et al. 2006). Figs. 2.6c and 2.6d show results produced using the dual-domain mass transfer model for Columns A and B, respectively. The flexibility of this model is reflected by the correspondence between observed and simulated concentrations during elution peaking in the initial response period; however, residuals increased significantly as experimental data began to display tailing. This finding likely reflects inadequate rate limitation in the secondary porosity portion of the dual-domain model that leads to excessive mass depletion from the sorbed phase. While the fit of the dual-domain model may be improved by further refinement to the mathematical representation, the results suggest that the first-order kinetic models perform as well if not better than the dual-domain model in simulating both the initial response and tailing behavior exhibited in the LAAP column elution data.

2.6.2.1 Assessment of Model Performance

RMSE values were calculated for each model scenario to quantitatively evaluate and compare Models 1 and 2. The Column A simulations produced noticeably different RMSE results (4.22 and 3.50 for Models 1 and 2, respectively), and the Column B simulations produced a slightly smaller difference between the models (1.32 and 1.05 for Models 1 and 2, respectively). When limited to residual evaluations after 10 days of elution, calculations produced RMSE values of 1.42 and 0.91 for Models 1 and 2, respectively, in the Column A simulations and 0.83 and 0.71 for Models 1 and 2, respectively, in the Column B simulations. The difference in RMSE values after 10 days verifies the improved fit to tailing conditions observed for Model 2 (Figs 2.5a and 2.5b).

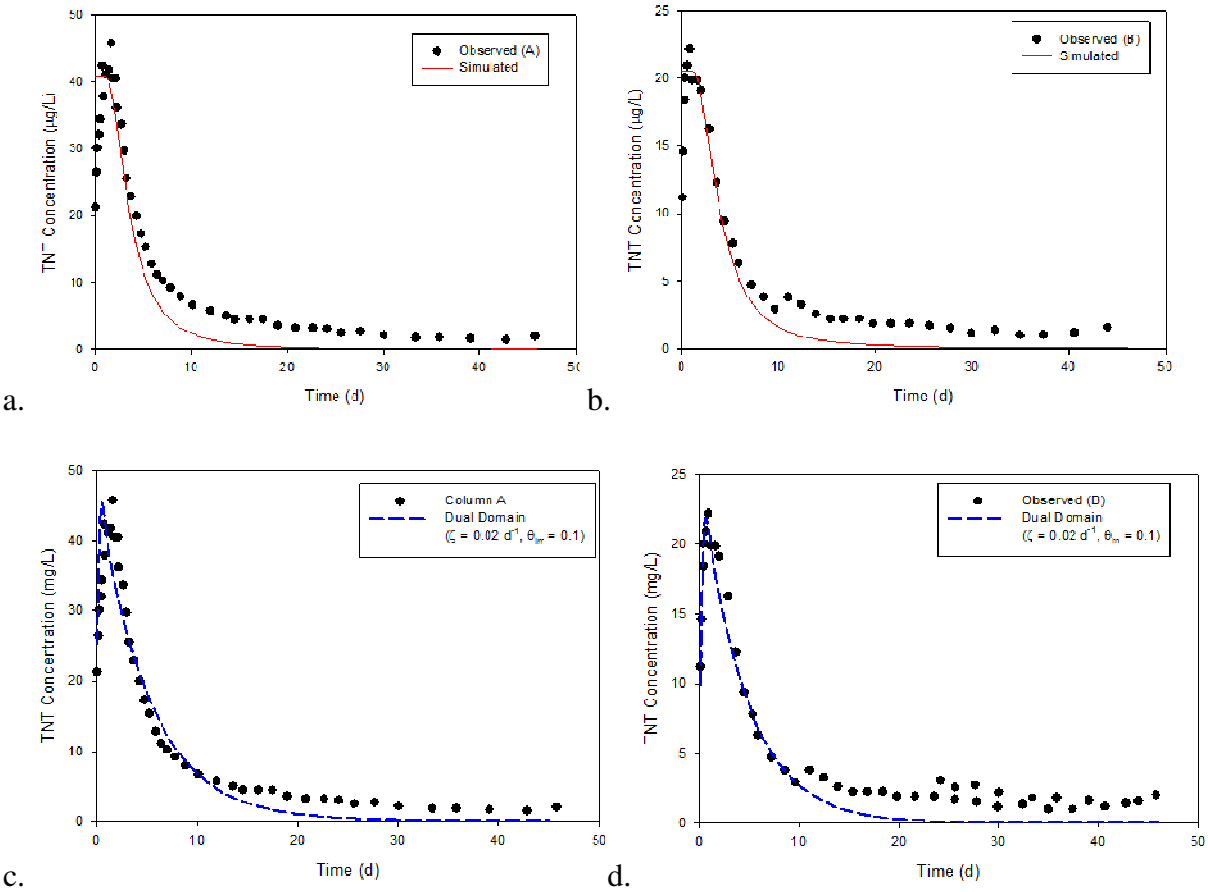

Figure 2.6 Simulation of column experiments of weathered TNT-contaminated soil (Sellm and Iskandar 1994) using instantaneous, non-linear sorption isotherm (Freundlich) for a. Column A and b. Column B and using the dual-domain model for c. Column A and d. Column B.

The estimated mass transfer coefficient values for Columns A and B are presented in Table 2.3. In general, predicted rate parameters were larger in the Column B simulations when compared to values determined in the Column A simulations. Given the larger initial sorbed phase concentration in the Column A sediment samples, the smaller mass transfer coefficient predictions may reflect the relative proportions of sorbed mass distributed between high and low energy sorption sites. In general, only minor differences were observed in mass transfer coefficient magnitudes when comparing Models 1 and 2, and the uncertainty associated with the parameter estimates was found to be negligible. However, it should be noted that the slight difference in parameter estimates reflects differences in the expression for equilibrium and forms of concentration gradients between phases employed by the two models.

Table 2.3 Model parameters for LAAP column elution data – Scenario 1

	Column A		Column B	
Parameter	Model 1	Model 2	Model 1	Model 2
Initial Concentration (mg kg^{-1})	164[1]	164[1]	76.1[1]	76.1[1]
α (d^{-1})	0.17 ± 0.02	-	0.34 ± 0.02	-
β (d^{-1})	-	0.27 ± 0.03	-	0.71 ± 0.04
K_f	6.09[2]	6.09[2]	6.09[2]	6.09[2]
N	0.67[2]	0.67[2]	0.67[2]	0.67[2]
RMSE	4.22	3.50	1.32	1.05

[1]Initial sorbed phase concentration reported by Sellm and Iskandar (1994) for LAAP soil samples A and B. [2]Freundlich isotherm parameter reported by Pennington and Patrick (1990) for LAAP soil samples A and B.

An additional metric used to evaluate goodness-of-fit to the experimental data (Figs. 2.5a and 2.5b) was a comparison of observed and simulated mass discharge. At the advent of tailing, the cumulative mass discharge for both Models 1 and 2 showed reasonable agreement with Column A data (percent error = 18.2% and 13.9%, respectively) and with Column B data (11.8% and 5.5%, respectively). In all cases, simulated results were greater than the experimental totals, which could be expected when considering the over-prediction of aqueous concentrations leading up to 10 days of simulation. At the conclusion of the Column A experiment, simulated results using Model 2 over-predicted cumulative mass discharge by 14.2% compared to 19.2% when using Model 1. In the case of the Column B experiment, the simulated results produced under-predictions of the experimental mass discharge by 6.0% and 8.5% for Models 1 and 2, respectively. However, the reliability of mass discharge comparisons associated with the Column B experiments was questionable given that the observed data produce an experimental total that exceeds the quantity of TNT initially present in the column by approximately 5.2%. This disparity was not identified in the Column A experiments.

The sensitivity of concentration predictions to the rate parameter β in Model 2 was further investigated using the Column A data (Fig. 2.7). The optimized β value of 0.27 day^{-1} was scaled up and down by one order-of-magnitude while the three other input parameters were held constant at their calibrated values. The results show that predictive errors were exacerbated by β scaling during the peak period (less than 10 days). However, predictive error was less significant

during the tailing period (after 10 days) where residual concentrations were actually minimized by the β reduction scenario. This observation suggests that larger values of the rate parameter (β) were providing conditions under which mass desorption occurred too rapidly. In this case, tailing behavior cannot be sustained because the simulated systems were mass-limited. This finding suggests that specific attention must be paid to quantifying β in the proposed model as overestimated rate parameters may result in under-predicted TORs.

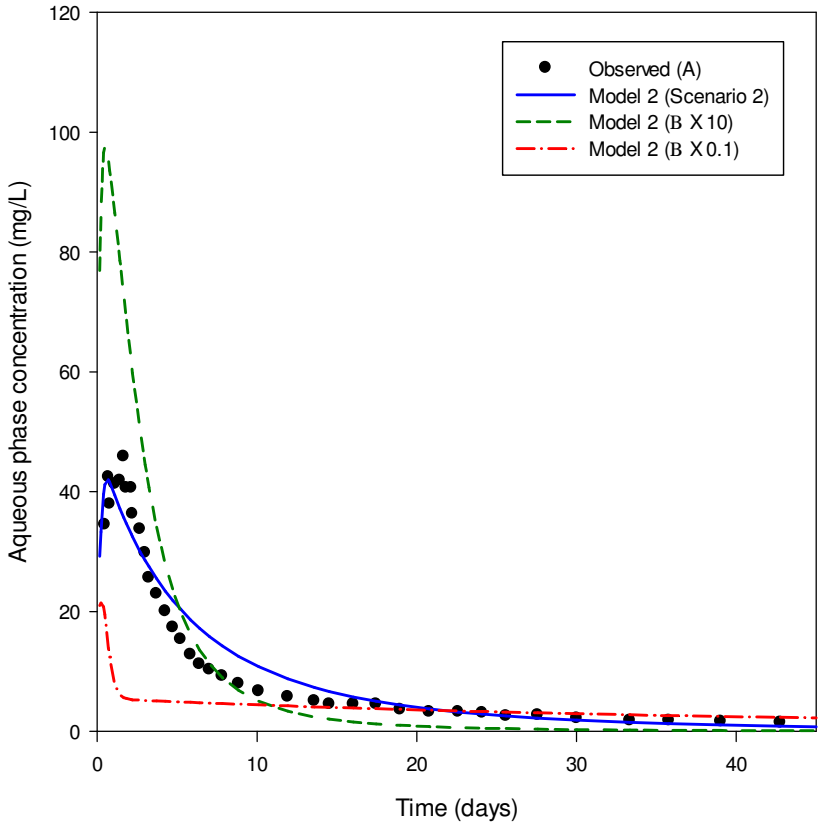

Figure 2.7 Sensitivity of Model 2 results to variations in the mass transfer coefficient (β) for simulation of Column A elution experiment with weathered TNT-contaminated sediment (Sellm and Iskandar 1994).

2.6.2.2 Extended uncertainty analysis

Three additional PEST simulations were conducted with each model for the purpose of evaluating the sensitivity of model predictions to potential variability from the reported Freundlich isotherm parameters and initial sorbed phase concentration. In Scenario 2, three parameters were optimized for Models 1 and 2: the mass transfer coefficients (α/β) and the Freundlich isotherm parameters (K_f and N). In Scenario 3, two parameters were estimated: the

mass transfer coefficient (α or β) and the initial concentration in the sorbed phase. In Scenario 4, all four model parameters were simultaneously optimized.

The results of extended scenario testing are shown in Figures 2.8a, 2.8b and 2.8c for Column A for Scenarios 2, 3 and 4, respectively. From a qualitative perspective, only minor differences were evident amongst the scenarios in the early period (less than 10 experimental days), though Model 2 still consistently provides a better fit to the observed data when compared to Model 1. In general, Scenario 2 provided the best overall fit to the observed data, particularly during tailing conditions; however, only a slight improvement was achieved when compared to Scenario 1 which was limited to rate parameter optimization. This finding suggests that the previously reported isotherm parameters reported by Pennington and Patrick (1990) are reasonable estimates for the experimental conditions in both columns.

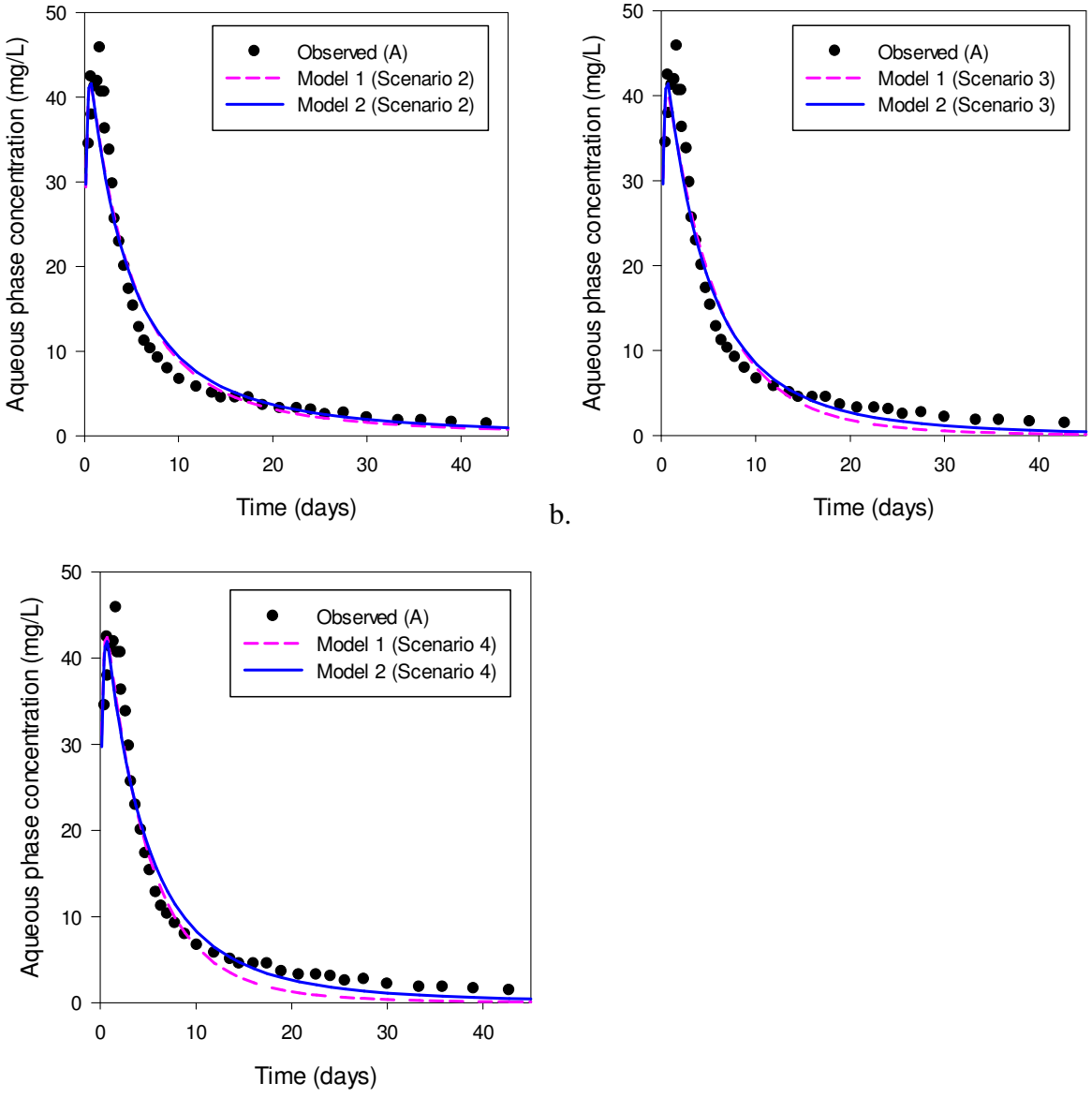

Figure 2.8 Simulation of column experiments (Sellm and Iskandar 1994) using Models 1 and 2 for Column A and Column B. Scenario 2 is a three-parameter fit (isotherm parameters and initial sorbed phase concentration). Scenario 3 is a two-parameter fit (initial sorbed phase concentration and mass transfer coefficient). Scenario 4 is a four-parameter fit (isotherm parameters, mass transfer coefficient and initial sorbed phase concentration).

Parameter estimates derived from extended scenario testing are presented in Tables 2.4, 2.5 and 2.6. While the results suggest improved fits when compared to the single-parameter optimization simulations (Scenario 1), it is important to note that the Scenario 2 simulations were the only alternatives which produced improvements in the RMSE values during tailing (i.e., after

10 days of experimentation). Furthermore, when compared to the isotherm parameter estimates from Pennington and Patrick (1990) for soil samples A and B, the estimated values derived in Scenario 2 generally represented drastic deviations from the expected values of K_f and N, particularly when considering the range of potential values within the reported 95% confidence intervals. The deviations may be partly explained by significant negative correlation coefficients between the isotherm parameters (less than -0.77 in all cases except Column B/Model 1). Considering these facts, it may be concluded that attempting to estimate isotherm parameters in the absence of reliable independent measures may produce erroneous results with respect to both the isotherm parameters themselves and the corresponding rate coefficients.

Scenarios 3 and 4 evaluated uncertainty with respect to the initial solid-phase concentrations in Columns A and B. The results presented in Table 5 show that the PEST-facilitated optimization process favored a reduction in the initial sorbed concentration in all cases except the Column B/Model 2 simulation. The legitimacy of the lower concentration estimates (relative to the reported initial conditions) could not be independently validated given the available data; however, the lower initial mass estimates produce under-predicted tailing conditions in the Scenario 3 and 4 simulations due to mass limitations.

Of the three sorption-desorption parameters estimated in Scenario 2, evaluation of sensitivity coefficients showed that both models were most sensitive to changes in the Freundlich exponent. For Model 2, the other parameters (K_f and β) showed approximately equal sensitivity, but for Model 1, simulation results were more sensitive to the mass transfer coefficient (α) compared to K_f. However, when considering the initial sorbed concentration in the analysis (Scenario 4), Model 1 showed equal sensitivity between the Freundlich exponent and the initial condition.

An additional issue encountered in Scenarios 3 and 4 was the identification of strongly correlated parameters, with a particularly strong positive offset existing between the initial sorbed-phase concentration and the isotherm distribution coefficient (K_f). This offsetting behavior was especially prevalent in the Column A simulations where the correlation coefficients reflecting the comparison between these two parameters were greater than 0.9 for Models 1 and 2. The Column B simulations produced lower positive correlations between these parameters (greater

Table 2.4 Model parameters for LAAP column elution data – Scenario 2

	Column A		Column B	
Parameter	Model 1	Model 2	Model 1	Model 2
Initial Concentration (mg kg^{-1})	164[1]	164[1]	76.1[1]	76.1[1]
α (d^{-1})	0.32 ± 0.05	-	0.46 ± 0.04	-
β (d^{-1})	-	0.45 ± 0.08	-	0.47 ± 0.03
K_f	36.8 ± 7.46	16.1 ± 1.39	16.8 ± 1.26	6.41 ± 1.64
N	0.30 ± 0.04	0.51 ± 0.03	0.36 ± 0.03	0.61 ± 0.06
RMSE	2.98	3.19	1.00	0.99

[1]Initial sorbed phase concentration reported by Sellm and Iskandar (1994) for LAAP soil samples A and B.

Table 2.5 Model parameters for LAAP column elution data – Scenario 3

	Column A		Column B	
Parameter	Model 1	Model 2	Model 1	Model 2
Initial Concentration (mg kg^{-1})	107 ± 5.23	131 ± 9.21	66.4 ± 3.14	78.1 ± 3.75
α (d^{-1})	0.49 ± 0.04	-	0.48 ± 0.04	-
β (d^{-1})	-	0.44 ± 0.06	-	0.63 ± 0.04
K_f	6.09[2]	6.09[2]	6.09[2]	6.09[2]
N	0.67[2]	0.67[2]	0.67[2]	0.67[2]
RMSE	3.22	3.06	1.15	1.08

[2]Freundlich isotherm parameter reported by Pennington and Patrick (1990) for LAAP soil samples A and B.

Table 2.6 Model parameters for LAAP column elution data – Scenario 4

	Column A		Column B	
Parameter	Model 1	Model 2	Model 1	Model 2
Initial Concentration (mg kg^{-1})	118 ± 23.5	132 ± 53.5	63.6 ± 6.49	74.7 ± 7.60
α (d^{-1})	0.45 ± 0.07	-	0.45 ± 0.04	-
β (d^{-1})	-	0.47 ± 0.03	-	0.48 ± 0.04
K_f	7.16 ± 3.29	6.24 ± 0.13	5.42 ± 1.63	5.66 ± 2.10
N	0.68 ± 0.08	0.67 ± 0.02	0.67 ± 0.07	0.64 ± 0.07
RMSE	3.06	3.05	1.12	0.99

than 0.7) but also showed a strong negative correlation between the isotherm parameters, as was the case in Scenario 2. Given the high degree of parameter correlation and the negligible improvement in RMSE values, it may be concluded that using column elution data to estimate

the initial sorbed-phase concentration and mass transfer parameters simultaneous may produce reasonable results; however, when the isotherm parameters are also uncertain, parameter correlations may produce unreasonable predictions.

2.7 Conclusions

This study represents a departure from previous research because contaminant desorption was analyzed in weathered soil instead of initially uncontaminated media. The first-order models (combined with parameter optimization) performed well in capturing the data trends in TNT elution experiments but under-predicted mass discharge during the tailing period. The alternative model (Model 2) demonstrated incremental improvement to the often-cited Model 1, showing an improved ability to matching the tailing of concentration data over time. Similar to the findings of previous research, transport simulations using a non-linear equilibrium sorption isotherm could not match the data trends observed in the column experiments. Although the dual-domain model was also able to capture the general data trends of the same experiments, Models 1 and 2 were superior to the dual-domain approach with respect to the tailing data. By excluding the initial response, model optimization to the tailing period provided an excellent match to the observed data but over-estimation of the initial sorbed mass demonstrate that further improvements to the calibration procedure are warranted.

These results suggest that the single-site, first-order desorption model may be useful for applications to contaminated field sites where hydrophobic organic compounds have been present and that the single-site representation may not be inferior to multiple-site, multiple-rate models. However, one motivation for this study is to first evaluate simpler models given the possibility that parameter-intensive models will lead to difficulties with optimization and result in significant uncertainty for long-range predictions. The utility of draw-and-fill experiments to provide an independent means of quantifying desorption mass transfer coefficients was not definitely demonstrated. However, a reasonable comparison between first-order mass transfer coefficients derived through the column experiments and values derived through batch desorption data suggests that with an improved experimental design, these parameters may be obtained without performing elution experiments. In general, because draw-and-fill experiments are less time- and labor-intensive compared to column experiments, this approach bears

consideration for quantifying a site-specific range of mass transfer coefficients prior to parameter optimization.

2.8 Acknowledgements

Funding for this work was provided through support of the U.S. Army Corps of Engineers, Norfolk, Virginia and Versar, Inc.

2.9 References

Amacher MC, Selim HM, Iskandar IK (1988) Kinetics of chromium (VI) and cadmium retention in soils. Soil Science Society of America Journal 52:398-408.

Ball WP, Goltz MN, Roberts PV (1991) Comment on "Modeling the transport of solutes influenced by multiprocess nonequilibrium;" by M. L. Brusseau, R. E. Jessup, and P. S. C. Rao. Water Resour Res 27 (4):653-656.

Bi E, Zhang L, Schmidt TC, Haderlein SB (2009) Simulation of nonlinear sorption of N-heterocyclic organic contaminates in soil columns. Journal of Contaminant Hydrology 107 (1–2):58-65.

Brusseau ML, Rao PSC, Gillham RW (1989) Sorption nonideality during organic contaminant transport in porous media. Crit Rev Environ Control 19 (1):33-99.

Chapelle FH, Widdowson MA, Brauner JS, Mendez E, Casey CC (2003) Methodology for estimating times of remediation associated with monitored natural attenuation. USGS Water Resource Investigation Report.

Doherty J (2005) PEST: Model-Independent Parameter Estimation. Fifth edn.

Dontsova KM, Hayes C, Pennington JC, Porter B (2009) Sorption of High Explosives to Water-Dispersible Clay: Influence of Organic Carbon, Aluminosilicate Clay, and Extractable Iron. Journal of Environmental Quality 38 (4):1458-1465.

Dontsova KM, Yost SL, Simunek J, Pennington JC, Williford CW (2006) Dissolution and transport of TNT, RDX, and Composition B in saturated soil columns. Journal of Environmental Quality 35 (6):2043-2054.

Fahrenfeld N, Zoeckler J, Widdowson MA, Pruden A Effect of biostimulants on 2,4,6-trinitrotoluene (TNT) degradation and bacterial community composition in contaminated aquifer sediment enrichments.

Fesch C, Simon W, Haderlein SB, Reichert P, Schwarzenbach RP (1998) Nonlinear sorption and nonequilibrium solute transport in aggregated porous media: Experiments, process identification and modeling. Journal of Contaminant Hydrology 31 (3-4):373-407.

Haderlein SB, Weissmahr KW, Schwarzenbach RP (1996) Specific adsorption of nitroaromatic explosives and pesticides to clay minerals. Environ Sci Technol 30 (2):612-622.

Haws NW, Ball WP, Bouwer EJ (2006) Modeling and interpreting bioavailability of organic contaminant mixtures in subsurface environments. Journal of Contaminant Hydrology 82 (3–4):255-292.

Huang W, Yu H, Weber WJ (1998) Hysteresis in the sorption and desorption of hydrophobic organic contaminants by soils and sediments: 1. A comparative analysis of experimental protocols. Journal of Contaminant Hydrology 31 (1-2):129-148.

Imhoff PT, Jaffé PR, Pinder GF (1994) An experimental study of complete dissolution of a nonaqueous phase liquid in saturated porous media. Water Resour Res 30 (2):307-320.
Johnson GR, Gupta K, Putz DK, Hu Q, Brusseau ML (2003) The effect of local-scale physical heterogeneity and nonlinear, rate-limited sorption/desorption on contaminant transport in porous media. Journal of Contaminant Hydrology 64 (1–2):35-58.
Larson SL, Martin WA, Escalon BL, Thompson M (2008) Dissolution, sorption, and kinetics involved in systems containing explosives, water, and soil. Environ Sci Technol 42 (3):786-792.
Lenke H, Warrelmann J, Daun G, Hund K, Sieglen U, Walter U, Knackmuss H (1998) Biological treatment of TNT-contaminated soil. 2. Biologically induced immobilization of the contaminants and full-scale application. Environ Sci Technol 32 (13):1964-1971.
Limousin G, Gaudet JP, Charlet L, Szenknect S, Barthès V, Krimissa M (2007) Sorption isotherms: A review on physical bases, modeling and measurement. Applied Geochemistry 22 (2):249-275.
Lindstrom FT, Boersma L (1971) A theory on the mass transport of previously distributed chemicals in a water saturated sorbing porous medium. Soil Science 111 (3):192-199.
Maraqa MA, Zhao X, Lee J-u, Allan F, Voice TC (2011) Comparison of nonideal sorption formulations in modeling the transport of phthalate esters through packed soil columns. Journal of Contaminant Hydrology 125 (1–4):57-69.
Miyares PH, Jenkins TF (1991) Improved salting out extraction-preconcentration method for the determination of nitroaromatics and nitramines in water. U.S. Army Corps of Engineers Cold Regions Research and Engineering Laboratory. Special Report 91-18.
Mukherji S, Peters CA, Weber WJ (1997) Mass transfer of polynuclear aromatic hydrocarbons from complex DNAPL mixtures. Environmental Science & Technology 31 (2):416-423.
Oddson JK, Letey J, Weeks LV (1970) Predicted distribution of organic chemicals in solution and adsorped as a function of position and time for various chemical and social properties. Soil Science Society of America Proceedings 34 (3):412-417.
Pennington JC, Patrick WH, Jr. (1990) Adsorption and desorption of 2,4,6-trinitrotoluene by soils. J Environ Qual 19 (3):559-567.
Roberts PV, Goltz MN, Summers RS, Crittenden JC, Nkedi-Kizza P (1987) The influence of mass transfer on solute transport in column experiments with an aggregated soil. Journal of Contaminant Hydrology 1 (4):375-393.
Seagren EA, Rittmann BE, Valocchi AJ (1999) An experimental investigation of NAPL pool dissolution enhancement by flushing. Journal of Contaminant Hydrology 37 (1–2):111-137.
Sellm HM, Iskandar IK (1994) Sorption-Desorption and Transport of TNT and RDX in Soils. U.S. Army Corps of Engineers Cold Regions Research & Engineering Laboratory. Report 944-7.
Spurlock FC, Huang K, van Genuchten MT (1995) Isotherm nonlinearity and nonequilibrium sorption effects on transport of fenuron and monuron in soil columns. Environmental Science & Technology 29 (4):1000-1007.
Van Genuchten MT, Davidson JM, Wierenga PJ (1974) An evaluation of kinetic and equilbrium equations for the prediction of pesticide movement through porous media. Soil Science Society of America Proceedings 38 (1):29-35.
Waddil DW, Widdowson MA (2000) SEAM3D: A numerical model for three-dimentional solute transport and sequential electron acceptor-based biodegradation in ground water.

ERD/EL TR-00X, U.S. Army Engineer Research and Development Center, Vicksburg, Mississippi.
Werner D, Karapanagioti HK, Sabatini DA (2012) Assessing the effect of grain-scale sorption rate limitations on the fate of hydrophobic organic groundwater pollutants. Journal of Contaminant Hydrology 129–130 (0):70-79.
Yamamoto H, Morley MC, Speitel Jr GB, Clausen J (2004) Fate and Transport of High Explosives in a Sandy Soil: Adsorption and Desorption. Soil & Sediment Contamination 13 (5):361-379.
Young DF, Ball WP (1995) Effects of column conditions on the first-order rate modeling of nonequilibrium solute breakthrough. Water Resour Res 31 (9):2181-2192.
Zheng C, Wang PP (1999) MT3DMS, A modular three-dimensional multi-species transport model for simulation of advection, dispersion and chemical reactions of contaminants in groundwater systems; documentation and user's guide. U.S. Army Engineer Research and Development Center Contract Report SERDP-99-1, Vicksburg, MS, 202 p.

2.10 Supplemental Information

For the purpose of comparison, two alternative mathematical models were employed for simulation of the TNT column elution experiments. *MT3DMS* was employed for both models with no changes to the code. The first model incorporates transport with the Freundlich instantaneous equilibrium isotherm, which allows Eq. (1) and Eq. (2) to be combined.

$$R\frac{\partial C}{\partial t} = -v_x \frac{\partial C}{\partial x} + D_x \frac{\partial^2 C}{\partial x^2} \tag{8}$$

where R is a dimensionless non-linear retardation factor, $R = 1 + \left(\rho_b K_f N / \theta\right) C^{N-1}$, that varies with space and time with the aqueous concentration.

The second model employs a dual domain approach with a linear instantaneous equilibrium sorption isotherm employed in both the mobile and immobile phases. Eq. (1) is modified to account for mass transfer between phases using a first-order mass transfer function proportional to the difference between the aqueous mobile concentration (C_m) and aqueous mobile concentration (C_{im})

$$R_m \frac{\partial C_m}{\partial t} = -v_x \frac{\partial C_m}{\partial x} + D_x \frac{\partial^2 C_m}{\partial x^2} - \frac{\zeta}{\theta_m}\left(C_m - C_{im}\right) \tag{9}$$

where θ_m is the mobile porosity [-]; ζ is the first-order coefficient for mass transfer between the mobile and immobile domains [T^{-1}]; and R_m is a dimensionless linear retardation factor for the mobile phase, such that $R_m = 1 + \rho_b K_d / \theta$, and K_d is the distribution coefficient [L^3 M^{-1}]. The equation of mass balance in the immobile domain is

$$R_{im} \frac{\partial C_{im}}{\partial t} = \frac{\zeta}{\theta_{im}}\left(C_m - C_{im}\right) \tag{10}$$

where θ_{im} is the immobile porosity [-];and R_{im} is a dimensionless linear retardation factor for sorption in the immobile domain, such that $R_{im} = 1 + \left(1 - f\right)\rho_b K_d / \theta$, where f is the fraction of sorption sites in contact with the mobile phase. The variable f implies the distribution coefficient does not vary between domains.

CHAPTER 3: Effect of biostimulants on 2,4,6-Trinitrotoluene (TNT) degradation and bacterial community composition in contaminated aquifer sediment enrichments

Submitted to Biodegradation, January 2012

3.1 Authors

Nicole Fahrenfeld, Jeffrey Zoeckler, Mark Widdowson, Amy Pruden

3.2 Abstract

2,4,6-Trinitrotoluene (TNT) is a toxic and persistent explosive compound occurring as a contaminant at numerous sites worldwide. Knowledge of the microbial dynamics driving TNT biodegradation is limited, particularly in native aquifer sediments where it poses a threat to water resources. The purpose of this study was to quantify the effect of organic amendments on anaerobic TNT biodegradation rate and pathway in an enrichment culture obtained from historically contaminated aquifer sediment and to compare the bacterial community dynamics. TNT readily biodegraded in all microcosms, with the highest biodegradation rate obtained under the lactate amended condition followed by ethanol amended and naturally occurring organic matter (extracted from site sediment) amended conditions. Although the same general reductive pathway of TNT degradation was observed across all conditions, denaturing gradient gel electrophoresis (DGGE) analysis revealed distinct bacterial community compositions. In all microcosms, Gram-negative γ- or β-Proteobacteria and Gram-positive Negativicutes or Clostridia were observed. A *Pseudomonas* sp. in particular was observed to be stimulated under all conditions. According to results of non-metric multidimensional scaling analysis of DGGE profiles, the microcosm communities were most similar to field site sediment corresponding to the highest TNT concentration, relative to moderately and uncontaminated sediments, suggesting that TNT contamination itself is a major driver of microbial community structure. Overall these results provide a new line of evidence of the key bacteria driving TNT degradation in aquifer sediments and their dynamics in response to organic carbon amendment, supporting electron donor addition as a promising technology for stimulating *in-situ* TNT bioremediation in the subsurface.

3.3 Introduction

Energetic compounds, or explosives, are of particular concern due to their toxicity and widespread contamination that has occurred during their manufacture, transport, testing, and disposal. 2,4,6-Trinitrotoluene (TNT) is an explosive present at numerous sites worldwide, including 20 of the current sites on the U.S. Environmental Protection Agency (EPA) National Priorities List (US EPA 2011b). TNT and its degradates have been found to be mutagenic (Alborg et al. 1988), toxic (Berthe-Corti et al. 1998), and teratogenic (Saka 2004). The EPA considers TNT an emerging contaminant and a possible human carcinogen based on epidemiological evidence (US EPA 2011a), underscoring the urgency to identify reliable remediation options.

Bioremediation harnesses the natural potential of microbes to effectively biodegrade or biotransform a variety of contaminants and is an attractive remedial technology from an economic and sustainability standpoint. TNT has been observed to biodegrade under both aerobic and anaerobic conditions via nitroreductive pathways in which TNT is successively reduced to (predominantly) 4-amino-2,6-dinitrotoluene (4ADNT) and 2,4-diamino-6-nitrotoluene (24DANT) (Hawari et al. 2000; Esteve-Nunez et al. 2001). Further reduction to 2,4,6-triaminotoluene (TAT) may ensue under strict anaerobic conditions (McCormick et al. 1976). A major benefit of the nitroreductive pathway is that as the amino character increases, so does sorption to organic rich sediment (Li et al. 1997), thus serving as a valuable attenuation mechanism for groundwater plumes. However, little is known about the bacterial communities driving TNT nitroreductive processes in contaminated aquifers.

Addition of fermentable substrates is commonly employed to stimulate reductive degradation pathways, particularly when the contaminant itself (such as TNT) does not readily serve as a carbon source. Electron donors and organic carbon sources have been observed to enhance TNT degradation in several studies: glucose and citrate stimulated TNT loss in contaminated landfill sediment (Tharakan and Gordon 1999); hydrogen, ethanol, propylene glycol, and butyrate supported a mixed TNT degrading culture grown from Milan Army Ammunition plant soil (Adrian et al. 2003); ethanol and propylene glycol supported a mixed TNT degrading culture from the Holston Army Ammunition plant (Adrian and Arnett 2007); and molasses, corn steep

liquor, potato starch, and soy bean oil supported loss of extractable TNT in soil slurries from the Massachusetts Military Reservation (Fuller et al. 2004). One of the few reported field scale demonstrations of *in situ* treatment was at the West Virginia Ordnance Works, in which they observed that Hydrogen Release Compound ® (a patented polylactate compound, Regenesis, Inc., San Clemente, CA) reduced TNT concentrations in groundwater as much as from 99.6µg/L to below 10µg/L in treated wells (Downey et al. 2005). However, no study to date has yet yielded robust rate data for microbes relevant to contaminated aquifer sediments.

Researchers have isolated a variety of bacteria that degrade TNT. While pure culture studies do provide important fundamental information, there is a general void in understanding of the microbial communities that drive TNT degradation, which are of greater relevance to conditions in contaminated environments. TNT contamination is known to reduce biological activity in soils (Meyers et al. 2007; George et al. 2008; Frische and Höper 2003), cause shifts in populations towards bacteria with higher TNT tolerances (Gong et al. 2000), select for Gram-negative bacteria (Fuller and Manning 1998), and reduce soil Acidobacter community and diversity (George et al. 2009). Biomass has been shown to increase in contaminated soils during treatment as observed using phospholipid fatty acid (PFLA) analysis for soil treated with manure (Wilke et al. 2004) and in molasses fed bioslurry reactor seeded with soil from the Joliet Army Ammunition Plant (Fuller and Manning 2004). However, TNT induced changes in community may not be consistent across different sediments (Wikström et al. 2000). While most of the above studies provide insight into microbial community shifts in terms of a toxic response to TNT, there is a general lack of molecular characterization of microbial communities associated with TNT biodegradation in aquifer sediments and their response to biostimulation.

The TNT contaminated site investigated here, located in the Atlantic Coastal Plain of Virginia, has a source dating back to World War I and is previously uncharacterized in the literature. At present, remediation has consisted of direct excavation of contaminated soil and unexploded ordnance in the source zone. A TNT plume is present in a surficial aquifer with concentrations of 440µg/L observed in source zone monitoring wells. Observed degradates include amino-dinitrotoluenes in the groundwater. The objectives of this study were to (1) compare the effect of a range of potential electron donors on the rate and pathway of TNT reduction, and (2)

determine the effect of electron donor addition on bacterial community composition with time. The overall goal is to gain fundamental insight into the microbial community dynamics that drive TNT remediation in the subsurface in order to better evaluate biostimulation as a viable remedial action for groundwater.

3.4 Materials and Methods

3.4.1 Sample Collection

Site sediment cores were collected from contaminated and uncontaminated sampling locations at depth corresponding to the water table and deeper using a direct push technology (i.e., Geoprobe™ rig). Core samples were encased in sterile acetate liners and were cut into 2ft sections, capped with Teflon tape, sealed, and stored on ice. Upon receipt in the laboratory, cores were transferred intact to storage in plastic bags filled with nitrogen at 4°C.

3.4.2 Microcosm preparation

An enrichment culture was developed from contaminated site sediment through a batch serial enrichment approach involving three generations of microcosms. Sediment samples used for seeding the first generation enrichment cultures were collected May 2009 at well B, characteristics of which are listed in Table 1.1. Homogenized sediment (1g) was placed in 50mL of anaerobic mineral media (Adrian et al. 2003) in quintuplet. TNT was spiked in (11µM) and bottles were sealed with 1" butyl rubber stoppers and aluminum crimps. Bottles were wrapped in foil, inverted, and incubated statically. Periodic liquid sampling was performed until TNT was below detection. Once TNT was below detection, bottles were respiked to the initial target concentration with TNT to verify biodegradation. This culture was used to inoculate second generation microcosms (1:10 dilution), which were prepared using natural carbon derived from site sediment and a modified version of the mineral media (Rectanus et al. 2007) used in the first generation. Rectanus et al. (2007) demonstrated a method to quantify readily extracted and labile fraction of organic carbon present in aquifer sediment, which is operationally defined as potentially bioavailable carbon (PBOC). The media was prepared using a trace vitamin solution reported by others (Adrian et al. 2003), minimal salts (Rectanus et al. 2007) and the addition of buffering to adjust the pH of PBOC extract to neutral. PBOC was extracted from core C, upgradient of the source zone, from a depth that was characterized by no solvent or NaOH

extractable TNT or degradates. The three experimental conditions differing in potential electron donor were PBOC only, PBOC with ethanol amendment, and PBOC with lactate amendment. Ethanol and lactate amendments were each added at 2.8mM.

Table 3.1 Characteristics of field site samples

Well	*Location*	*Depth (m)*	*% Sand*	*% Silt*	*% Clay*	*Classification*	*TNT (mg/kg)*
A	Source zone	5.79	80.9	8.0	11.1	Loamy sand	3406
B	Outside source zone	4.27	79.9	7.5	12.6	Sandy loam	20.7
C	Upgradient of source zone	4.88	81.2	7.0	11.9	Sandy loam	b.d.[a]

[a] = below detection, detection limit 0.4mg/kg.

To obtain rate data, third generation microcosms were prepared in an identical manner as the 2nd generation bottles, in quintuplet for each test condition. Triplicate biologically inhibited ("killed") controls were prepared in parallel identically to experimental bottles, except that $HgCl_2$ (3.7mM) was added to inhibit microbial growth. Aqueous samples were taken periodically for explosives analysis and at the same time aliquots (10mL) were filtered (0.2µm nitrocellulose filters) and filters were preserved at -20°C for molecular analysis.

3.4.3 Chemical analysis

Analysis was performed on reserved liquid from microcosms or acetonitrile sediment extracts for 2,4-diamino-6-nitrotoluene (24DANT), 2,6-diamino-4-nitrotoluene (26DANT), 1,3,5-trinitrobenzene (135TNB), 1,3-dinitrobenzene, TNT, tetryl, 2,4-dinitrotoluene, 2,6-dinitrotoluene, 2-amino-4,6-dinitrotoluene (2ADNT), 4-amino-2,6-dinitrotoluene (4ADNT) (Accustandard). Gradient-grade methanol and acetonitrile (EMD Chemicals) were used and all other chemicals were ACS grade. Quantification was performed using a liquid chromatograph with ultra violet detection (Shimatdzu Prominence) on an Ultra C8 column (Restek) according to EPA Method 8330b. A gradient method was used for the mobile phase which consisted of nanopure water mixed with 30% methanol for 10.5 min, 40% methanol for 26.5 min, 50% methanol for 9.5 min, followed by 3 min at 30% methanol to reequilbirate to starting conditions adapted from (Lenke et al. 1998).

Particle size analysis (Soil Survey Staff 2004) was performed on aliquots of sediment. Total organic carbon analysis on the PBOC extracts was performed using catalytic combustion (Shimadzu TOC V CSN Total Organic Carbon Analyzer).

3.4.4 Biomolecular analysis

DNA was extracted from preserved filters from replicate bottles corresponding to key microcosm rate time points using a FastDNA SPIN Kit (MP Biomedicals, Solon, OH) according to manufacturer's instructions and from field sediment samples using FastDNA SPIN Kit for Soil (MP Biomedicals). A 1:50 dilution of DNA extract was demonstrated to minimize PCR inhibition and therefore was implemented in all downstream analyses. PCR was performed using an Eppendorf MasterTaq kit in a 25µL reaction volume. Total bacterial 16S rRNA genes were amplified using forward primer 8f and universal reverse primer 1492r (Weisburg et al. 1991). A nested PCR was performed using this PCR product as template to yield a PCR product suitable for denaturing gradient gel electrophoresis (DGGE) using 341GC and 533r primers and previously defined conditions (Watanabe et al. 2001).

DGGE was performed using D Code system (Bio-Rad, Hercules, CA). The gels were prepared using 8% acrylamide with a denaturing gradient from 35-65% (100%=40% (v/v) deionized formamide and 42% (w/v) urea) and electrophoresed at 50V for 18hr. The gels were stained with 1X SYBR Gold (Molecular Probes) and documented using a Gel Doc XR System (BioRad). Bands of interest were excised, placed in 36µL ddH2O, amplified with PCR, and subject to DNA sequencing.

Extracted DNA from one replicate of each experimental treatment taken at 6days, was subject to 16S rRNA gene amplification using primers 8f/1492r, as described above, and cloned into *Escherichia coli* using a TOPO TA Cloning Kit (Invitrogen, Carlsbad, CA). Eighty clones from each sample were analyzed via restriction digest with *MspI* to identify unique operational taxonomical units. Unique clones were further analyzed by DGGE in parallel with experimental samples. Clones with the same migration pattern as bands from experimental samples were noted. Corresponding clone inserts were subject to DNA sequencing by the Virginia Bioinformatics Institute (Blacksburg, VA). GenBank DNA sequences with the highest similarity

to those represented by the DGGE bands were identified using the BLAST alignment tool (http://www.ncbi.nlm.nih. gov/BLAST/). Sequences for bands of interest (bands a-n) have been submitted to EMBL database and are available under accession numbers HE614130-HE614143.

3.4.5 Data analysis

DGGE banding patterns were digitized using Quantity One software (Bio-Rad). Statistical analysis of banding patterns (band number and intensity) was performed by non-metric multidimensional scaling (MDS) using PRIMER 6 (Prime E, United Kingdom). Relative abundance was estimated from digitized band intensity and the abundance of bacterial classes was compared by t-test in R. Modeling of degradation rates was performed in R using linear regression. Rates from the replicate microcosms were compared as described above, with a Bonferonni correction for multiple comparisons.

3.5 Results

3.5.1 Effect of Amendment on TNT Biodegradation Rate and Pathway

Rapid loss of aqueous TNT was observed in all experimental microcosms, with TNT below detection after 200hr for all conditions (Fig. 3.1). Zero, first, and second order models of the rates were compared and zero order provided the best fit to the data, based on R^2 value (Table C.1). Thus, rates of TNT loss were approximated as zero order with the estimated rates for lactate, ethanol, and PBOC amended conditions being 0.14±0.015µM/hr, 0.087±0.0046µM/hr, 0.047±0.013µM/hr, respectively. All experimental microcosms yielded significantly greater rates of TNT loss than killed controls (compared using t-test lactate: $P=3x10^{-11}$, ethanol: $P=1.5x10^{-10}$, PBOC: $P=2.9x10^{-7}$) indicating that $HgCl_2$ inhibited microbial degradation of TNT. Among the experimental conditions, lactate stimulated more rapid TNT loss than ethanol (P=0.042), which was more rapid than PBOC ($P=5.0x10^{-4}$). A consistent rate of TNT loss was observed among the killed controls (P=1.0 for all), though at a significantly slower rate than the biologically active treatments as noted above.

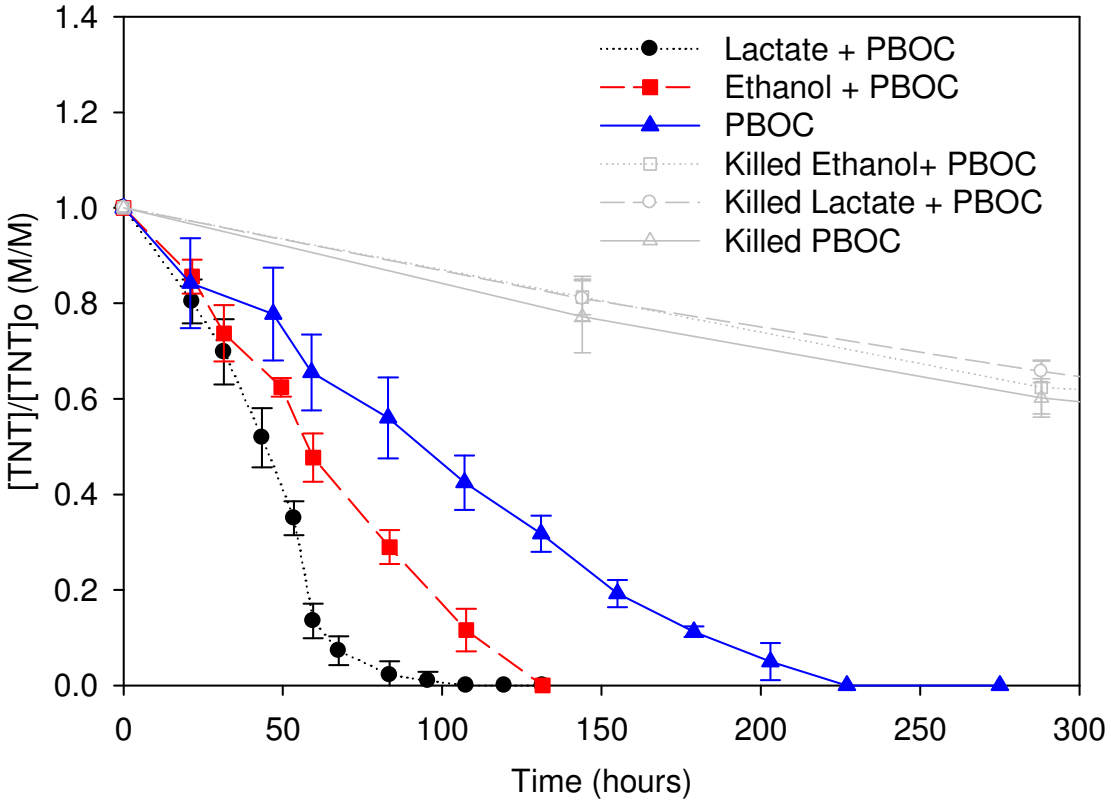

Figure 3.1 TNT transformation with time in microcosms amended with lactate (circles), ethanol (squares), and PBOC (triangles) as well as killed controls for each (open circles, open squares, and closed triangles, respectively). $[TNT]_o$ = 10.8+/-1.2µM, across all conditions

The primary pathway of TNT degradation was observed to be consistent across the three experimental conditions. A nitroreductive pathway beginning with the appearance of ADNT followed by DANT was observed in all microcosms, with 4ADNT and 24DANT as the dominant isomers (data not shown). All intermediates were non-detectable by 800hr in the lactate and ethanol microcosms and by 1000hrs in the PBOC microcosms (data not shown). TAT quantification was not pursued given challenges in quantification of this short lived degradation product. No intermediate production was observed in the killed controls; and no other explosives related compounds analyzed for were detected, including 135TNB, indicating that photolysis was not occurring in the microcosms.

3.5.2 Bacterial community response to amendments

DGGE was performed to compare the bacterial community profiles of the final TNT degradation time point of 144hrs across amendment conditions and to field site sediments, as shown in Figure 3.2a. A unique array of bands was observed for each experimental condition and the contaminated sediment, while only four visible bands were resolved from the uncontaminated sediment sample.

MDS analysis was performed on digitized banding profiles to gain insight into broad similarities among the dominant bacterial communities, as shown in Figure 3.2b. Significant differences in DGGE profiles were observed with respect to the different amendments applied in the microcosms, in spite of the fact that same nitroreductive biodegradation products were observed. Previous comparison of electron donor addition to TNT reduction demonstrated some differences in the isomers produced with different electron donors (Adrian et al. 2003). Among the amendment conditions, the banding profiles corresponding to ethanol and lactate were observed to be the most similar. No significant difference was observed between duplicate DNA extracts from microcosms or sediment samples, except in the case of sediment sample A (likely a gel-edge artifact).

According to MDS analysis, all experimental microcosms clustered together relative to the field site sediments (Fig. 3.2b), indicating that while significantly different banding profiles were observed by the end of the experiment, microcosms receiving different amendments still were more similar to each other than they were to native sediment samples. However, experimental microcosms did cluster most closely with field sediment sample A, which was the most heavily contaminated with TNT. Notably, this was despite the fact that the culture employed in the microcosms was originally enriched from Well B, which was characterized by intermediate contamination. Converse to the experimental microcosms, killed controls clustered with the moderately contaminated Well B sediment.

a.

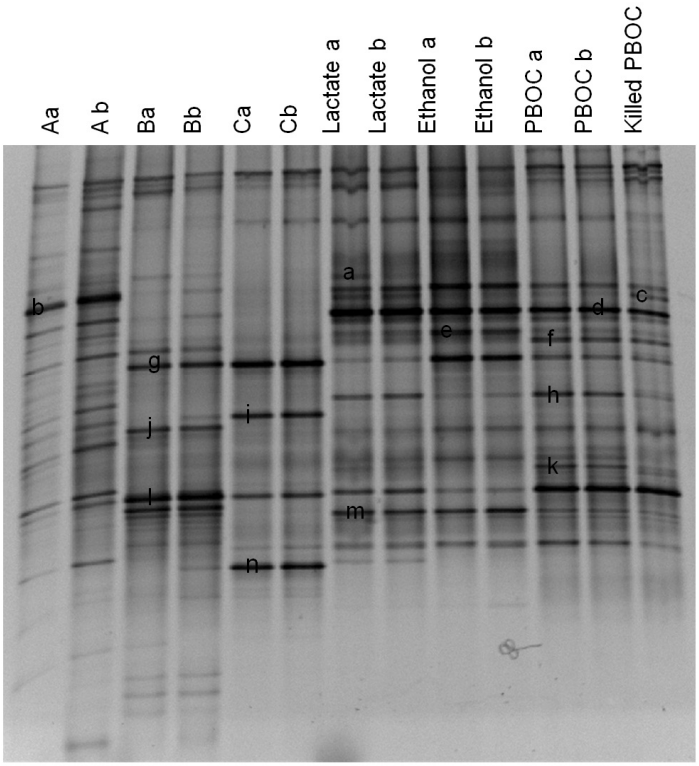

b.

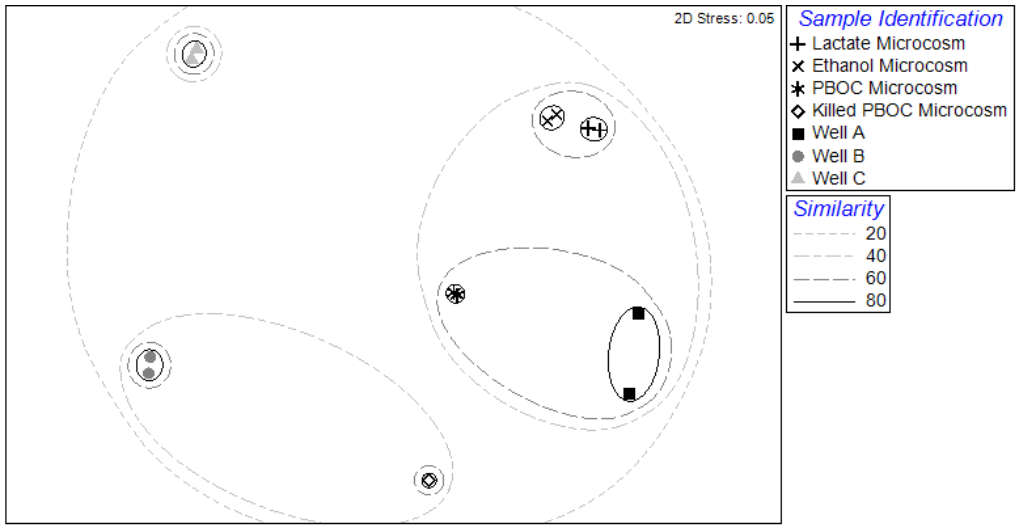

Figure 3.2 a. DGGE comparing DNA extracted from field sediment samples collected from groundwater Wells A (3406µgTNT/g sediment), B (20.7µg TNT/g sediment), and C (TNT below detection) with DNA extracted from microcosms after 144hrs. Labelled bands (a-n) were excised and subject to DNA sequence analysis (Table 2.2). DGGE analysis of each sample was conducted on DNA extractions from duplicate microcosms (a, b). b. MDS analysis of DGGE fingerprints for lactate (+), ethanol (x), PBOC (*), and the killed PBOC (open diamonds) microcosms and Wells A (squares), B (circles), and C (triangles).

3.5.3 Temporal patterns in bacterial community dynamics

MDS analysis was also performed on DGGE profiles corresponding to various biodegradation time points for each condition, shown in Fig. 3.3. For all experimental microcosms, significant differences in banding patterns were observed between 0hrs and later time points. Experimental lactate microcosms resulted in three significantly different clusters for 0, 24 and 72, versus 144hr time points (Fig. 3.3a) while ethanol resulted in two significantly different clusters for time 0hr versus all later time points (Fig. 3.3b). PBOC elicited less consistent clustering; however earlier time points did still cluster more closely than latter samplings (Fig. 3.3c). DGGE images are shown in Fig. 3.4a-c.

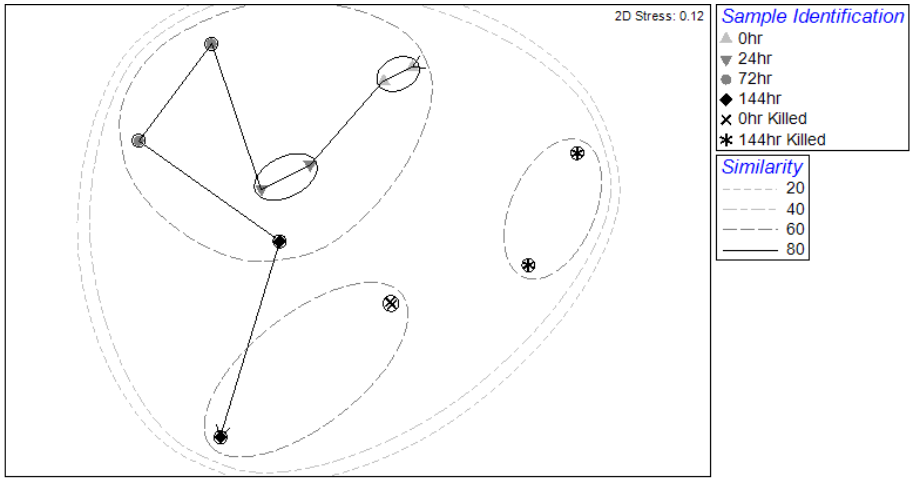

a.

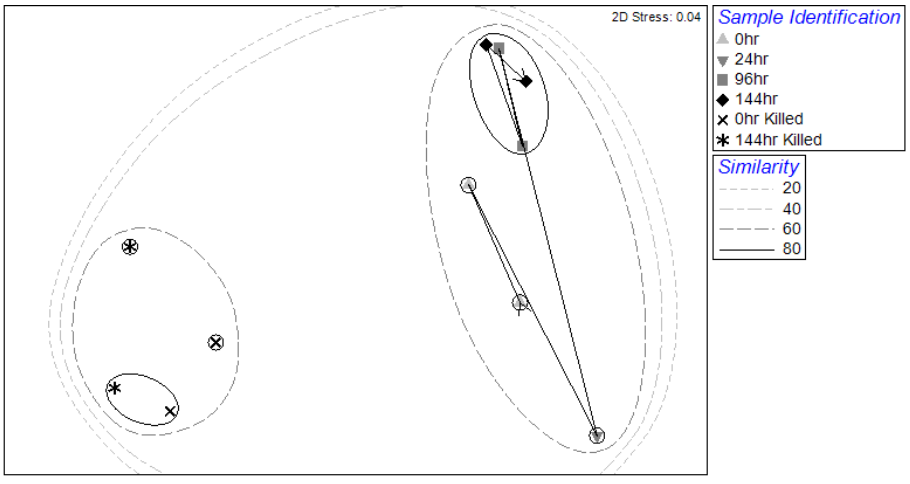

b.

c.

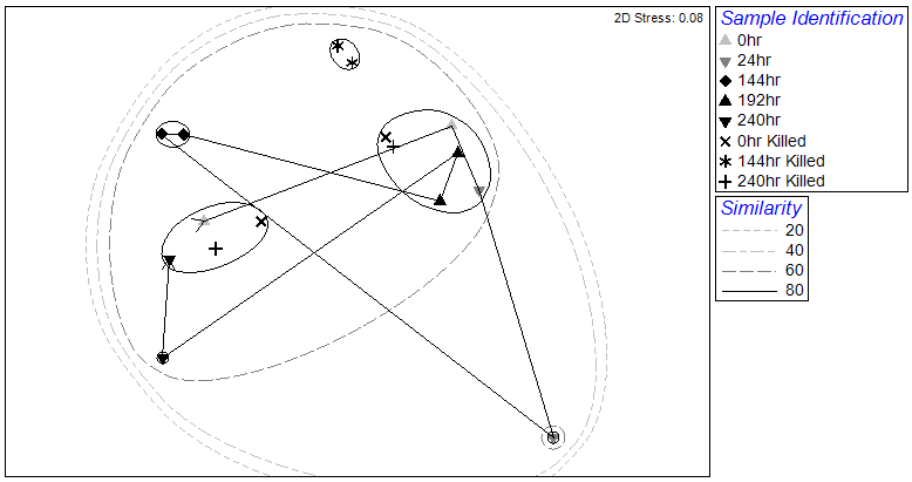

Figure 3.3 MDS analysis of DGGE fingerprints of microcosms with time for a. Lactate, b. Ethanol, c. PBOC for 0hr (triangle), 24hr (inverted triangle; available only in singlet for ethanol), 72hr (circle), 96hr (square), and 144hr (diamond) for experimental microcosms and 0hr (x) and 144hr (*) for killed controls. Results demonstrate temporal changes in microbial community profile.

a.

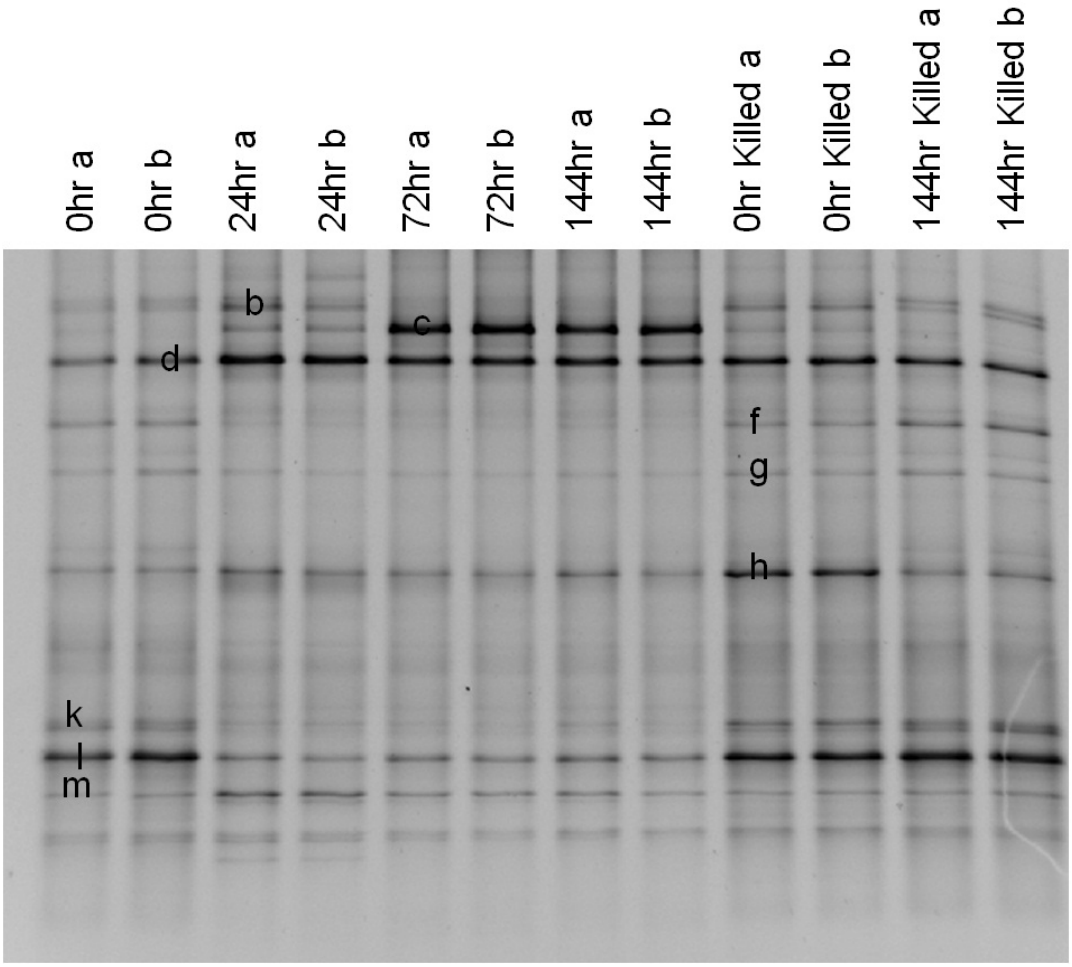
0hr a
0hr b
24hr a
24hr b
72hr a
72hr b
144hr a
144hr b
0hr Killed a
0hr Killed b
144hr Killed a
144hr Killed b
b
c
d
f
g
h
k
l
m

b.

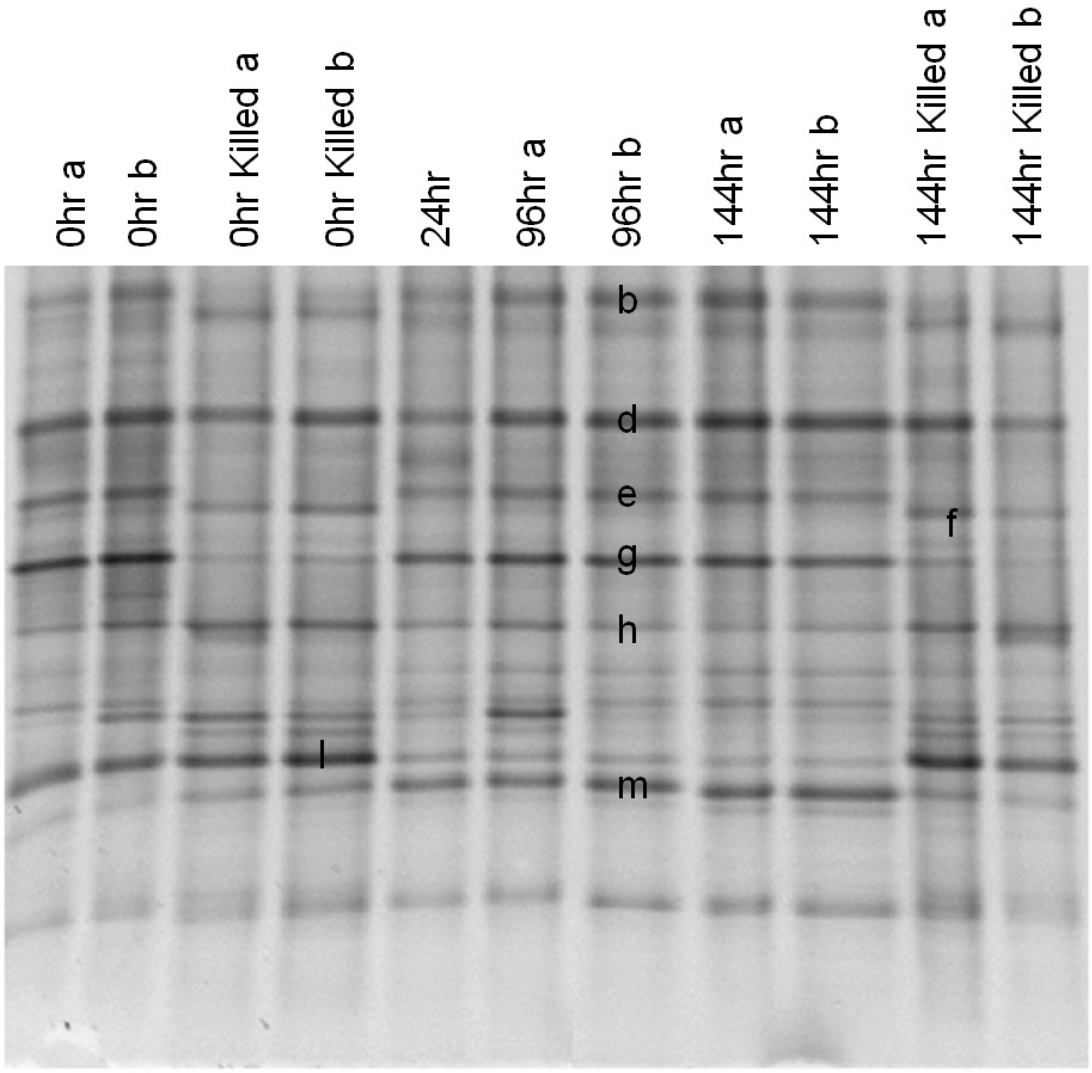
0hr a
0hr b
0hr Killed a
0hr Killed b
24hr
96hr a
96hr b
144hr a
144hr b
144hr Killed a
144hr Killed b
b
d
e
f
g
h
l
m

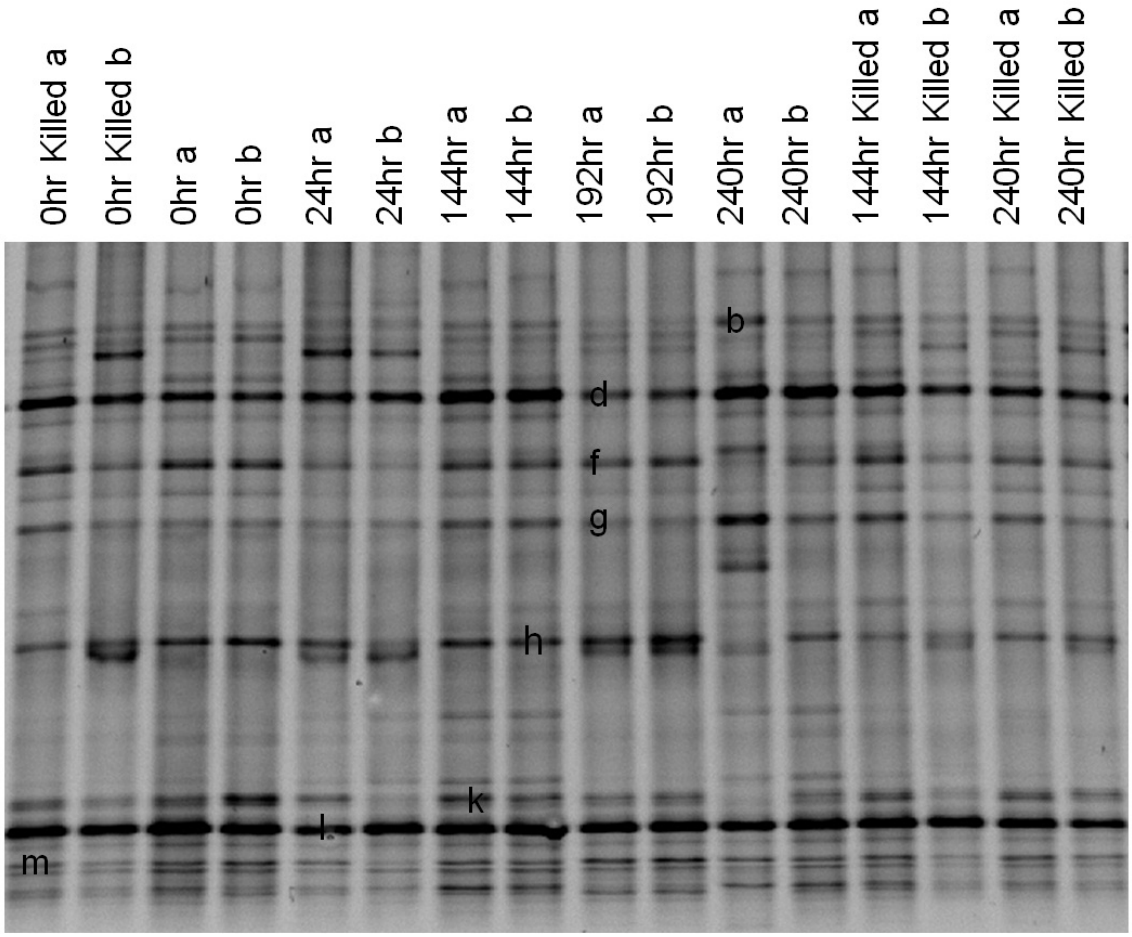

c.

Figure 3.4 DGGE of DNA extracted for microcosms and killed controls for key degradation time points for a. lactate stimulated bottles, b. ethanol stimulated bottles, and c. PBOC only bottles

3.5.4 Identification of dominant bacteria

DNA sequencing results are summarized in Table 3.2 and corresponding DGGE bands are labeled in Fig 3.2. Identified bacteria from the microcosms all were classified as either Gram-negative bacteria belonging to the γ- or β-Proteobacteria class or Gram-positive bacteria (specifically Firmicutes) belonging to the Negativicutes or Clostridia class. Similar results were found for contaminated sediment where γ- and β-proteobacteria as well as Firmicutes were identified. In contrast, only γ- and β-proteobacteria were identified in the uncontaminated sediment. Several *Pseudomonas* strains corresponded to dominant bands (bands b, d, and g) across all microcosm conditions at 144hrs. In ethanol microcosms in particular, increased band

intensity (e) was noted corresponding to Clostridia. In lactate and PBOC microcosms with more prevalent band (l) corresponding to *Methylobacterium*.

Relative abundance of each class of bacteria was estimated by band intensity (Fig. 3.5). Gram-negative (Proteobacteria) were more abundant than Gram-positive (Firmicutes) in all samples ($p<0.05$ in all cases). However, the relative abundance of the classes of identified Proteobacteria varied (statistical significance determined via t-test): β-Proteobacteria were more abundant than γ-Proteobacteria in field sediment sample B ($p=2.9x10^{-3}$) and C ($p= 7.6x10^{-4}$) and the PBOC ($p= 1.9x10^{-2}$) microcosms; γ-Proteobacteria were more abundant than β-Proteobacteria in lactate ($p= 7.8x10^{-3}$) and ethanol ($p= 5.0x10^{-3}$) amended microcosms, and no significant difference was observed in field sediment sample A ($p=0.24$). Clostridia were detected in all samples except field sediment sample C, ranging from 12.1-29.0% of the bacterial community.

Table 3.2 Highest sequence similarities found for DGGE bands

Band	***Phylum***	***Class***	***Highest Similarity from BLAST (accession number)***	***% Match***
a	Proteobacteria	γ -proteobacteria	*Pseudomonas* sp. (FM161516)	94%
b	Proteobacteria	γ -proteobacteria	Uncultured soil bacterium clone GO0VNXF07H8RDO 16S ribosomal RNA gene, partial sequence. (JF383105)	89%
c	Firmicutes	Negativicutes	Uncultured *Pelosinus* sp. clone PAGW1_64 (GQ257723)	89%
d	Proteobacteria	γ -proteobacteria	Uncultured *Pseudomonas* sp. clone LJH D 16S ribosomal RNA gene, partial sequence (HM192823)	93%
e	Firmicutes	Clostridia	*Desulfitobacterium* sp. CR1 (AB299028)	95%
f	Firmicutes	Clostridia	Eubacterium saburreum clone ATC_H74_12 (GU413453)	98%
g	Proteobacteria	γ -proteobacteria	Uncultured *Pseudomonas* sp. clone adm 34 16S ribosomal RNA gene, partial sequence (JF812373)	96%
h	Proteobacteria	β-proteobacteria	*Ralstonia* sp. LIG5GB 16S ribosomal RNA gene, partial sequence. (HM587786)	99%
i	Proteobacteria	β -proteobacteria	Uncultured beta proteobacterium clone THz2 30 16S ribosomal RNA gene, partial sequence. (HM854322)	96%
j	Firmicutes	Clostridia	Eubacterium saburreum clone ATC_H74_12 16S ribosomal RNA gene, partial sequence (GU413453)	98%
k	Proteobacteria	β -proteobacteria	Cupriavidus basilensis isolate TFD8 (EF177353)	97%
l	Proteobacteria	β proteobacteria	*Methylobacterium* sp. T34 partial 16S rRNA gene, strain T34 (FR869835)	95%
m	Proteobacteria	β -proteobacteria	*Cupriavidus* sp. DE7 16S ribosomal RNA gene, partial sequence (JN226398)	97%
n	Proteobacteria	β -proteobacteria	Uncultured Betaproteobacteria bacterium 16S rRNA gene from clone (CU920167)	97%

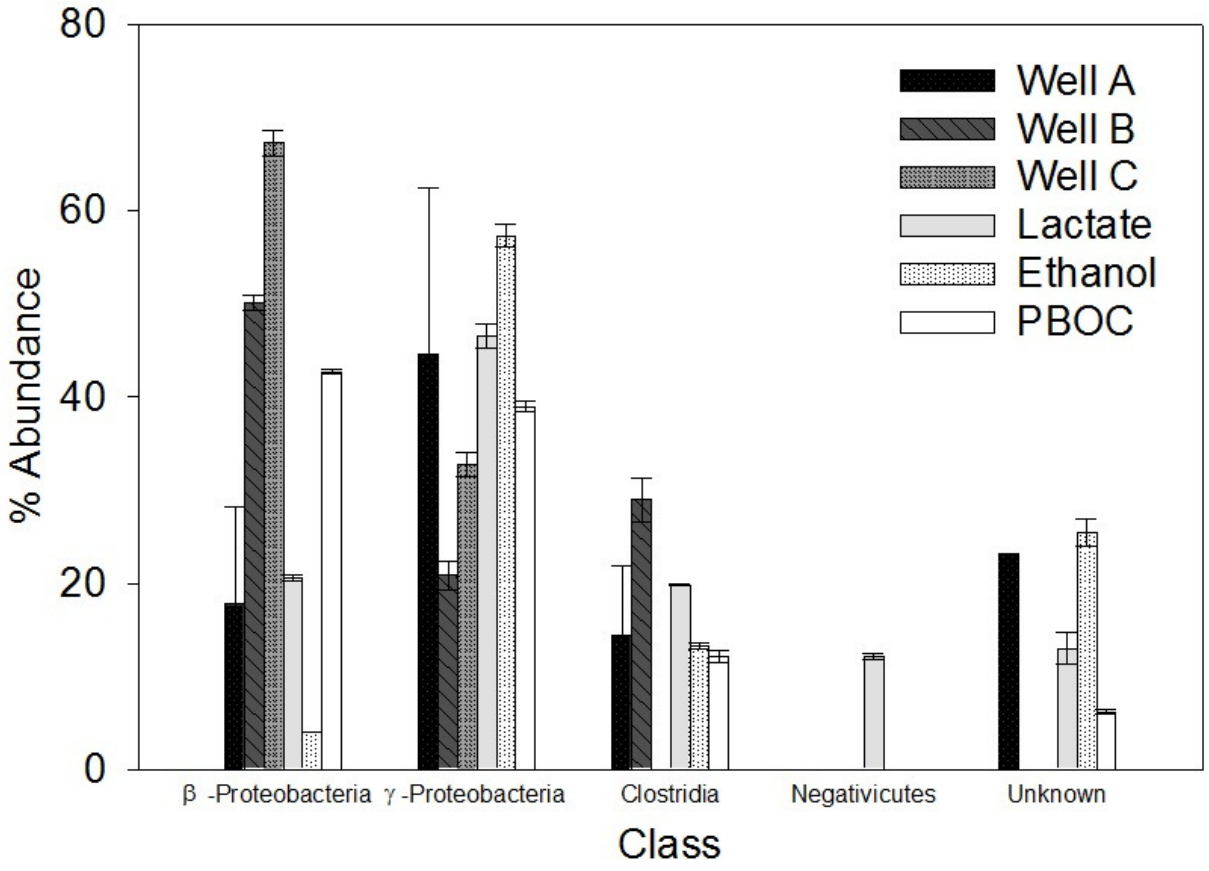

Figure 3.5 Relative abundance of each class of bacteria as estimated by band intensity, corresponding to the DGGE image shown in Fig. 3.2a.

3.6 Discussion

3.6.1 Potential for Biostimulation of TNT Biodegradation

This study provided new insight into bacterial community dynamics relevant to TNT bioremediation in contaminated aquifers and supports organic carbon amendment as a promising *in-situ* bioremediation approach. Both lactate and ethanol, which were amended above the PBOC background, were better stimulants than PBOC alone likely because the presence of each increased the total bioavailable organic matter. To represent complex organic matter typically present in groundwater, PBOC was maintained in the background across all conditions at 190mg/L TOC, although not all this TOC is expected to be readily degradable. Likewise, lactate

was a likely superior stimulant than ethanol as it is readily fermentable and provides more energy (1.11kJ/electron equivalent) than ethanol upon reduction. Additionally, lactate and ethanol may have stimulated TNT degradation by generating H_2, which can then serve as an electron donor for nitroreduction. Zero order was the best model fit and implies that rate is independent of TNT concentration, correspondingly suggesting that the TNT concentration was well above the Michaelis-Menton half saturation constant. All rates for the third generation microcosms that were the focus of this study were significantly faster than those observed in earlier generation microcosms prepared with sediment slurries (data not shown), supporting the conclusion of a high concentration of active biomass consistent with zero order kinetics.

Losses of TNT observed in the killed controls indicate that $HgCl_2$ may not have been sufficient to fully inhibit the microbial culture. A second possibility is that bacteria were in fact killed by the $HgCl_2$, but bacterial enzymes remained active. A third possibility is that there were slow losses of TNT to the PBOC matrix. The latter is in agreement with the slow kinetic losses of TNT to Aldrich humic acids in batch studies (Li et al. 1997), considering that the PBOC extract is heavily enriched in humic acids (Rectanus et al. 2007).

3.6.2 Key Characteristics of TNT-Degrading Bacterial Communities

The observation that the bacterial community in amended microcosms resembled the heavily contaminated sediment provides evidence that TNT concentration is a driving factor governing the bacterial community composition (Fig 3.2). Similarly, differences among the field sediment samples themselves may be due to differences in TNT concentration, though other heterogeneities between sediment cores (organic carbon, dissolved oxygen, etc.) could have also played a role. The reason killed controls clustered with Well B sediment is likely because $HgCl_2$ does not destroy DNA and thus it effectively acted to preserve the initial condition of the killed microcosms, which, like the others, were originally inoculated from enrichment culture generated from Well B sediment.

This MDS comparison at key biodegradation time points provides a snapshot of how the microbial community changes during TNT biodegradation. These findings indicate that the

bacterial community was in a dynamic state during TNT biodegradation, highlighting bands that intensify during TNT biodegradation as being of keen interest. Generally, the dominant bacteria identified corresponded well with the anaerobic conditions characteristic of the contaminated site sediment and imposed on the microcosms. Further, several highest band DNA sequence similarities corresponded to relatives of previously described TNT degraders known to be able to reduce nitro groups.

3.6.3 Putative Roles of Bacteria Identified

Several identified bacteria had high sequence similarity to those know to degrade TNT in pure culture. Clostridia are obligate anaerobes, thus their presence in microcosms and contaminated sediments provides evidence of anaerobic conditions. Likewise, the lack of identified Clostridia in the uncontaminated sediment may imply that conditions there are aerobic (Fig 3.2). Clostridia have been found to reduce TNT in pure cultures (Regan and Crawford 1994). Two genes, *nit*A and *nit*B, (Kutty and Bennett 2005) and an Fe-only hydrogenase (Watrous et al. 2003) have been implicated in nitro- reduction and tied to growth in *Clostridia.* Interestingly, the other Gram-positive bacteria class identified, Negativicutes, corresponded to a *Pelosinus* clone found in RDX contaminated sediments at the Picatinny Arsenal stimulated with lactate (Fuller et al. 2010). This suggests a potentially important role for *Pelosinus* in energetics remediation. *Pelosinus* are iron reducing bacteria and have been found in sediment contaminated with chlorinated solvents (Moe et al. 2011). *Pseudomonas* spp. were also identified across the contaminated sediment and microcosms and represent an extremely diverse and metabolically versatile genus, existing both as aerobes and facultative anaerobes. Several *Pseudomonas* strains have been implicated in TNT biodegradation (Duque et al. 1993). Specifically, in *P. putida,* nitroreductase genes *pnr*A and *pnr*B have been identified (Caballero et al. 2005b). Evidence suggests that *Pseudomonas* spp. can use TNT as a terminal electron acceptor and perhaps facilitate the release of nitrite that may be used as N source for growth (Duque et al. 1993; Caballero et al. 2005a). High band sequence similarity corresponding to β-Proteobacteria included *Cupriavidus*, an aerobe not previously implicated in TNT degradation and *Methylobacteria*, species of which have been confirmed to degrade TNT (Van Aken et al. 1999). Further, *Ralstonia* are aerobic or facultative anaerobes that have previously been identified in pristine soil contaminated with TNT (George et al. 2008).

The dominance of Gram-negative bacteria in all sediment samples is in agreement with previous research: a weak negative association of Gram-positive bacteria with high concentrations of TNT in sediments (Fuller and Manning 1998).

Intensifying bands correspond to bacteria that found the TNT microcosm environment relatively favorable. For example, they may possess a higher tolerance for the toxicity of TNT and its degradates, received growth benefit from reduction of TNT, or are able to outcompete other bacteria for use of the amended carbon substrates. Shifts in microbial community structure demonstrated by MDS across time in the lactate bottles included increases in band c and d intensities, corresponding to the *Pelosinus* and *Pseudomonas*, respectively. In the ethanol bottles, bands b, d, g, and m increased in intensity with time corresponding to various strains of *Pseudomonas* and *Ralstonia*. PBOC only bottles displayed increased intensity for bands b and g, both corresponding to *Pseudomonas* spp. Other researchers have also observed that the addition of TNT to uncontaminated soils stimulated an increase in *Pseudomonas* populations in aerobically incubated soils (George et al. 2008). A notable band that decreased in intensity with time across all conditions was Band l, which corresponds to the obligate aerobic TNT degrading *Methylobaceterium*. This observation further supports in the conclusion that anaerobic conditions were maintained in the microcosms.

3.7 Conclusions

This work demonstrated that TNT is readily biodegradable by cultures enriched from historically contaminated aquifer sediments. Biodegradation was possible in the presence of natural site organic matter (PBOC) and rates were significantly stimulated by the addition of lactate or ethanol. DGGE revealed a dynamic bacterial community response to organic amendment and biodegradation with time among the microcosm conditions, yet demonstrated a broad similarity in terms of the dominant bacteria identified and their high DNA sequence similarity to known TNT degraders. These included various *Clostridia* spp., *Pseudomonas* spp., and possibly a *Pelosinus* spp. that has previously been found at an RDX contaminated site. The same nitroreductive TNT biodegradation pathway, through concomitant production of ADNT followed by DANT, was also observed across conditions indicating that this may be a robust TNT

biodegradation pathway among various groundwater bacteria. Interestingly, the organic carbon stimulated microcosms actively degrading TNT aligned more closely with the most heavily TNT contaminated field sediment, relative to less contaminated sediments, indicating that TNT itself may be a driving factor in the bacterial community structure.

3.8 Acknowledgements

Funding for this work was provided by Versar, Inc. and the U.S. Army Corps of Engineers, Norfolk, Virginia. Thanks to H. Clarkson Meredith (Versar), Jody Smiley (VT), and Rachel Kistler (VT) for technical and laboratory assistance.

3.9 References

Adrian N, Arnett C (2007) Anaerobic biotransformation of explosives in aquifer slurries amended with ethanol and propylene glycol. Chemosphere 66 (10):1849-1856.

Adrian N, Arnett C, Hickey R (2003) Stimulating the anaerobic biodegradation of explosives by the addition of hydrogen or electron donors that produce hydrogen. Water Res 37 (14):3499-3507.

Alborg J, G, Einisto P, Sorsa M (1988) Mutagenic activity and metabolites in the urine of workers exposed to trinitrotoluene (TNT). British J Industr Med 45:353-358.

Berthe-Corti L, Jacobi H, Kleihauer S, Witte I (1998) Cytotoxicity and mutagenicity of a 2,4,6-trinitrotoluene (TNT) and hexogen contaminated soil in S. typhimurium and mammalian cells. Chemosphere 37 (2):209-218.

Caballero A, Esteve-Nunez A, Zyltra G, Ramos J (2005a) Assimilation of nitrogen from nitrite and trinitrotoluene in Pseudomonas putida JLR11. J Bacteriol 187 (1):396-399.

Caballero A, Lazaro J, Ramos J, Esteve-Nunez A (2005b) PnrA, a new nitroreductast-family enzyme in the TNT-degrading strain Pseudomonas putida JLR11. Environ Microbiol 7 (8):1211-1219.

Downey S, Ladaa T, Mullendore D (2005) In situ enhanced bioremediation to treat nitroaromatics in groundwater. Federal Facilities Environ J 16 (1):85-96.

Duque E, Haidour A, Godoy F, Ramos J (1993) Construction of a Pseudomonas hybrid strain that mineralizes 2,4,6-trinitrotoluene. J Bacteriol 175 (8):2278-2283.

Esteve-Nunez A, Caballero A, Ramos JL (2001) Biological Degradation of 2,4,6-Trinitrotoluene. Microbiology and Molecular Biology Reviews 65 (3):335-352.

Frische T, Höper H (2003) Soil microbial parameters and luminescent bacteria assays as indicators for in situ bioremediation of TNT-contaminated soils. Chemosphere 50 (3):415-427.

Fuller M, Hatzinger P, Rungmakol D, Schuster R, Steffan R (2004) Enhancing the attenuation of explosives in surface soils at military facilities: combined sorption and biodegradation. Environ Toxicol Chem 23 (2):313-324.

Fuller M, Manning J (1998) Evidence for differential effects of 2,4,6-trinitrotoluene and other munitions compounds on specific subpopulations of soil microbial communities. Environ Toxicol Chem 17 (11):2185-2195.
Fuller M, Manning J (2004) Microbiological changes during bioremediation of explosives-contaminated soils in laboratory and pilot-scale bioslurry reactors. Bioresource Technol 91 (2):123-133.
Fuller M, McClay K, Higham M, Hatzinger P, Steffan R (2010) Hexahydro-1,3,5-trinitro-1,3,5-triazine (RDX) bioremediation in groundwater: Are known RDX-degrading bacteria the dominant players? Bioremediation J 14 (3):121-134.
George I, Eyers L, Stenuit B, Agathos S (2008) Effect of 2,4,6-trinitrotoluene on soil bacterial communities. J Ind Microbiol Biotechnol 35 (4):225-236.
George I, Liles M, Hartmann M, Ludwig W, Goodman R, Agathos S (2009) Changes in soil Acidobacteria communities after 2,4,6-trinitrotoluene contamination. FEMS Microbiol Lett 296 (2):159-166.
Gong P, Gasparrini P, Rho D, Hawari J, Thiboutot S, Ampleman G, Sunahara G (2000) An in situ respirometric technique to measure pollution-induced microbial community tolerance in soils contaminated with 2,4,6-trinitrotoluene. Ecotoxicol Environ Safety 47 (1):96-103.
Hawari J, Beaudet S, Halasz A, Thiboutot S, Ampleman G (2000) Microbial degradation of explosives: biotransformation versus mineralization. Appl Microbiol Biotechnol 54 (5):605-618.
Kutty R, Bennett G (2005) Biochemical characterization of trinitrotoluene transforming oxygen-insensitive nitroreductases from Clostridium acetobutylicum; ATCC 824. Arch Microbiol 184 (3):158-167.
Lenke H, Warrelmann J, Daun G, Hund K, Sieglen U, Walter U, Knackmuss H (1998) Biological treatment of TNT-contaminated soil. 2. Biologically induced immobilization of the contaminants and full-scale application. Environ Sci Technol 32 (13):1964-1971.
Li A, Marx K, Walker J, Kaplan D (1997) Trinitrotoluene and metabolites binding to humic acid. Environ Sci Technol 31 (2):584-589.
McCormick N, Feeherry F, Levinson H (1976) Microbial transformation of 2,4,6-trinitrotoluene and other nitroaromatic compounds. Appl Environ Microbiol 31 (6):949-958.
Meyers S, Deng S, Basta N, Clarkson W, Wilber G (2007) Long-term explosive contamination in soil: Effects on soil microbial community and bioremediation. Soil Sed Contam 16 (1):61-77.
Moe W, Stebbing R, Rao J, Bowman K, Nobre M, da Costa M, Rainey F (2011) Pelosinus defluvii sp. nov., isolated from chlorinated solvent contaminated groundwater, emended description of the genus Pelosinus, and transfer of Sporotalea propionica to Pelosinus propionicus comb. nov. Int J Syst Evol Micr.
Rectanus H, Widdowson M, Chapelle F, Kelly C, Novak J (2007) Investigation of reductive dechlorination supported by natural organic carbon. Ground Water Monitoring & Remediation 27 (4):53-62.
Regan K, Crawford R (1994) Characterization of Clostridium bifermentans and its biotransformation of 2,4,6-trinitrotoluene (TNT) and 1,3,5-triaza-1,3,5-trinitrocyclohexane (RDX). Biotechnol Lett 16 (10):1081-1086.
Saka M (2004) Developmental toxicity of p,p'-dichlorodiphenyl tricholorethane, 2,4,6-trinitrotoluene, ther metabolites and benzo(a)pyrene in Xenopus laevis embryos. Environ Toxicol Chem 23 (4):1065-1073.

Soil Survey Staff (2004) Soil Survey Field and Laboratory Methods Manual. Soil Survey Investigations Report No. 52, Version 4.0. R. Burt (ed.). U.S. Department of Agriculture, Natural Resources Conservation Service.

Tharakan J, Gordon J (1999) Cometabolic biotransformation of trinitrotoluene (TNT) supported by aromatic and non-aromatic cosubstrates. Chemosphere 38 (6):1323-1330.

US EPA (2011a) Emerging contaminants – 2,4,6-trinitrotoluene (TNT) fact sheet. http://www.epa.gov/fedfac/documents/emerging_contaminant_tnt.pdf. Accessed 4/30/2012

US EPA (2011b) National Priorities List. http://www.epa.gov/superfund/sites/npl/. Accessed 11/5/2011

Van Aken B, Godefroid L, Peres C, Naveau H, Agathos S (1999) Mineralization of 14C-U-ring labeled 4-hydroxylamino-2,6-dinitrotoluene by manganese-dependent peroxidase of the white-rot basidiomycete Phlebia radiata. J Biotechnol 68 (2-3):159-169.

Watanabe K, Kodama Y, Harayama S (2001) Design and evaluation of PCR primers to amplify bacterial 16S ribosomal DNA fragments used for community fingerprinting. J Microbiol Methods 44 (3):253-262.

Watrous M, Clark S, Kutty R, Huang S, Rudolph F, Hughes J, Bennett G (2003) 2,4,6-Trinitrotoluene reduction by an Fe-only hydrogenase in Clostridium acetobutylicum. Appl Environ Microbiol 69 (3):1542-1547.

Weisburg W, Barns S, Pelletier D, Lane D (1991) 16S ribosomal DNA amplification for phylogenetic study. J Bacteriol 173 (2):697-703.

Wikström P, Andersson A, Nygren Y, Sjöström J, Forsman M (2000) Influence of TNT transformation on microbial community structure in four different lake microcosms. J Appl Microbiol 89 (2):302-308.

Wilke B, Gattinger A, Fröhlich E, Zelles L, Gong P (2004) Phospholipid fatty acid composition of a 2,4,6-trinitrotoluene contaminated soil and an uncontaminated soil as affected by a humification remediation process. Soil Biology Biochem 36 (4):725-729.

CHAPTER 4: Kinetic and pathway modeling of reductive 2,4,6-trinitrotoluene (TNT) degradation with different electron donors

In preparation for submission

4.1 Authors

Nicole Fahrenfeld, Amy Pruden, Mark Widdowson

4.2 Abstract

Simulation of 2,4,6-trinitrotoluene (TNT) degradation rate and pathway is presented for cultures enriched from historically contaminated sediments undergoing biostimulation by addition of lactate, ethanol, and natural organic matter. Lactate amended microcosms were 1.7 times faster than ethanol amended microcosms and 3.0 times faster than natural organic matter amended microcosms. This is likely due to increased biomass concentration observed for lactate over ethanol over natural organic matter. TNT degradation pathway modeling included determination of branching coefficients representing whether the first reduction of nitro group occurred in the ortho or para position or whether TNT was removed from the aqueous phase (i.e. bound to dissolved organic matter). Branching coefficients were greater for initial reduction of para (17-27% initial TNT concentration) over ortho (3-9% initial TNT concentration) for all test conditions. However, greater degradate recovery and a different (lower para/ortho) ratio was observed for ethanol compared to lactate and un-amended conditions. Given the difference in sorption parameters for degradate isomers, these results suggest that differences in pathway branching stimulated by different electron donors are potentially relevant to long term site models.

4.3 Introduction

2,4,6-trinitortoluene (TNT) is a toxic and recalcitrant contaminant. TNT is a challenging contaminant to remediate in groundwater and existing predictive models applied to contaminated sites all indicate extended times-of-remediation (Robertson et al. 2007; Martel et al. 2008). These modeling studies focused on time-of-remediation for TNT at a field site using first order kinetic losses, but did not report predictions for fate of its degradates. More detailed modeling of TNT degradation pathway and kinetics may be beneficial for understanding the environmental

fate of TNT and better inform remedial actions. TNT biodegradation is particularly complex, as it may be transformed to a wide array of intermediates. TNT degradation generally occurs via a reductive pathway, regardless of whether conditions are aerobic or anaerobic. A commonly observed degradation pathway involves TNT reduction to either 2-hydroxyamino-4,6-diaminonitrotoluenes (2HDANT) or 4-hydroxyamino-2,6-dimainonitrotoluene (4HDANT), then 2-amino-4,6-dinitrotoluene (2ANDT) or 4-amino-2,6-dinitrotoluene (4ADNT), followed by 2,4-diamino-6-nitrotolueune (24DANT) and 2,6-diamino-4-nitrotoluene (26DANT), finally to 2,4,6-triaminonitrotoluene (TAT) (Smets et al. 2007). While its formation is believed to prevent mineralization, TAT is considered a desirable end product because it binds irreversibly to soil (Daun et al. 1998). However, more complex branched pathways have been reported. One commonly observed involves the formation of azoxy dimers (i.e. 2,2',6,6'-tetranitro-4,4'azoxytoluene or 2,4',6,6'-tetranitro,4,2'-azoxytoluene) after intial reductions under aerobic conditions [i.e. (Pavlostathis and Jackson 1999)].

Most previous modeling efforts focused solely on TNT degradation (Pavlostathis and Jackson 1999; Riefler and Smets 2002; Admassu et al. 1998), in which model pathway branching and rates for daughter products were not evaluated. TNT modeling studies have employed pseudo first order degradation kinetics to *Cyanobacterium* in pure culture (Pavlostathis and Jackson 1999) or Michaelis–Menten kinetics to describe TNT reduction by NAD(P)H:Flavin mononucleotide oxidoreductase with inactivation (Riefler and Smets 2002) and *Clostridia bifermentans* in pure culture (Admassu et al. 1998). Previous researchers that addressed modeling the fate of degradates using Monod equations achieved good fit to biomass, TNT, and HADNT concentration versus time data, but were unable to match concentration time data for other daughter products (ADNT and DANT) (Daun et al. 1999). Given the complex network of TNT degradation pathways and the varying sorption parameters and therefore mobilities of intermediates, a comprehensive modeling approach for TNT biodegradation pathways and kinetics is desirable. Recently, a modeling approach was proposed that improved upon previous TNT degradation models by applying the modified Michaelis-Menten kinetics and including downstream products and accounting for pathway branching (Gupta 2011). The model was validated using data from the literature (Daun et al. 1998; Hwang et al. 1998). The model

achieved good fit, in part, by including terms for parent compounds inhibiting degradation of daughter compounds, as others have done to describe growth in pure culture (Park et al. 2002).

Of further interest is a modeling approach that enables evaluation of the effect of various electron donors on kinetics and branching. Several researchers have demonstrated that the addition of electron donors can support TNT biodegradation (Gerlach et al. 1999; Adrian et al. 2003; Adrian and Arnett 2007; Fuller and Manning 2004; Tharakan and Gordon 1999); however, robust comparison of electron donor addition on rate and pathway branching has not previously been examined. Preference for the reduction of the para over the ortho nitro group to amine is expected based on Eh; therefore, more 4ADNT can be expected to form than 2ADNT during the reductive degradation of TNT (Hofstetter et al. 1999). Empirically, a 10:1, preference for reduction of the para over the ortho nitro group has been reported for pure cultures of *E. coli* (Yin et al. 2005). But, observation of 2ADNT as the dominant ADNT has been reported for methanogenic TNT degrading cultures (Hwang et al. 2000) and using contaminated loam soil culture (Robertson et al. 2007). Modeling the results of Hwang et al. (2000) revealed 44% of TNT degraded to 2ADNT and 15% degraded to 4ADNT (the remaining 40% unknown) (Gupta 2011). Understanding TNT pathway branching is useful for modeling of long-term site conditions as bioavailability of the individual isomers for degradation may be influenced by sorption parameters that differ for each isomer. For example, 2ADNT has a 5-10 times higher distribution coefficient (K_d) for illite, kaoline, and montmorillonite (Haderlein et al. 1996; Daun et al. 1998) while 4ADNT has a 1.6 times higher K_d for synthetic organoclay (hexadecyltrimethylammonium bromide with bentonite, used as a potential remedial sorbent) (Upson and Burns 2006). Furthermore, applying a model to representative complex groundwater microbial communities, rather than single model pure cultures, is desirable.

Previously, the effect of electron donor addition on TNT degradation rate using pseudo zero order kinetics and the associated shifts in groundwater microbial communities were demonstrated (Fahrenfeld, in review; see Chapter 3). Here, the recently developed branched kinetic modeling approach (Gupta 2011) is applied to this bench-scale TNT biodegradation study including the ADNT and DANT degradates. Kinetic parameters and the effect of electron donor addition (ethanol, lactate and chemically-extracted natural organic carbon) on degradation rates

and pathway branching are presented here, which may help inform decision making and modeling efforts related to long term remediation of TNT contaminated sites.

4.4 Experimental Methods

4.4.1 Batch microcosm preparation, sampling, analysis

Batch microcosms were prepared as described previously (Fahrenfeld et al., in review; see Chapter 3). Briefly, a reduced sediment TNT-degrading microbial culture was grown using sediment from FNOD in anaerobic media (Adrian et al. 2003) spiked with ~11µM TNT. Analysis was performed on LC with photodiode array detection using a C8 column (Restek) and methanol/water mobile phase, based on the method of Lenke et al. (Lenke et al. 1998) and previously detailed. Once degradation was confirmed, second generation microcosms were prepared using 1:10 dilution of this culture in potentially bioavailable organic carbon (PBOC) extracted from uncontaminated FNOD sediment (Rectanus et al. 2007), 11µM TNT, and either ethanol or lactate were added as electron donors at concentration 100x stoichiometric requirement. Third generation bottles were prepared the same as second generation bottles, in quintuplet, and sampled periodically without sacrifice. Liquid samples were analyzed via EPA Method 8330 for explosives.

4.4.2 Molecular analysis

Aqueous samples (5mL) from the microcosms were filter-concentrated (0.22µm), and filters were preserved at -20°C until DNA extraction. DNA was extracted from preserved filters using FASTSpin Kit (MoBio) following manufacturer instructions. Microbial biomass was approximated by converting 16S gene copies measured using Q-PCR. Serial dilutions of cloned genes (10^8-10^2 gene copies/µL) were used to create standard curves. DNA extracts were diluted 1:50 to reduce inhibition. The dilution chosen based on serial dilutions of select standards and comparing PCR efficiencies. Samples were analyzed in triplicate, with a standard curve and negative control included in each run. The Ribosomal Database Project (Cole et al. 2008) was used to estimate the 5.3 gene copies per cell, based on the microbial community member's median number of 16S gene copies per cell. To convert the number of cells to biomass, a cell size of 0.95fg was assumed (Neidhardt 1996).

4.4.3 Batch sorption isotherms

Batch 48-hr sorption tests were performed using uncontaminated FNOD sediment sampled at 24-25ft-bgs. Briefly, uncontaminated sediment samples were collected from FNOD in May 2010 in polyacteate sleeves using direct push technology (i.e. GeoProbe). Sediment cores were stored at 4C until use then air dried to constant mass, sieved (2 mm), and homogenized. Aliquots were extracted with acetonitrile and analyzed via EPA Method 8330B for explosives to ensure sediment was not contaminated. Sorption isotherms for the FNOD sediment were prepared in triplicate by spiking varying concentrations of TNT, 2ADNT, 4ADNT, or 26DANT (Accustandard, New Haven, CT) into glass vials containing 0.5 g of upgradient FNOD sediment and 1.5 mL Ultrapure (18 mΩ) distilled deionized water. Vials were capped with Teflon-lined septa and allowed to equilibrate, mixing end-to-end on a shaker table. After 48 hr of mixing, vials were centrifuged at 2500 rpm, and the decanted supernatant was analyzed for explosives. The batch sorption experiments were repeated in triplicate for each concentration as described above except the aqueous phase contained 0.08% (v/v) ethanol. The 0.08% (v/v) ethanol represents a concentration four times that added to ethanol amended microcosms and was added to determine if there was any co-solvent effect on sorption parameters.

4.4.4 Modeling and statistical analyses

All modeling was performed in Microsoft Excel using data from the third generation experimental microcosms. Microbial growth parameters were estimated using 16S qPCR data from duplicate microcosms by assuming exponential growth during the early stages of the experiment (from 0hr until 30-34.5hr). Best-fit of the biomass growth parameters was achieved through trial-and-error calibration.

TNT degradation parameters and branching were modeled in Microsoft Excel for each replicate individually to facilitate statistical comparison of the different electron donor test conditions. Degradation rate ($v_{\max}$), half saturation coefficient ($K_{lc,lp}$), and initial TNT concentration were calibrated to the data using Excel's parameter optimization tool, Solver, and where necessary, by trial-and-error, to maximize R^2 between observed and simulated concentration data. The difference between initial measured TNT concentration and initial calibrated TNT concentration was defined as Initially Bound, as described in Section 4.5.1. Branching coefficients for

reductive degradate isomers, defined in Section 4.5.2, were determined by taking the ratio of the maximum 4ADNT or maximum 2ADNT concentration to initial calibrated TNT concentration.

Statistical analyses were performed using R (http://www.r-project.org/). Normality of data was checked using a Shapiro test and equal variance tested using Bartlett test. Given results that were non-parametric with unequal variance, a Kruskal test followed by a pairwise t-test with a Bonferroni correction for multiple comparisons was applied to compare test conditions.

Full simulations, including ADNT and DANT data, were performed for each experimental condition using the mean concentrations of quintuplet microcosms to calibrate parameters for TNT degradation, branching, and daughter product formation and degradation. Proxy 2HADNT and 4HADNT data were manually generated and simulated to achieve fit of downstream daughter products. These manually generated data and the resultant parameter values could not be generated with sufficient consistency to allow for robust comparison across replicates; hence, full simulation was pursued only for the averaged data for each test condition and, thus, these parameters are not statistically evaluated. TNT degradation parameters and branching coefficients were determined as described above using average data. To determine degradation parameters for ADNTs and 24DANT, the same method was applied as for TNT with the addition of inhibition coefficients. Inhibition coefficients were applied for daughter product parents. Additionally, coefficients were included for 4HADNT inhibition on 2HADNT and 2ADNT inhibition on 4ADNT.

4.5 Model Description

4.5.1 Conceptual framework

Modeling of branched reductive degradation pathways requires a framework that allows for simulating when one parent forms multiple daughter products and multiple parents forms a single daughter compound. For TNT reductive degradation, an example of the former branching is when TNT degrades to either 2HADNT or 4HADNT. An example of the latter is that both 4ADNT and 2ADNT can be reduced to form 24DANT. Thus, describing these scenarios requires determination of the stoichiometric relationship between and parent and daughter as

well as a branching coefficient. This branching coefficient will be used to describe what percentage of loss of a parent compound results in formation of a given daughter compound. Branching coefficients can be used to account for irreversible mass balance losses (e.g. losses to sediment matrix, for hydrophobic compounds like TNT). Here, an Initially bound fraction of TNT was determined by allowing initial TNT concentration to be a calibrated model parameter and taking the ratio of initially calibrated TNT to initially measured TNT. A second loss branch was defined as Final Bound, represents the fraction of the mole balance not accounted for in observed degradates. This represents the remainder of the mass balance and was calculated as % Final Bound = 100% - % Initially bound - % 4-branch - % 2-branch.

4.5.2 Mathematical model

The mathematical framework for this model is based on previously presented work (Gupta 2011). A general form of the mass balance on the aqueous phase concentration of the compound lc, C_{lc}^{aq} [ML^{-3}], with a biological source and sink that is subject to sorption can be written:

$$\frac{dC_{lc}^{aq}}{dt} = R_{source,lc}^{bio} - R_{sink,lc}^{bio,EA} - \frac{\rho_b dC_{lc}^{s}}{\theta dt} \qquad \text{Eq (1)}$$

where t is time [T], $R_{source,lc}^{bio}$ is rate of biological formation [ML^{-3}T^{-1}] of lc, $R_{\sin k,lc}^{bio,EA}$ [ML^{-3}T^{-1}] is the rate of biological degradation of lc, ρ_b is the solution bulk density [ML^{-3}], C_{lc}^{s} [ML^{-3}] is the sorbed concentration of lc, and θ porosity [dimensionless]. Assuming sorption is represented using the linear instantaneous isotherm, Eq. 1 can be rearranged as:

$$\left(1 + \frac{\rho_b K_{d,lc}}{\theta}\right)\frac{dC_{lc}^{aq}}{dt} = R_{source,lc}^{bio} - R_{sink,lc}^{bio,EA} \qquad \text{Eq (2)}$$

where K_d is the linear sorption coefficient. To determine the rate ($R_{\sin k,lc}^{bio,EA}$) of loss of a compound, a modified Michaelis-Menten equation was used:

$$R_{sink,lc}^{bio,EA} = \frac{f_{lc} M_{red}}{\theta} v_{lc}^{max,EA} \left(\frac{\overline{C_{lc}}}{K_{lc}^{Ea} + \overline{C_{lc}}}\right) I_{lc,li} I_{lc,lj} \qquad \text{Eq (3)}$$

where f_{lc} is fraction of the microbial population participating in degradation, M_{red} the microbial population density, $v_{lc}^{\max,EA}$ [T^{-1}] is maximum specific rate of degradation, and $\overline{C}_{lc}$ [ML^{-3}] is the effective concentration (defined as the difference between the aqueous phase concentration and

the minimum concentration at which biodegradation occurs), and K_{lc}^{Ea} [ML^{-3}] is the effective half saturation constant. Inhibition was defined as

$$I_{lc,lj} = \prod_{lj}\left[\frac{K_{lc,lj}}{K_{lc,lj}+\bar{C}_{lj}}\right] \qquad \text{Eq (4)}$$

where $\kappa_{lc,lj}$ [ML^{-3}] is the inhibition coefficient for compound lj on compound lc, and $\overline{C}_{lj}$ [ML^{-3}] is the effective concentration for compound lj.

Branching ($\zeta_{lc,lp}^{dau}$) was defined as the product of branching coefficient ($\xi_{lc,lp}^{dau}$), the percent of the parent going to the daughter product, and the stoichiometric coefficient ($\sigma_{lc,lp}^{dau}$) defining the relationship of the parent and daughter (in all cases here, $\sigma_{lc,lp}^{dau}$=1, based on the stoichiometry of the TNT degradation pathway:

$$\zeta_{lc,lp}^{dau} = \xi_{lc,lp}^{dau}\sigma_{lc,lp}^{dau} \qquad \text{Eq (5)}$$

Thus, to define the source of a daughter compound, the sink of the parent compound must be adjusted to account for branching. For the case of a daughter, lc, originating from a single parent, lp, the following equation applies:

$$R_{source,lc,lp}^{bio} = \zeta_{lc,lp}^{dau}R_{sink,lp}^{bio,EA} = \xi_{lc,lp}^{dau}\sigma_{lc,lp}^{dau}R_{sink,lp}^{bio,EA} \qquad \text{Eq (6)}$$

This equation would apply, for example, where 4ADNT is the daughter product of 4HADNT, as it is assumed that formation of an amino group in the para position is the only product of a hydroxylamine group in that position. However, when a single daughter product has multiple parent compounds, as is the case for 24DANT which can be the daughter of both 2ADNT and 4ADNT, instead the sum of branching-adjusted sink terms for each parent contributes to daughter product formation, as described below.

$$R_{source,lc}^{bio} = \sum_{lp}R_{source,lc,lp}^{bio} = \sum_{lp}\xi_{lc,lp}^{dau}\sigma_{lc,lp}^{dau}R_{sink,lp}^{bio,EA} \qquad \text{Eq (7)}$$

4.5.3 Model solution

If one takes the finite difference approximation of Eq. 3 and Eq. 4, the following equation defines the change in concentration due to biodegradation losses in a given time interval (Δt) can be defined as:

$$\Delta C_{lc}^{sink,\Delta t} = min\left\{\frac{v_{lc}^{max,EA} C_{lc}^{t} M_{red} \Delta t}{\left(K_{lc}^{EA}+C_{lc}^{t}\right)\theta} \prod_{lp} \frac{K_{lc,lp}}{K_{lc,lp}+C_{lp}^{t+\Delta t}} \prod_{lj} \left[\frac{K_{lc,lj}}{K_{lc,lj}+C_{lj}^{t+\Delta t}}\right], C_{lc}^{t}\right\} \quad \text{Eq (8)}$$

where f_{lc} was set to one, and inhibition from compound lj is included when appropriate to represent inhibition from a second parent compound or a competing sister compound. Finite difference approximation of Eq. 7 yields an equation describing the change concentration due to biological generation :

$$\Delta C_{lc}^{source,\Delta t} = \sum_{lp} \xi_{lc,lp}^{dau} \sigma_{lc,lp}^{dau} \left(C_{lp}^{t} - C_{lp}^{t+\Delta t}\right) \quad \text{Eq (9)}$$

Substituting E. 8 and 9 into Eq 1 and taking the finite difference approximation, the concentration of any given compound is defined as:

$$C_{lc}^{t+\Delta t} = \Delta t \left[C_{lc}^{t} + \frac{\Delta C_{lc}^{source,\Delta t} - \Delta C_{lc}^{sink,\Delta t}}{\left(1+\frac{\rho_b K_{d,lc}}{\theta}\right)}\right] \quad \text{Eq (10)}$$

Finally, to estimate the microbial growth, bacterial growth was fitted to the following equation for exponential growth:

$$M_{red,t+\Delta t} = M_{red,t0} e^{k(t+\Delta t)} \quad \text{Eq (11)}$$

where $M_{red,t0}$ is the initial TNT-reducing biomass concentration [ML^{-3}], k is the biomass growth rate [T^{-1}], and $M_{red,t+\Delta t}$ is the TNT-reducing biomass concentration [ML^{-3}].

4.6 Results and Discussion

4.6.1 Bacterial Growth

Bacterial growth parameters were estimated using biomass density estimates based on quantification of 16S rRNA genes by qPCR (Table 4.1). Growth parameters were determined using Eq. 11 where the biomass growth rate was obtained from the slope of the semi-log plot of biomass versus time using the first two sampling points. Biomass was modeled as exponential

growth for simplicity. Results of the manually calibrated fit are shown in Fig 4.1. Exponential grow was chosen for simplicity. Initial biomass concentration, $M_{red,t0}$, ranged about an order of magnitude across test conditions and final biomass, $M_{red,t+\Delta t}$, over 2 orders of magnitude with lactate having the greatest and PBOC only with the least for both time points (Table 4.1). The initial difference in biomass was due to the fact that while 2nd generation microcosms were prepared with a 1:10 dilution of the same inoculum, 3rd generation microcosms were prepared using a 1:10 dilution from 2nd generation microcosms which received either lactate, ethanol, or no amendment. Given that microbial growth rate was consistent across test conditions, the difference in the final biomass resulted from differences in initial biomass concentration given that exponential growth was assumed.

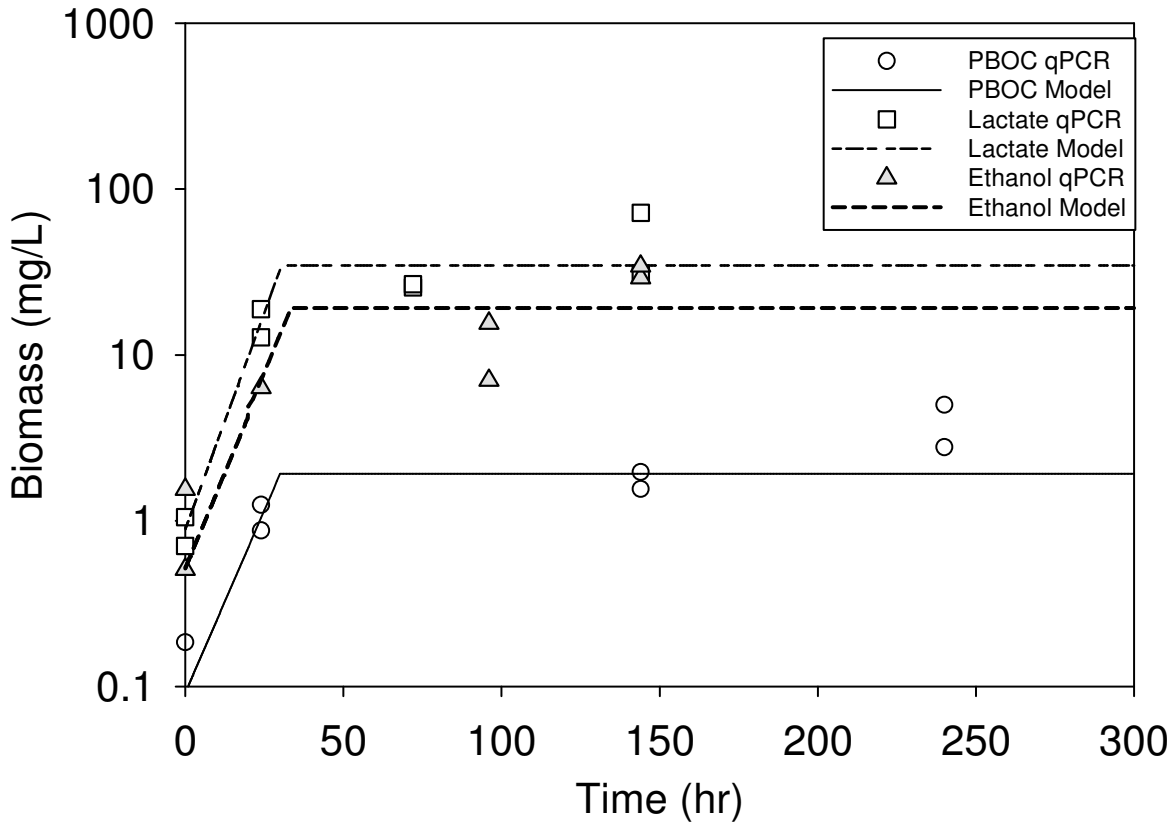

Figure 4.1 Growth curve data and model fit for lactate, ethanol, and unamended microcosms. Biomass was estimated by converting 16s rRNA gene copies assuming an estimated 5.3copies/cell (Cole et al. 2008) and an assumed mass per cell (Neidhardt 1996).

It is acknowledged that 16S rRNA gene measurements did not provide a precise measurement of bacterial cells. Different bacterial species varied in the number of copies of 16S rRNA genes present in their genome [catalogued by (Cole et al. 2008)] so a direct conversion between 16S rRNA genes and cells did not exist. However, given that the microbial communities present in the microcosms were derived from the same inoculum, it was assumed that the average number of 16S rRNA genes per bacterial cell was similar across the microcosms, despite changes observed previously via DGGE (see Chapter 2). Alternatively, direct measurement of TNT-degrading bacteria, rather than total bacteria estimated by 16S rRNA gene measurements, would have been ideal. This has been achieved with some success for other contaminants by quantifying using primers specific to 16s rRNA for known degraders or functional genes known to be vital in its degradation, such as the *tce*A, *bvc*A, and *vcr*A genes involved in dechlorination (Ritalahti et al. 2006). However, such a method has not yet been successfully developed for TNT degraders. Further, a variety of non-specific nitroreductase and oxidoreductase genes (as reviewed by (Roldán et al. 2008)) have been implicated in TNT reduction, which complicates primer design. In this study, previously verified primers for functional genes of bacteria related to those identified in the microbial community were tested [*pnr*A (van Dillewijn et al. 2008), *nit*A and *nit*B (Kutty and Bennett 2005), and *xlp*A (Fuller and Steffan 2008)), but all resulted in non-specific PCR product when applied to mixed samples (results not shown). Previous modeling efforts approximated growth using traditional techniques, like optical density data (Daun et al. 1999), or using pure cultures or with purified enzymes (Pavlostathis and Jackson 1999; Riefler and Smets 2002; Admassu et al. 1998; Park et al. 2002) and applying these reported growth parameters to this inherently different system is likely even less precise. Thus, bacterial growth parameters were reported as estimated values and the lumped $v_{\max} M_{red,t+\Delta t}$ term was used to compare TNT reduction rates.

4.6.2 Modeling: TNT & Branching Coefficients

Modeling of TNT degradation rate was performed for each replicate corresponding to each experimental condition and these values were compared as described above (Table 4.1). The overall rate of degradation, the product of $v_{\max}$ and $M_{red,t+\Delta t}$, was significantly greater for the lactate than the ethanol condition ($p= 3x10^{-5}$) and for both lactate and ethanol than PBOC ($p= 2.4x10^{-7}$ and 0.001, respectively). This trend is in agreement with the pseudo zero order kinetics,

a simplified approach previously assumed for this study (see Chapter 3). Performing robust simulation demonstrates that lactate resulted in higher biomass than ethanol, which had higher biomass concentrations than PBOC background conditions. This trend was expected given that lactate generates more energy (1.11kJ/eeq) than ethanol upon reduction and that both the lactate and ethanol amendments increased the total organic carbon above that provided by the PBOC; thus, lactate provides more favorable conditions for bacterial growth than ethanol which provides more favorable conditions than PBOC alone. The greatest overall degradation rate observed here for lactate was 100x slower than previously reported for (1) a culture derived from municipal wastewater that was fed glucose as a carbon source (Daun et al. 1998; Daun et al. 1999; Gupta 2011) and (2) a methanogenic culture derived from Holston Army Ammunition Plant wastewater fed sludge and glucose (Hwang et al. 2000; Gupta 2011). The slower rate observed for the FNOD derived culture is likely due to the difference in biomass concentration, which for the former study reached a maximum concentration of 41.5mg biomass/L (Daun et al. 1998), 1.2-22 times higher than observed here. Another potential reasons for faster rates observed pervious are inherent differences in microbial community structure and function in wastewater and aquifer sediments. Wastewater bacteria are known quickly degrade a wide variety of contaminants and are faster growing than groundwater bacteria because, by design, they are maintained under peak kinetic conditions.

Table 4.1 Growth parameters applied to all simulations and rate, half saturation constants, and lumped rate parameters determined for simulation of replicates

	μ (hr^{-1}) [a]	$R_{sink,lc}^{bio,EA}$ (mg/L·hr)[b]	$M_{red,t0}$ (mg/L)[c]	$M_{red,t+\Delta t}$ (mg/L)[d]	v_{max} (hr^{-1})[e]	K_s (mg/L)[f]
Ethanol	0.1052	0.027+/-0.054	0.51	19.2	0.0014 +/- 0.0003	0.229+/-0.188
Lactate	0.1205	0.045+/-0.013	0.88	34.6	0.0013 +/- 0.001	0.010+/-0.015
PBOC	0.1015	0.015+/-0.001	0.091	1.92	0.0081 +/- 0.0008	0.279+/-0.261

[a] Estimated microbial growth rate constant, [b] $v_{max} \times M_{red,t+\Delta t}$, [c] Estimated initial microbial density, [d] Estimated final microbial density, [e] Maximum rate of degradation, [f] Half saturation constant

Branching for each electron donor is illustrated in Fig 4.2 and branching coefficients are listed in Table 4.2. The percent of initially bound TNT was determined by allowing the initial TNT concentration to be a model parameter by excluding concentration at the initial time points from calibration and R^2 calculation. The calibrated initial TNT concentration was compared to the initial observed TNT concentration and this percent lost is referred to as initially bound. Initially bound TNT accounted for 13-15% of the total TNT concentration and was not significantly different for different test conditions. This term was included to account for initial TNT drops observed before the inflection point in the degradation curves. Examples of this fitting technique for the averaged data sets is shown in Fig 4.3, for TNT between initial sampling and 24hrs a greater drop in concentration was observed than that seen for 24-48hrs.

Branching for the individual isomers was determined by comparing the maximum observed 2ADNT and 4ADNT to the total maximum observed for TNT. This value was adjusted for initial losses for discussion and reporting in Fig 4.2. The 4-branch (4HADNT followed by 4ADNT) accounted for 17-27% of initial TNT concentration with the highest values observed corresponding to the ethanol amended microcosms. The 2-branch (2HADNT followed by 2ADNT) accounted for 3-9% of the initial TNT concentration, again, with the highest value corresponds with the ethanol amended microcosms. This trend, greater observed 4ADNT than 2ADNT is consistent with previous reports (Yin et al. 2005; Hofstetter et al. 1999). Significantly more TNT followed the 4 than the 2 branch for the ethanol test condition ($p=0.0019$) but differences observed were not significant for lactate or PBOC. Freundlich sorption isotherms ($C_{sorb}=K_f C_{aq}^{n}$) were fit to 2ADNT ($K_f=5.2$, $n=0.38$, $R^2=0.80$) and 4ADNT ($K_f=2.7$, $n=0.65$, $R^2=0.93$). Isotherm results indicate that 2ADNT has slightly greater interactions with the uncontaminated site sediment than does 4ADNT: for the same aqueous phase concentration the corresponding calculated sorbed phase concentration is higher for 2ADNT than 4ADNT (Figure D.1). Matrix spiked PBOC (which was extracted from the uncontaminated sediment), however, revealed greater recovery for 2ADNT (83+/-4%) than for 4ADNT (64+/-6%). Therefore, even by accounting for rapid matrix losses implied by lower matrix spike recoveries for 4ADNT, 4ADNT was likely preferentially produced in the ethanol condition. How potential losses of 2HADNT compare to 4HADNT losses is not known, although rapid losses are expected for both to the PBOC matrix as it is rich in humic acids. Daun et al. (1998) demonstrated that HADNTs

bound irreversibly to humic acids, accounting for mass balance losses in humic acid spiked biotic experiments. Here, no differences were observed in branching coefficients comparing between test conditions for the mole fraction proceeding down the 4 pathway nor the 2 pathway.

The 4:2 branch, defined as maximum observed 4ADNT/maximum observed 2ADNT was 3.1+/-0.2, 6.3+/-1.0, and 5.9+/-2.3 for the ethanol, lactate, and PBOC test conditions, respectively. Therefore, a greater 4:2 branch is seen for PBOC ($p=0.04$) and lactate ($p=0.027$) compared to ethanol, and no difference ($p=1.0$) is observed between PBOC and lactate. Insignificant differences between sorption isotherms created with and without the ethanol spike were observed, in agreement with the general view that completely water miscible solvents like ethanol at v/v fractions less than 1% (here <0.02%) have negligible effect on solubility (Schwarzenbach et al. 2003). Killed controls spiked with ethanol did not exhibit higher concentrations of TNT than the PBOC or lactate killed controls. Therefore, the cosolvent effect was believed to be unlikely for the compounds analyzed. However, HADNTs were not observed nor were sorption isotherms created for these short lived intermediates, therefore, the effect of sorption on ethanol concentration was unknown. It is also possible that differences observed in the ethanol test condition may be microbially-mediated differences. Potential for different

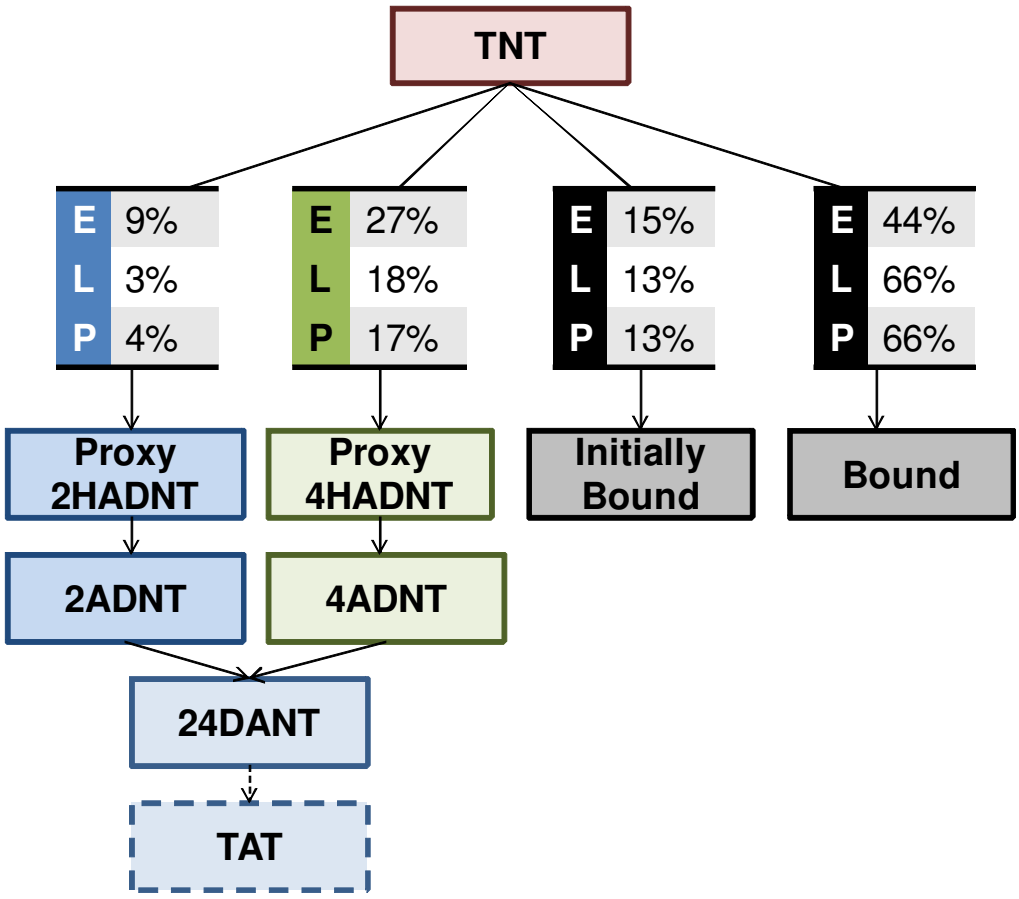

Figure 4.2 Pathway branching, estimated from mole balance for ethanol (E), lactate (L), and PBOC (P) test conditions. Initially bound and bound represent moles lost before TNT degradation and downstream of TNT degradation, respectively. Proxy HADNTs were included in model pathway to account for extended retardation between TNT degradation and ADNT formation.

branching with different microbial communities is apparent in the reported differences in 4:2 branch ratios, 10:1 (Pavlostathis and Jackson 1999) and 0.34 (Hwang et al. 2000), for different bacteria incubated without sediment.

The remainder of the mass balance (100% - % Initially bound - % 4-branch - % 2-branch) was termed Final Bound and represents the fraction of the mole balance not accounted for in observed degradates. This branch made up more of the lactate ($p=0.0012$) and PBOC ($p=0.0066$) branching than it did for ethanol, as more of the initial TNT was observed as 4ADNT and 2ADNT. This may be a result of faster degradation kinetics of the intermediates, preventing retardation from reversible matrix interactions from occurring in the ethanol test condition, as

will be discussed below. Overall the bound fraction (Initially bound + Final Bound) accounts for 59-79% of the initial TNT concentration. It is possible that this bound fraction could represent unidentified products. Although unidentified (ghost) peaks were observed in the HPLC chromatograms, they did not share retention times with previously described degradates for which standards were available (2-nitrotoluene, 3-nitrotoluene, 4-nitrotoluene, nitrobenzene, 2,2',6,6'-tetranitro-4,4'-azoxytoluene, 2,2',6,6'-tetranitro-4,4'-azotoluene, 4,4',6,6'-tetranitro-2,2'azotoluene, 2HADNT, 4HADNT, TAT). However, the observed mass balance losses were not surprising as TNT and its reductive degradates are characterized by strong interactions with dissolved organic matter (Li et al. 1997) and sediment. For example, in the presence 10.3% (w/v) montmorillonite clay, only 10% of initial TNT was observed as degradation products, the rest presumably bound to clay (Daun et al. 1998).

4.6.3 Degradate Modeling

Full degradation path modeling was pursued for average values from replicate microcosms (Fig 4.3). The same approach as detailed above for determining branching coefficients and initially bound was applied to the average data for each experimental condition. The lag between the time point when TNT was first observed to be degrading and when ADNT appeared could not be simulated using inhibition terms. This necessitated the use of proxy 2HADNT and 4HADNT to serve as intermediates. However, these compounds were below detection during the experiment. This is not surprising because low HADNT isomer recovery (<25% initial TNT concentration) has been reported in the presence of 1% w/v humic acid (Daun et al. 1998). Here, the PBOC matrix is rich in humic and fulvic acids, likely higher than the 1%w/v spike previously reported, providing more potential for interference with HADNT quantification. Sorption to humics increases with increasing amino character (Li et al. 1997; Daun et al. 1998; Lenke et al. 1998). Such sorptive losses of degradates have been suggested as a scheme for long term remediation of TNT (Lenke et al. 1998) and demonstrated in various humification schemes (Breitung et al. 1996; Esteve-Nunez et al. 2001; Thorn et al. 2008; Wilke et al. 2004; Fuller et al. 2004; Pennington et al. 1995; Drzyzga et al. 1998).

Formation of 2ADNT and 4ADNT was more rapid than degradation, as seen through the right skew and resultant flattening of these peaks. To model this phenomenon, inhibition terms were

added for 4HADNT inhibiting 2HADNT degradation as well as 2ADNT inhibiting 4ADNT. These terms were justified based on Eh: reducing TNT to 4ADNT is energetically favorable to reduction to 2ADNT (130mV compared to 90mV) whereas reducing 2ADNT to 24DANT (or 26DANT) is energetically favorable to reducing 4ADNT to 24DANT (125mV compared to 85mV) (Hofstetter et al. 1999). Model fit using these inhibition terms was good with root mean square values greater than 0.89 for all ADNT isomers under all test conditions (Supplemental Table 4.2a-c).

TNT degradation was faster than ADNT and DANT degradation, in agreement with what is expected based on reduction potential as well as previous observations (Daun et al. 1999). ADNT isomers were below detection in ethanol (4ADNT 419.5hr, 2ADNT 323.5hr) and lactate (4ADNT and 2ADNT both 419.5hr) microcosms before PBOC microcosms (4ADNT 731hr, 2ADNT 731hr). DANT was below detection first in lactate (611.5hr), followed by ethanol (803.5hr) then PBOC (1019hr) microcosms, following the same trend as observed for TNT degradation.

Only 24DANT was observed to form in this study and it was assumed that all 2ADNT degradation contributed to formation of 24DANT. It is possible that 26DANT was formed and lost to the matrix, but no matrix spike interference was observed for either DANT isomer. Further, the formation of 24DANT is energetically favorable to formation of 26DANT from 2ADNT (Hofstetter et al. 1999),. Thus, for the model, 24DANT had two parent compounds (both ADNT isomers) and separate inhibition coefficients pertaining to each isomer. Degradation beyond DANTs (i.e. TAT) was not quantified.

The model was more sensitive to rate parameters and inhibition coefficients than to half saturation coefficient, this result is consistent with past model sensitivity analyses using similar model formations (Gupta 2011).

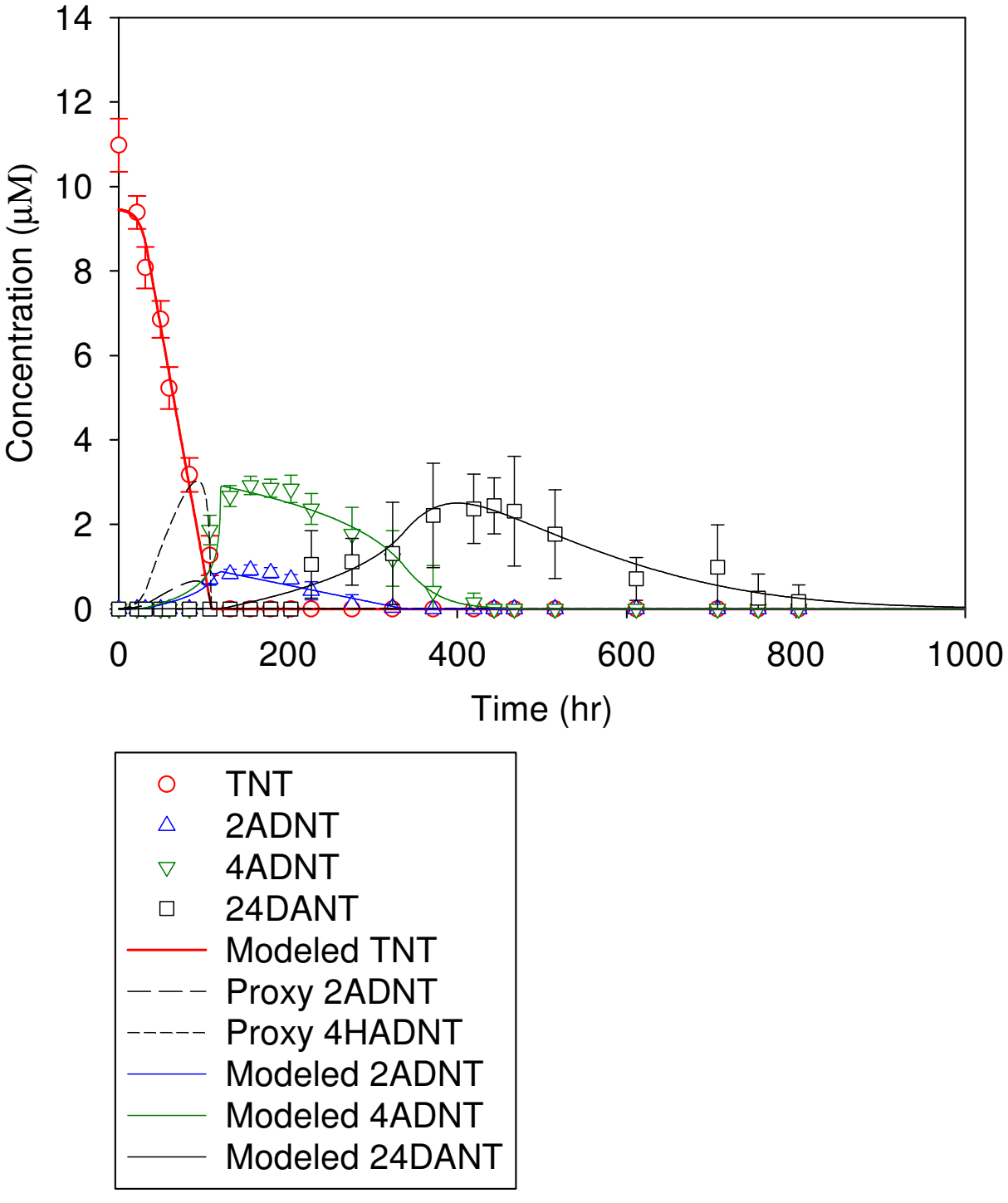
Concentration (µM)
Time (hr)
0
2
4
6
8
10
12
14
0
200
400
600
800
1000
TNT
2ADNT
4ADNT
24DANT
Modeled TNT
Proxy 2ADNT
Proxy 4HADNT
Modeled 2ADNT
Modeled 4ADNT
Modeled 24DANT

a.

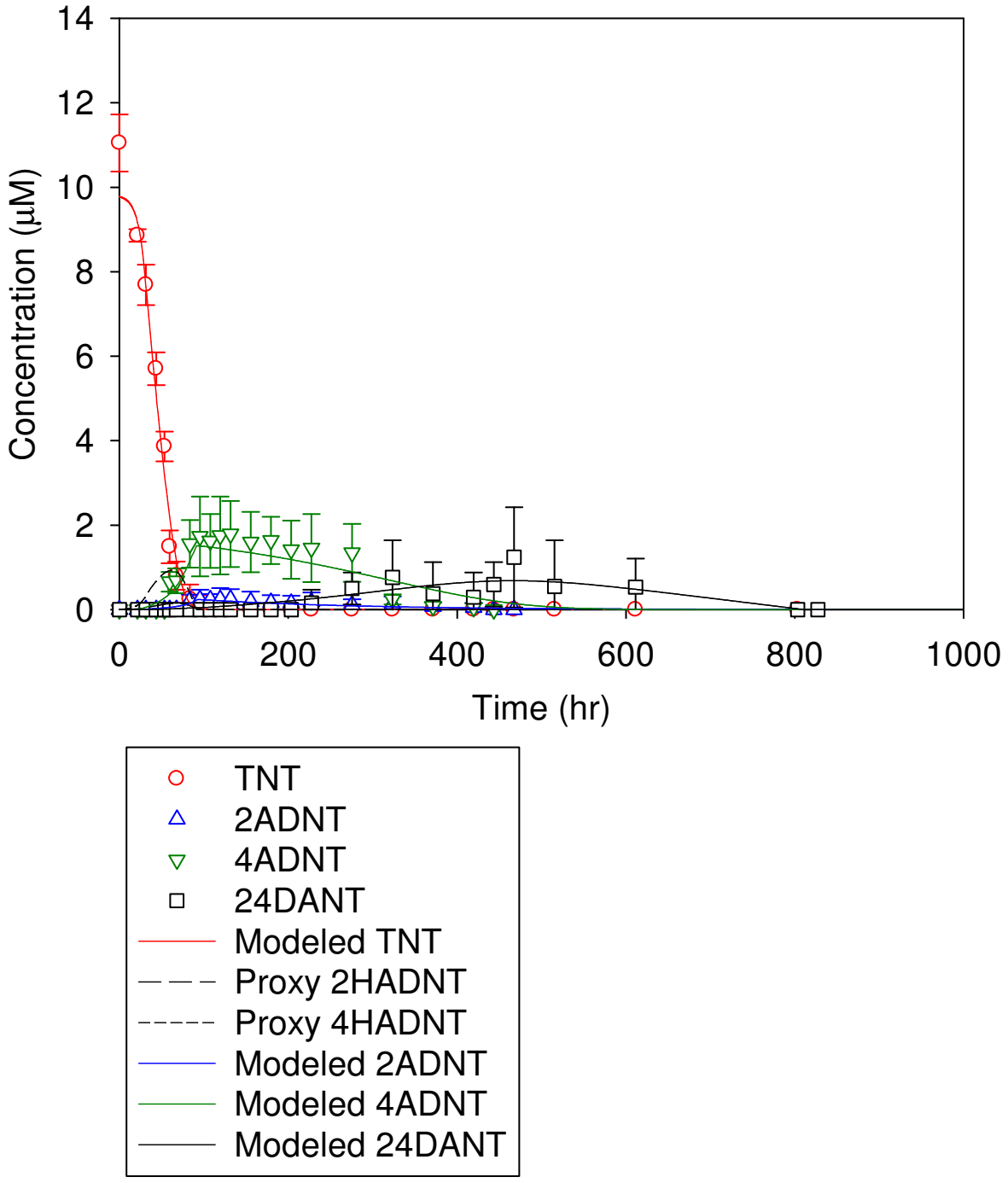
14
12
10
8
6
4
2
0
Concentration (µM)
0
200
400
600
800
1000
Time (hr)
TNT
2ADNT
4ADNT
24DANT
Modeled TNT
Proxy 2HADNT
Proxy 4HADNT
Modeled 2ADNT
Modeled 4ADNT
Modeled 24DANT

b.

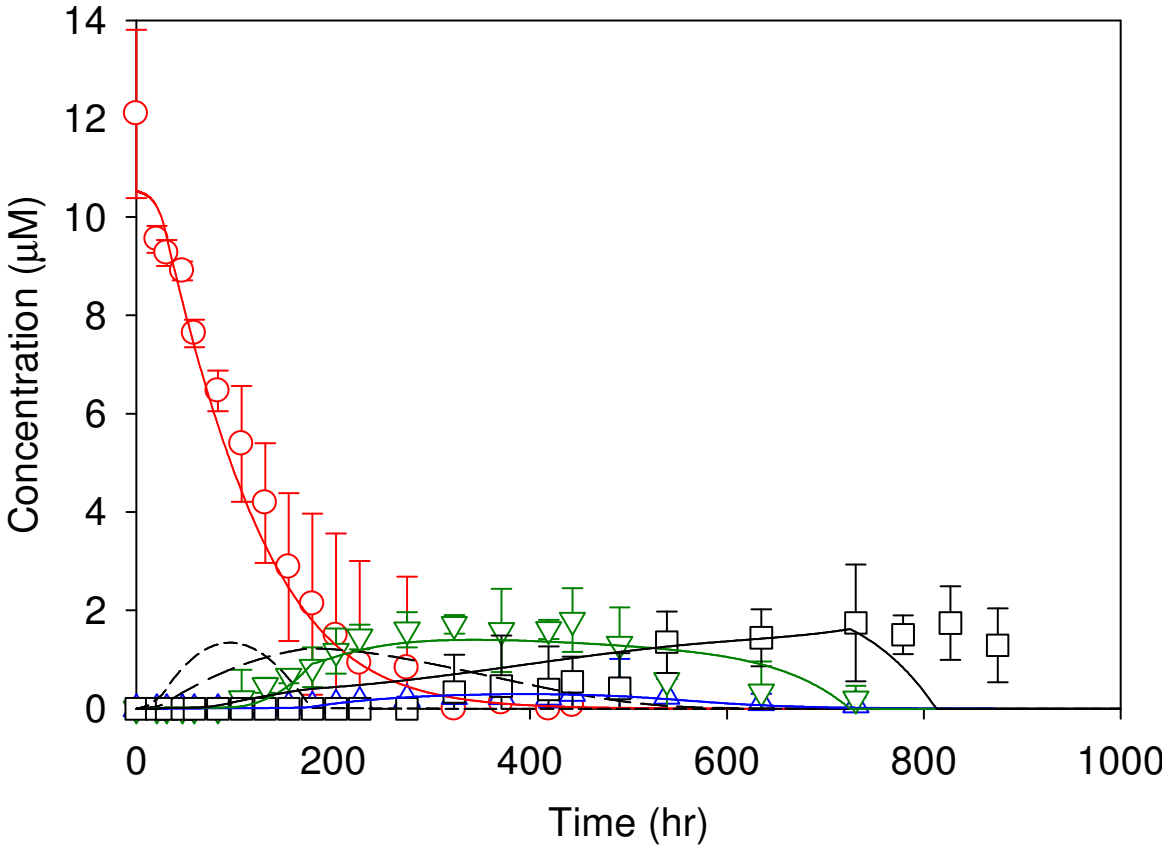

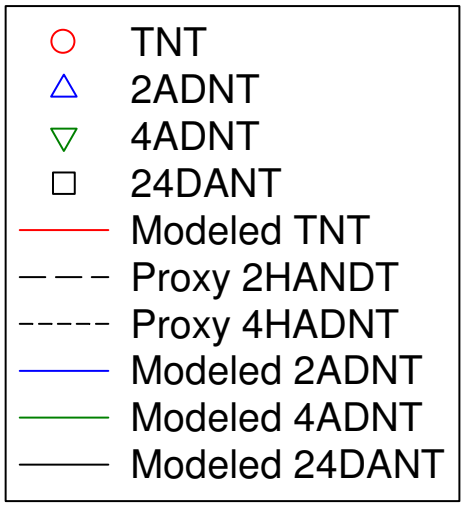

c.

Figure 4.3 Observed and modeled degradation pattern for TNT and its intermediates in microcosms stimulated with a. ethanol, b. lactate, and c. PBOC.

4.7 Conclusions

These modeling results provide the first of kinetic parameter estimation and comparison for a complex TNT-degrading community undergoing stimulation with different electron donors. Introduction of inhibition terms to this previously validated model among degradate siblings (4HADNT inhibiting 2HADNT and 2ADNT inhibiting 4ADNT) was needed to simulate concentration-time curve flattening, providing support to observations that enzymes catalyzing nitroreduction are non-specific and is potentially necessary for long term degradate modeling. A significantly lower 4:2 isomer branching ratio was observed for microcosms stimulated by ethanol compared to lactate and PBOC. This difference is either caused by co-solvent effects on unquantified intermediates (HADNTs) or due to microbially mediated pathway differences. The different pathway branching has implications for long term modeling given different sorptive properties of the two isomers. Overall, these results suggest that when choosing a biostimulant that there is more to consider than simply rate of TNT loss as differences in degradate pathway branching were observed between ethanol and lactate.

4.8 References

Admassu W, Sethuraman AV, Crawford R, Korus RA (1998) Growth kinetics of Clostridium bifermentans and its ability to degrade TNT using an inexpensive alternative medium. Bioremediation J 2:17-28.

Adrian N, Arnett C (2007) Anaerobic biotransformation of explosives in aquifer slurries amended with ethanol and propylene glycol. Chemosphere 66 (10):1849-1856.

Adrian N, Arnett C, Hickey R (2003) Stimulating the anaerobic biodegradation of explosives by the addition of hydrogen or electron donors that produce hydrogen. Water Res 37 (14):3499-3507.

Breitung J, Bruns-Nagel D, Steinbach K, Kaminski L, Gemsa D, von Löw E (1996) Bioremediation of 2,4,6-trinitrotoluene-contaminated soils by two different aerated compost systems. Appl Microbiol Biotechnol 44 (6):795-800.

Cole JR, Wang Q, Cardenas E, Fish J, Chai B, Farris RJ, Kulam-Syed-Mohideen AS, McGarrell DM, Marsh T, Garrity GM, J. M. Tiedje JM (2008) The Ribosomal Database Project: improved alignments and new tools for rRNA analysis. Nucleic Acids Res 37 (D):141-145.

Daun G, Lenke H, Knackmuß H-J, Reuß M (1999) Experimental investigations and kinetic models for the cometabolic biological reduction of trinitrotoluene. Chemical Engineering & Technology 22 (4):308-313.

Daun G, Lenke H, Reuss M, Knackmuss HJ (1998) Biological treatment of TNT-contaminated soil. 1. Anaerobic cometabolic reduction and interaction of TNT and metabolites with soil components. Environ Sci Technol 32 (13):1956-1963.

Drzyzga O, Bruns-Nagel D, Gorontzy T, Blotevogel K-H, Gemsa D, von Low E (1998) Incorporation of 14C-labeled 2,4,6-trinitrotoluene metabolites into different soil fractions after anaerobic and aerobic treatment of soil/molasses mixtures. Environ Sci Technol 32 (22):3529-3535.

Esteve-Nunez A, Caballero A, Ramos JL (2001) Biological Degradation of 2,4,6-Trinitrotoluene. Microbiology and Molecular Biology Reviews 65 (3):335-352.

Fuller M, Hatzinger P, Rungmakol D, Schuster R, Steffan R (2004) Enhancing the attenuation of explosives in surface soils at military facilities: combined sorption and biodegradation. Environ Toxicol Chem 23 (2):313-324.

Fuller M, Manning J (2004) Microbiological changes during bioremediation of explosives-contaminated soils in laboratory and pilot-scale bioslurry reactors. Bioresource Technol 91 (2):123-133.

Fuller ME, Steffan R (2008) Groundwater Chemistry and Microbial Ecology Effects on Explosives Biodegradation - Final Report. SERDP Project ER-1378. http://www.serdp.org/Program-Areas/Environmental-Restoration/Contaminants-on-Ranges/Characterizing-Fate-and-Transport/ER-1378. Accessed 5/1/2012

Gerlach R, Steiof M, Zhang C, Hughes JB (1999) Low aqueous solubility electron donors for the reduction of nitroaromatics in anaerobic sediments. Journal of Contaminant Hydrology 36 (1-2):91-104.

Gupta A (2011) Mathematical modeling of reductive transformation kinetics of branched degradation pathways of groundwater contaminants (Masters Thesis). Virginia Tech, Blacksburg, VA

Haderlein SB, Weissmahr KW, Schwarzenbach RP (1996) Specific adsorption of nitroaromatic explosives and pesticides to clay minerals. Environ Sci Technol 30 (2):612-622.

Hofstetter TB, Heijman CG, Haderlein SB, Holliger C, Schwarzenbach RP (1999) Complete Reduction of TNT and Other (Poly)nitroaromatic Compounds under Iron-Reducing Subsurface Conditions. Environ Sci Technol 33 (9):1479-1487.

Hwang P, Chow T, Adrian NR (1998) Transformation of TNT to Triaminotoluene by Mixed Cultures Incubated Under Methanogenic Conditions. USACERL Technical Report 98/116. http://owww.cecer.army.mil/techreports/Adr_TTT/Adr_TTT.ULI.post.pdf. Accessed 5/1/2012

Hwang P, Chow T, Adrian NR (2000) Transformation of Trinitrotoluene to triaminotoluene by mixed cultures incubated under methanogenic conditions Environ Toxicol Chem 19 (4):836-841.

Kutty R, Bennett G (2005) Biochemical characterization of trinitrotoluene transforming oxygen-insensitive nitroreductases from Clostridium acetobutylicum; ATCC 824. Arch Microbiol 184 (3):158-167.

Lenke H, Warrelmann J, Daun G, Hund K, Sieglen U, Walter U, Knackmuss H (1998) Biological treatment of TNT-contaminated soil. 2. Biologically induced immobilization of the contaminants and full-scale application. Environ Sci Technol 32 (13):1964-1971.

Li A, Marx K, Walker J, Kaplan D (1997) Trinitrotoluene and metabolites binding to humic acid. Environ Sci Technol 31 (2):584-589.

Martel R, Robertson T, Doan M, Thiboutot S, Ampleman G, Provatas A, Jenkins T (2008) 2,4,6-Trinitrotoluene in soil and groundwater under a waste lagoon at the former Explosives Factory Maribyrnong (EFM), Victoria, Australia. Environmental Geology 53 (6):1249-1259.

Neidhardt FC (1996) Escherichia coli and Salmonella: Cellular and Molecular Biology. Vol 1. pp. 14, ASM Press.
Park C, Kim T-H, Kim S, Lee J, Kim S-W (2002) Biokinetic parameter estimation for degradation of 2,4,6-trinitrotoluene (TNT) with Pseudomonas putida KP-T201. Journal of Bioscience and Bioengineering 94 (1):57-61.
Pavlostathis SG, Jackson GH (1999) Biotransformation of 2,4,6–trinitrotoluene in Anabaena sp. cultures. Environmental Toxicology and Chemistry 18 (3):412-419.
Pennington JC, Hayes CA, Myers KF, Ochman M, Gunnison D, Felt DR, McCormick EF (1995) Fate of 2,4,6-trinitrotoluene in a simulated compost system. Chemosphere 30 (3):429.
Rectanus H, Widdowson M, Chapelle F, Kelly C, Novak J (2007) Investigation of reductive dechlorination supported by natural organic carbon. Ground Water Monitoring & Remediation 27 (4):53-62.
Riefler RG, Smets BF (2002) NAD(P)H:Flavin mononucleotide oxidoreductase inactivation during 2,4,6-trinitrotoluene reduction. Appl Environ Microbiol 68 (4):1690-1696.
Ritalahti KM, Amos BK, Sung Y, Wu Q, Koenigsberg SS, Löffler FE (2006) Quantitative PCR Targeting 16S rRNA and Reductive Dehalogenase Genes Simultaneously Monitors Multiple Dehalococcoides Strains. Applied and Environmental Microbiology 72 (4):2765-2774.
Robertson TJ, Martel R, Quan DM, Ampleman G, Thiboutot S, Jenkins T, Provatas A (2007) Fate and transport of 2,4,6-trinitrotoluene in loams at a former explosives factory J Soil Sed Contam 16 (2):159-179.
Roldán MD, Pérez-Reinado E, Castillo F, Moreno-Vivián C (2008) Reduction of polynitroaromatic compounds: the bacterial nitroreductases. FEMS Microbiol Lett 32 (3):474-500.
Schwarzenbach RP, Gschwend PM, Imboden DM (2003) Activity coefficient and solubility in water. In: Environmental organic chemistry, second edition. John Wiley and Sons, Hoboken, New Jersey, p 166.
Smets B, Yin H, Esteve-Nuñez A (2007) TNT biotransformation: when chemistry confronts mineralization. Appl Microbiol Biotechnol 76 (2):267-277.
Tharakan J, Gordon J (1999) Cometabolic biotransformation of trinitrotoluene (TNT) supported by aromatic and non-aromatic cosubstrates. Chemosphere 38 (6):1323-1330.
Thorn KA, Pennington JC, Kennedy KR, Cox LG, Hayes CA, Porter BE (2008) N-15 NMR study of the immobilization of 2,4- and 2,6-dinitrotoluene in aerobic compost. Environ Sci Technol 42 (7):2542-2550.
Upson RT, Burns SE (2006) Sorption of nitroaromatic compounds to synthesized organoclays. Journal of Colloid and Interface Science 297 (1):70-76.
van Dillewijn P, Couselo JL, Corredoira E, Delgado A, Wittich R-M, Ballester A, Ramos JL (2008) Bioremediation of 2,4,6-trinitrotoluene by bacterial nitroreductase expressing transgenic aspen. Environ Sci Technol 42 (19):7405-7410.
Wilke B, Gattinger A, Fröhlich E, Zelles L, Gong P (2004) Phospholipid fatty acid composition of a 2,4,6-trinitrotoluene contaminated soil and an uncontaminated soil as affected by a humification remediation process. Soil Biology Biochem 36 (4):725-729.
Yin H, Wood TK, Smets BF (2005) Reductive transformation of TNT by Escherichia coli: pathway description. Appl Microbiol Biotechnol 67 (3):397-404.

4.9 Supplemental Information

Table 4.2 a. PBOC model parameters and fit for averaged data, b. Ethanol model parameters and fit for averaged data, c. Lactate model parameters and fit for averaged data

a.

	Units	TNT	4HADNT	2HADNT	4ADNT	2ADNT	24DANT
Maximum Rate of Degradation (Vmax)	/hr	1.23×10^{-2}	1.05×10^{2}	25.0	3.82×10^{-3}	7.45×10^{-5}	1.18×10^{-1}
Half Saturation Constant (K_s)	mg/L	1.16	1.00×10^{-3}	1.00×10^{-2}	$1.00\times^{-7}$	1.00×10^{-8}	30.0
Initial Microbial Density (& Other Constants) (A_0)	mg/L			0.091			
Microbial Growth Rate Constant	/hr			0.1015			
Daughter Product Branching Coefficient (d)	--	--	0.17	0.04	0.92	0.92	0.85
Inhibition Coefficient (K_{inh}) Parent	mg/L	--	1.00×10^{-3}	1.00×10^{-3}	5.85×10^{-4}	1.00×10^{-4}	1.58×10^{-3}[a]
Inhibition Coefficient (K_{inh}) Sibling/2nd Parent	mg/L	--	--	1.00[b]	5.19×10^{-3}[c]	--	3.83×10^{3}[c]
R-Square (With Sorption)	--	0.99	--	--	0.94	0.94	0.90

[a]4ADNT, [b]4HADNT inhibition, [c] 2ADNT inhibition

b.

	Units	TNT	4HADNT	2HADNT	4ADNT	2ADNT	24DANT
Maximum Rate of Degradation (Vmax)	/hr	1.20×10^{-3}	10.0	1.00	7.27×10^{-4}	4.19×10^{-5}	1.32×10^{-4}
Half Saturation Constant (K_s)	mg/L	1.00×10^{-3}	1.00×10^{-3}	1.00×10^{-3}	3.75×10^{-1}	1.00×10^{-6}	2.48×10^{-1}
Initial Microbial Density (& Other Constants) (A_0)	mg/L	0.509					
Microbial Growth Rate Constant	/hr	0.1052					
Daughter Product Branching Coefficient (d)	--	--	0.28	0.09	0.92	0.92	0.85
Inhibition Coefficient (K_{inh}) Parent	mg/L	--	1.00×10^{-2}	1.00×10^{-1}	1.00×10^{-4}	1.00×10^{-4}	3.52×10^{-2} [a]
Inhibition Coefficient (K_{inh}) Sibling/2nd Parent	mg/L	--	--	1.00 [b]	1.92×10^{-2} [c]	--	10.5 [c]
R-Square	--	0.99	--	--	0.95	0.90	0.95

[a] 4ADNT, [b] 4HADNT inhibition, [c] 2ADNT inhibition

c.

	Units	TNT	4HADNT	2HADNT	4ADNT	2ADNT	DANT
Maximum Rate of Degradation (Vmax)	/hr	1.65×10^{-3}	70.0	20.0	1.48×10^{-4}	3.62×10^{-6}	1.36×10^{-5}
Half Saturation Constant (K_s)	mg/L	3.78×10^{-1}	1.00×10^{-3}	1.00×10^{-3}	1.55×10^{-1}	1.00×10^{-4}	1.00×10^{-4}
Initial Microbial Density (& Other Constants) (A_0)	mg/L	0.878					
Microbial Growth Rate Constant	/hr	0.1205					
Daughter Product Branching Coefficient (d)	--	--	0.17	0.02	0.92	0.92	0.85
Inhibition Coefficient (K_{inh}) Parent	mg/L	--	1.00×10^{-3}	1.00×10^{-3}	9.93	1.00×10^{-4}	20.1 [a]
Inhibition Coefficient (K_{inh}) Sibling/2nd Parent	mg/L	--	--	$1.00\times10^{-}$ [1b]	1.00×10^{-2} [c]	--	1.22 [c]
R-Square (With Sorption)	--	0.99	--	--	0.89	0.92	0.71

[a]4ADNT, [b]4HADNT inhibition, [c] 2ADNT inhibition

CHAPTER 5: CONCLUSIONS

TNT is a widespread, toxic, and recalcitrant contaminant. Despite the fact that biostimulation by electron donor addition is known to promote biodegradation and is being applied at field sites, little is known about (1) the effect of different electron donors on biodegradation rate and pathway in historically contaminated sediments nor (2) what changes in the microbial community are taking place during stimulation. This research aimed to address these knowledge gaps, and in addition, to improve methods for determining bioavailability through improved models of kinetic desorption in two historically contaminated sediments. Better understanding of bioavailability and biostimulation should help guide remediation and predictive modeling for contaminated aquifers. Contributions of this work to broader understanding of the fate of TNT in historically contaminated sediments include:

- ***First-order desorption rate parameters for a historically TNT contaminated sediment and surface soil using two different approaches at the first order, non-linear model.*** Two first-order models for kinetic desorption were evaluated for the purpose of predicting the long-term release of TNT from a saturated zone source area. While one model (Model 1) is widely used in the literature, and the second model (Model 2) is widely used reactive transport modeling software (MT3DMS and SEAM3D), this work represents the first systematic comparison of the two approaches. In addition, Model 2 was updated to incorporate the Freundlich isotherm. Parameter values and fit were evaluated for both models, demonstrating that while both performed comparably, Model 2 may represent a better behaved and bounded approach. Further, rate values corresponding to historically contaminated sediments were provided, rather than lab contaminated sediments, which are more relevant to site conditions.

- ***First study of biostimulation with historically contaminated aquifer sediment derived microbial community.*** Previous biostimulation studies were performed with enrichment cultures derived from uncontaminated sediment or wastewater. Applying electron donor studies across enrichment cultures derived from different sources is problematic as the community structure is likely disparate. Here, a historically contaminated sediment

derived enrichment culture was grown and was demonstrated to be representative of the bacterial community in the contaminated aquifer. Comparing electron donors, lactate was shown to stimulate faster TNT degradation than ethanol and PBOC.

- ***First modeling of biostimulation of TNT-acclimated community***. Degradation rates for Lactate > Ethanol > PBOC, and estimated parameters are presented. An initial drop in TNT concentration before degradation of TNT was observed and simulated by allowing initial TNT to be an adjustable model parameter. The difference between TNT observed at 0hr and the model parameter for initial TNT concentration was identified as the Initially Bound portion of TNT. Branching coefficients were defined to calculate the amount of TNT forming degradates (4HADNT and 2ADNT) as well as that lost to the dissolved organic matter in the matrix (Bound). Retardation could not account for the lag between TNT disappearance and ADNT formation and thus proxy-HADNT intermediates were included in the simulation. Lag between degradate (2ADNT, 4ADNT, and 24DANT) appearance and loss was simulated by adding in inhibition terms for competing isomers. Interestingly, different branching (more 2ADNT relative to 4ADNT) and greater degradate recovery than for observed for other test conditions was achieved for biostimulation with ethanol. This result implies that there may be more to consider than simply TNT degradation rate when choosing a biostimulant.

- ***Application of DGGE to demonstrate distinct changes in microbial community upon electron donor addition.*** The structure of a bacterial community, grown from an enrichment derived from moderately contaminated sediment, approached the structure present at heavily contaminated sediment. This suggests that TNT drives microbial communities more than the biostimulant. Different bacteria were shown to dominate under stimulation with different electron donors, for example the predominance of *Pelosinus* in cultures stimulated by lactate. Comparing individual test conditions across time, it is apparent that *Pseudomonas* grew in each condition. The strain obtained in pure culture was able to rapidly degrade TNT. Another candidate degrader identified was *Pelosinus*, which has been found at another biostimulated munitions contaminated site.

This result is potentially useful in determining bacterial signatures of biodegradation and for future functional gene design, as published functional gene primers did not work with our mixed culture.

Finally, the study site used for this research benefited from the work.

- ***Demonstration of feasibility of TNT biodegradation and biostimulation through electron donor addition for the FNOD site.*** FNOD remains on the NPL and the work presented here served as a feasibility study that site decision makers can use to help inform the remedial design and remedial action at the site. This research clearly suggests that lactate and possibly ethanol could serve as biostimulants to the TNT-degrading population of microorganisms present in the surficial aquifer at the TNT Area. Integration of results of this research into a site model for the fate and transport of TNT showed promising results in terms of reducing the TNT plume footprint and accelerating time of remediation. This involved increasing the rate of TNT biotransformation in the source zone. At the field scale, this would be achieved through the combination of biostimulation and bioaugmentation. In this study it was demonstrated that TNT degraders at FNOD can be cultured and enriched for this purpose and rates of biotransformation can be increased with the addition of an electron donor. Bioaugmentation provides a means to overcome limitations of a biostimulation-only approach by artificially boosting the active enzyme concentration needed to push contaminant concentrations beyond the minimum threshold.

Future research directions based on this work are suggested to include:

- ***Comparison of batch/column first order desorption rates to those present in calibrated site models.*** Being able to independently determine first-order model parameters is potentially useful at newly discovered sites where there is a lack of sufficient sampling history to calibrate models for making long term predictions of time-of-remediation. Thus, validation of the first order model with hydrophobic compounds at the field scale

and comparison of the rate coefficients to those observed at the bench scale is necessary if this model will continue to be applied.

- ***Pilot study of electron donor addition at FNOD***. The bench scale biostimulation study suggests that electron donor addition of either lactate or ethanol may increase biodegradation rates in-situ. Recommendations for next steps include a pilot test in the source zone at the TNT Area combined with updates to the solute transport model. The purpose of the pilot project would be to optimize biostimulation and bioaugmentation as a remediation strategy to shrink and manage the TNT plume at FNOD through accelerated attenuation.

- ***Identification of molecular markers for monitoring TNT biodegradation in-situ.*** This work highlighted the fact that currently known qPCR primers for nitroreductase genes are not general enough for widespread application. However, here there were several candidate degraders identified and this information can aid in the design of general qPCR primers for functional genes or primers specific for bacteria potentially unique to reductive degradation, for example, *Pelosinus.*

APPENDIX A. Supplemental FNOD site background characterization

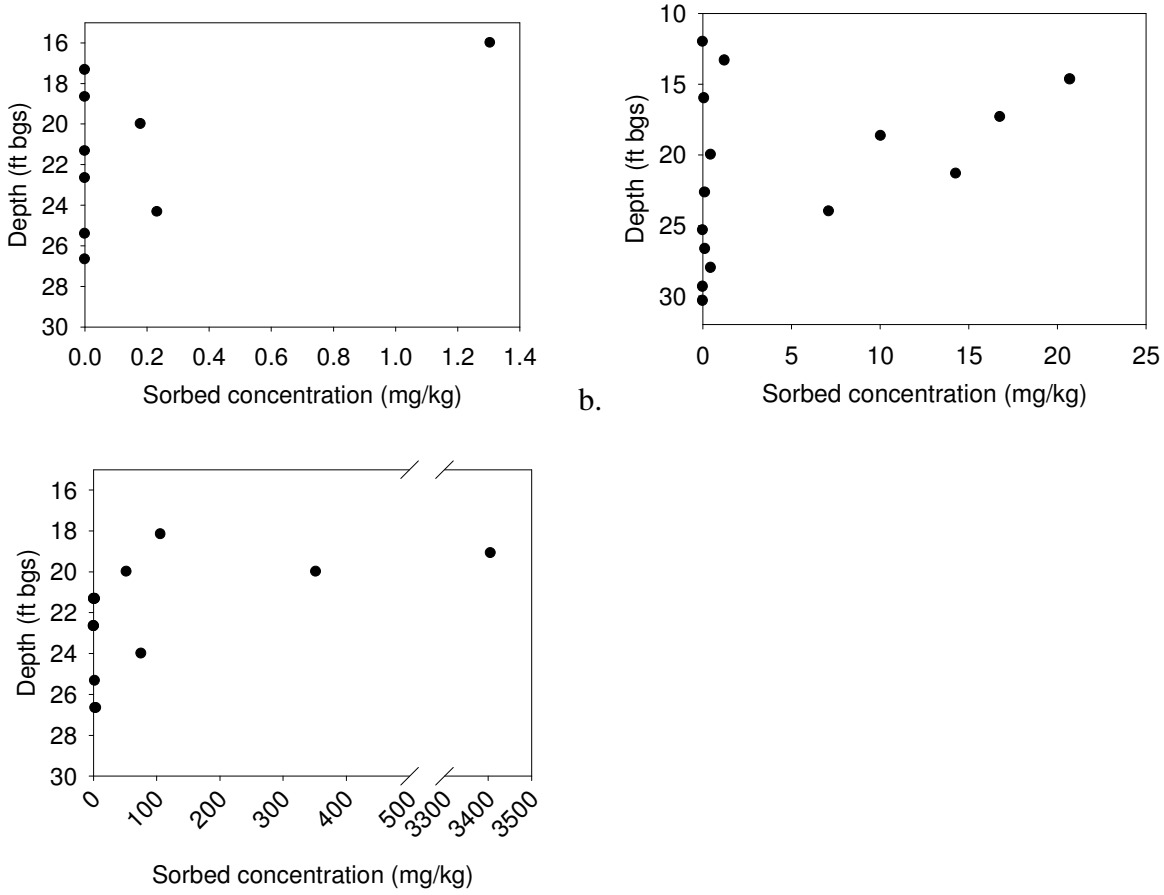

Figure A.1 Sorbed TNT concentrations for a. Uncontaminated column, b. Well 7, c. Well 18.

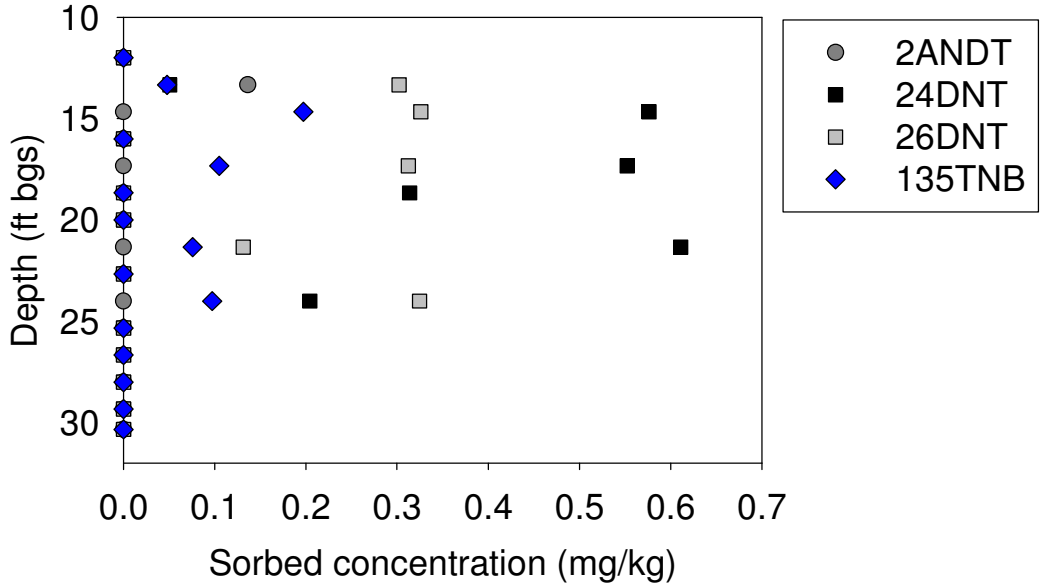

a.

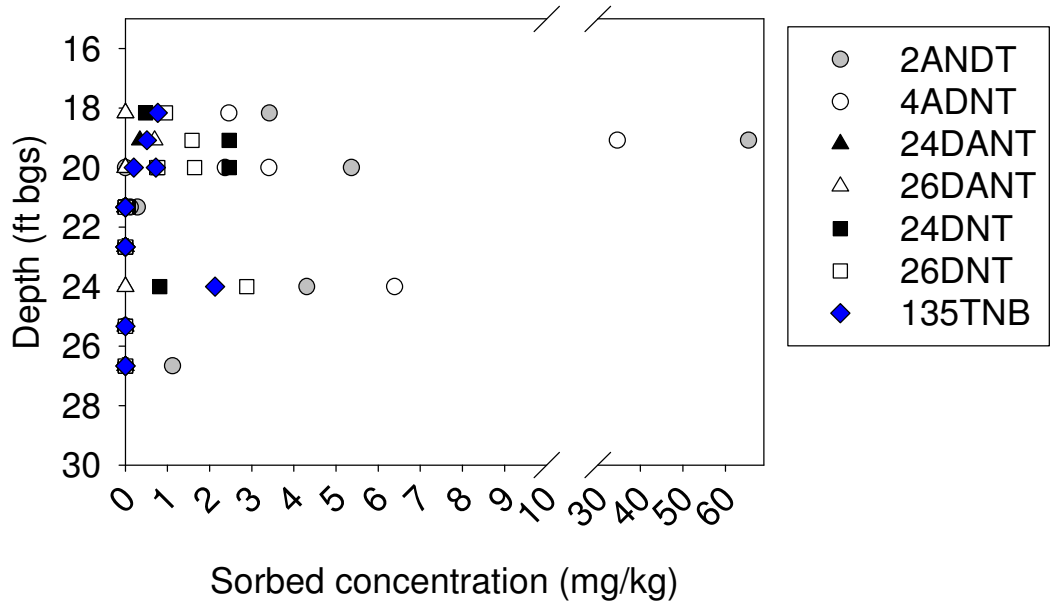

b.

Figure A.2 Sorbed co-contaminant concentrations for a. Well 7 and b. Well 18.

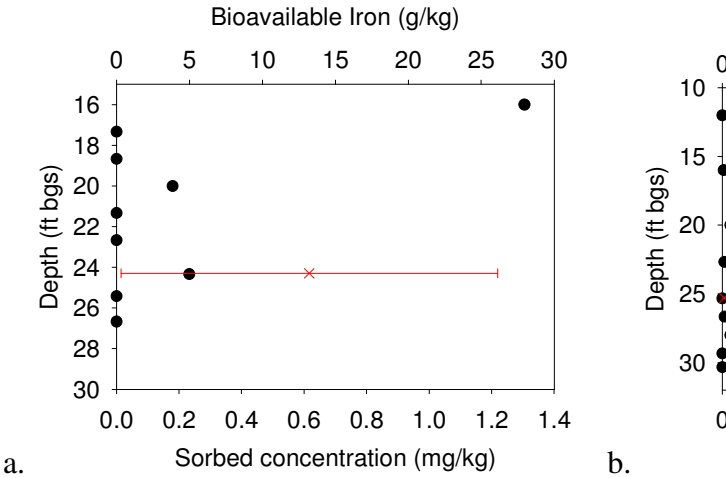

a.

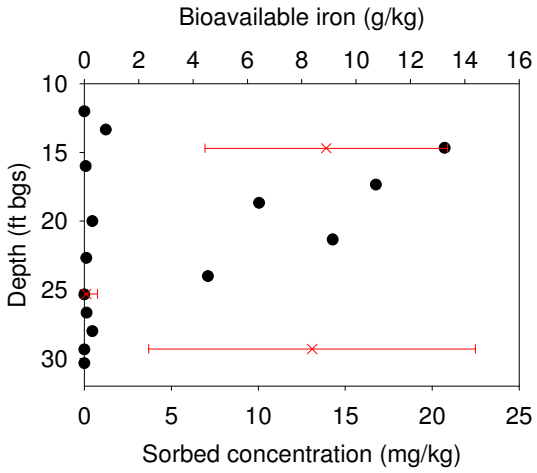

b.

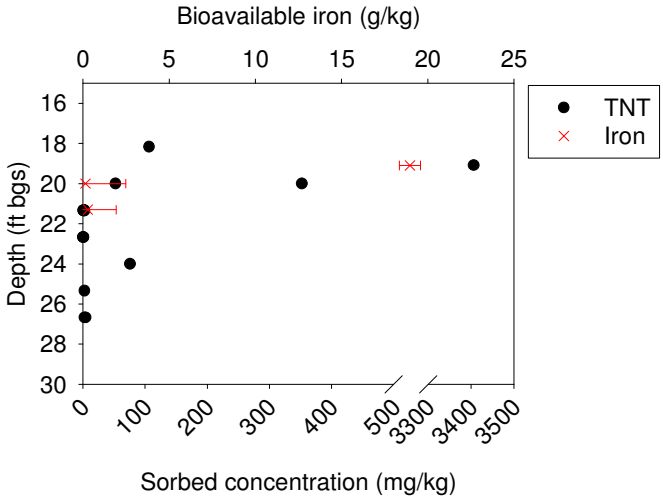

c.

Figure A.3 Bioavailable iron test results for a. Uncontaminated, b. Well 7, c. Well 18.

APPENDIX B. Supplemental desorption results

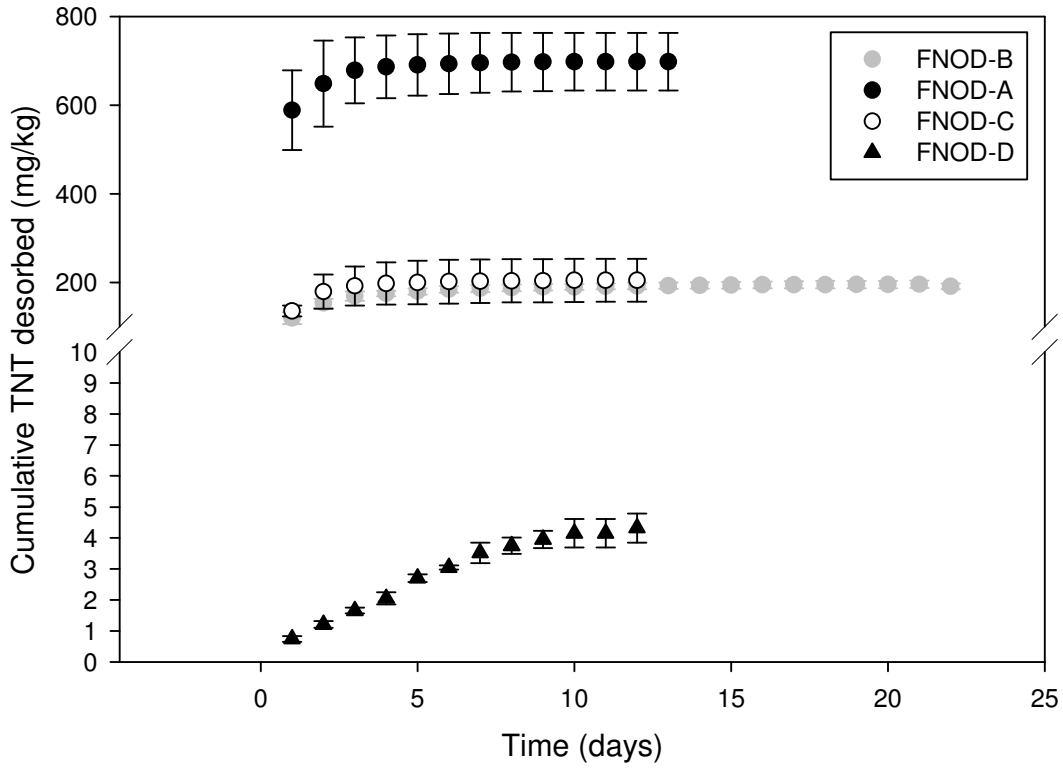

Figure B. 1 Batch desorption cumulative TNT desorbed with time.

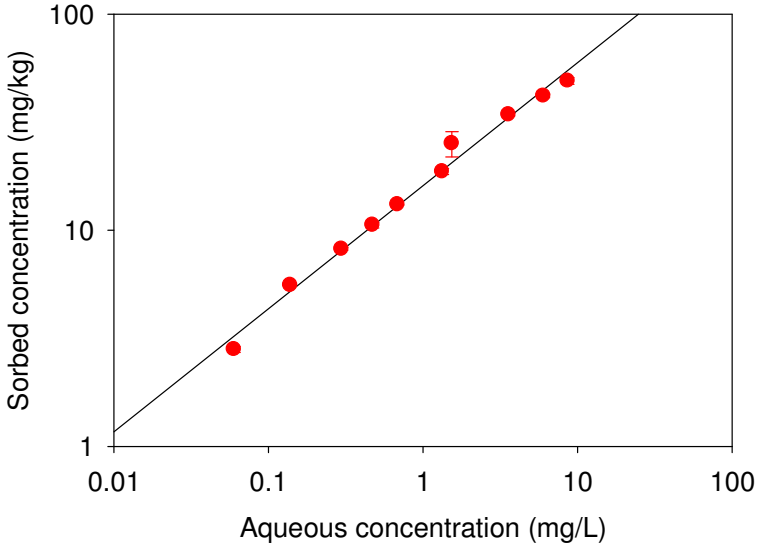

Figure B.2 Freundlich sorption isotherm for TNT

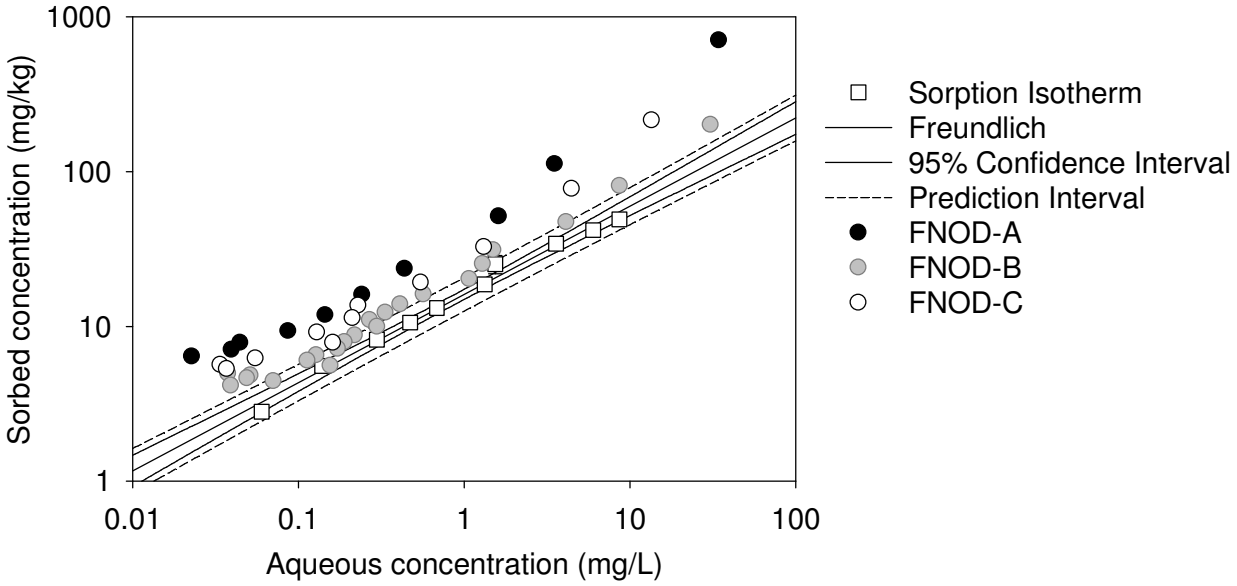

Figure B.3 Combined desorption isotherm and batch desorption isotherm.

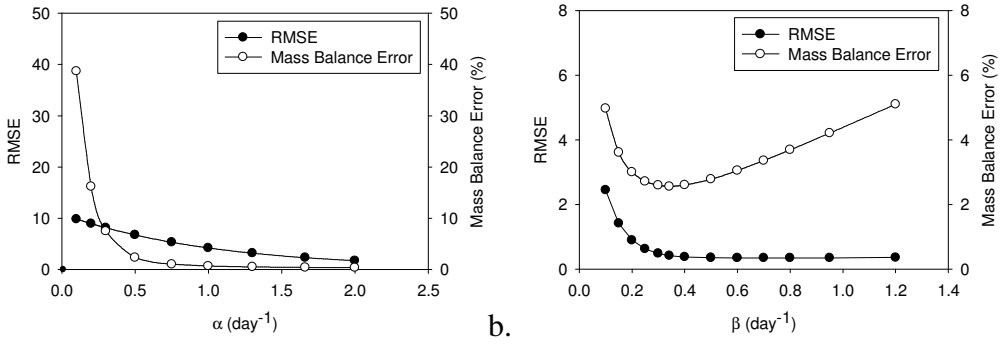

a. b.

Figure B.4 RMSE and mass balance error for a range of mass transfer coefficients for FNOD-A sediment using a. Model 1 and b. for Model 2.

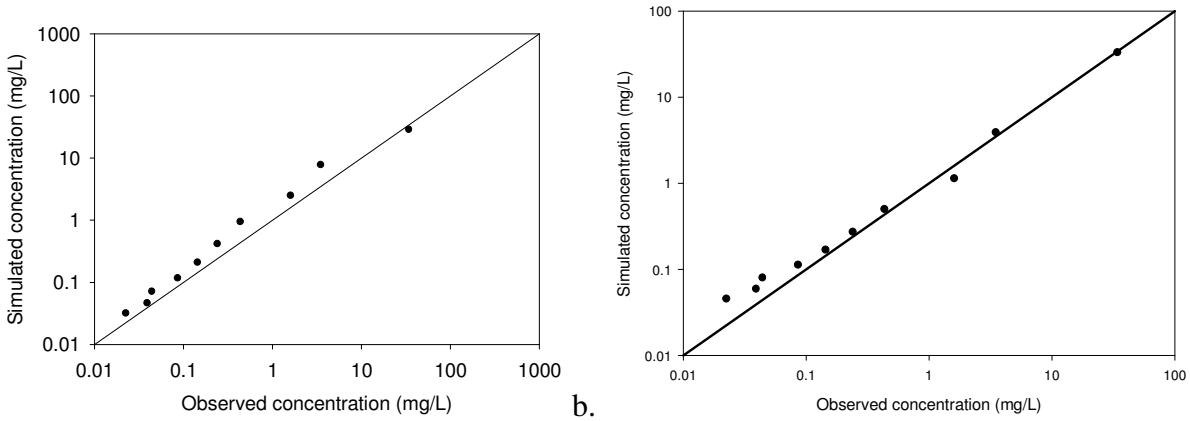

a. b.

Figure B.5 Comparison of simulated and observed aqueous phase concentration for FNOD-A sediment using a. Model 1 and b. for Model 2.

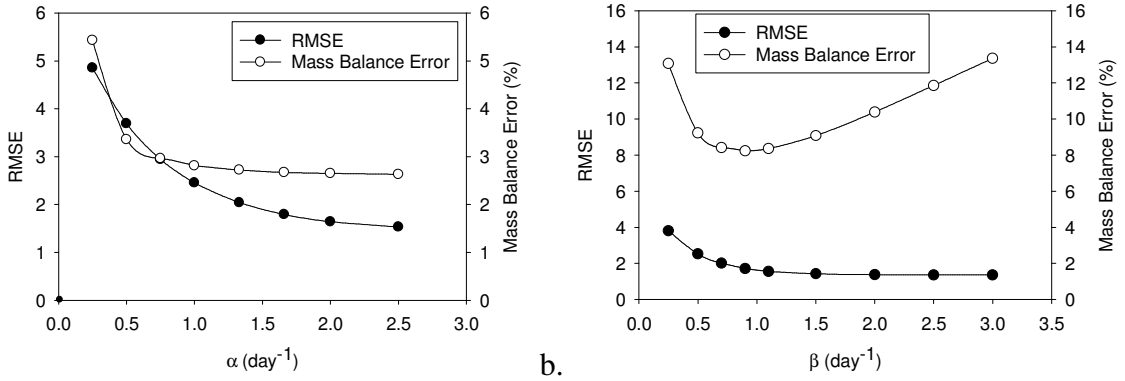

a. b.

Figure B.6 RMSE and mass balance error for a range of mass transfer coefficients for FNOD-B sediment using a. Model 1 and b. for Model 2.

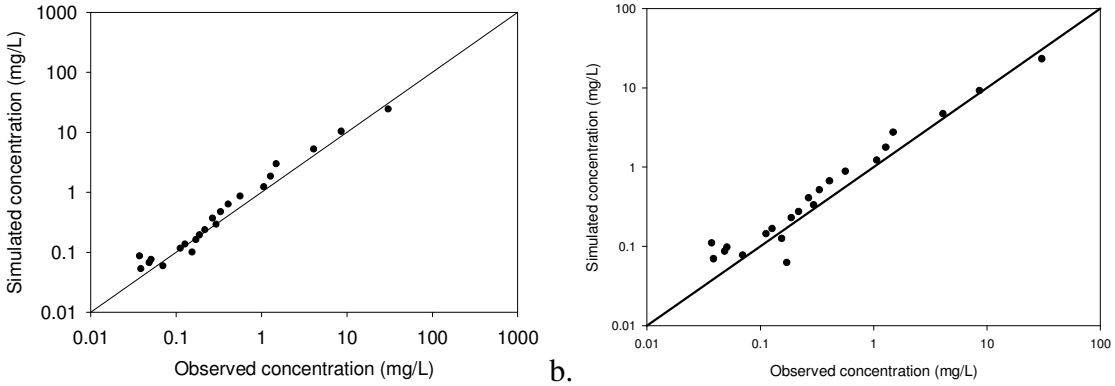

a. b.

Figure B.7 Comparison of simulated and observed aqueous phase concentration for FNOD-B sediment using a. Model 1 and b. for Model 2.

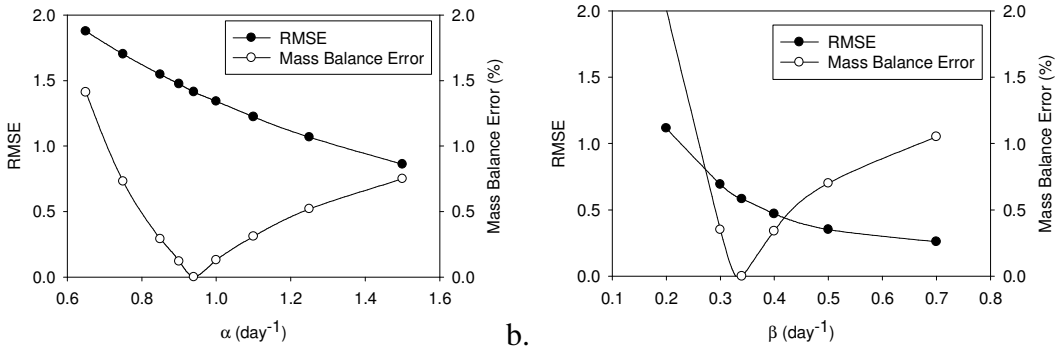

a. b.

Figure B.8 RMSE and mass balance error for a range of mass transfer coefficients for LAAP-B sediment (Sellm and Iskandar 1994) using a. Model 1 and b. for Model 2.

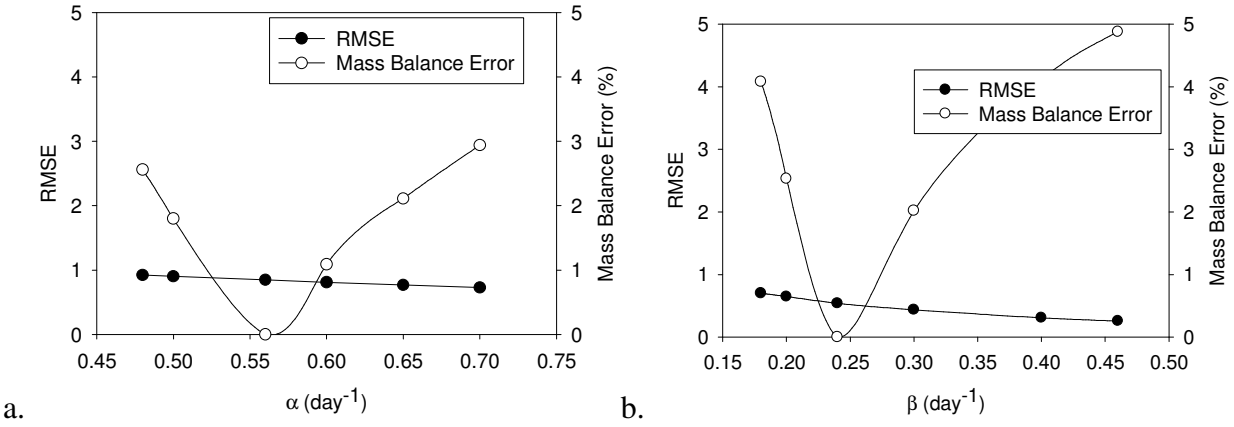

Figure B.9 RMSE and mass balance error for a range of mass transfer coefficients for LAAP-B sediment (Sellm and Iskandar 1994) using a. Model 1 and b. for Model 2.

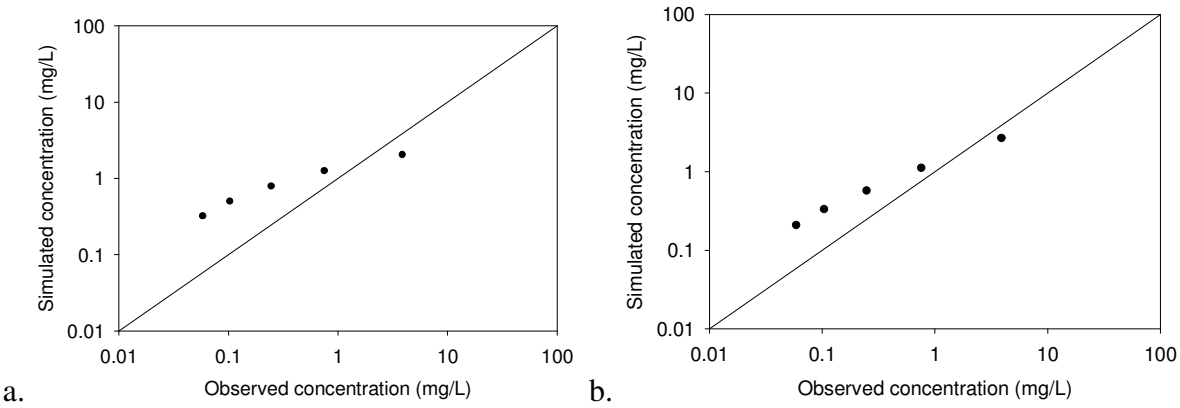

Figure B.10 Comparison of simulated and observed aqueous phase concentration for LAAP-B sediment (Sellm and Iskandar 1994) for LAAP-B sediment using a. Model 1 and b. for Model 2.

B.1 References

Sellm HM, Iskandar IK (1994) Sorption-Desorption and Transport of TNT and RDX in Soils. U.S. Army Corps of Engineers Cold Regions Research & Engineering Laboratory. Report 944-7.

APPENDIX C. Supplemental biodegradation results

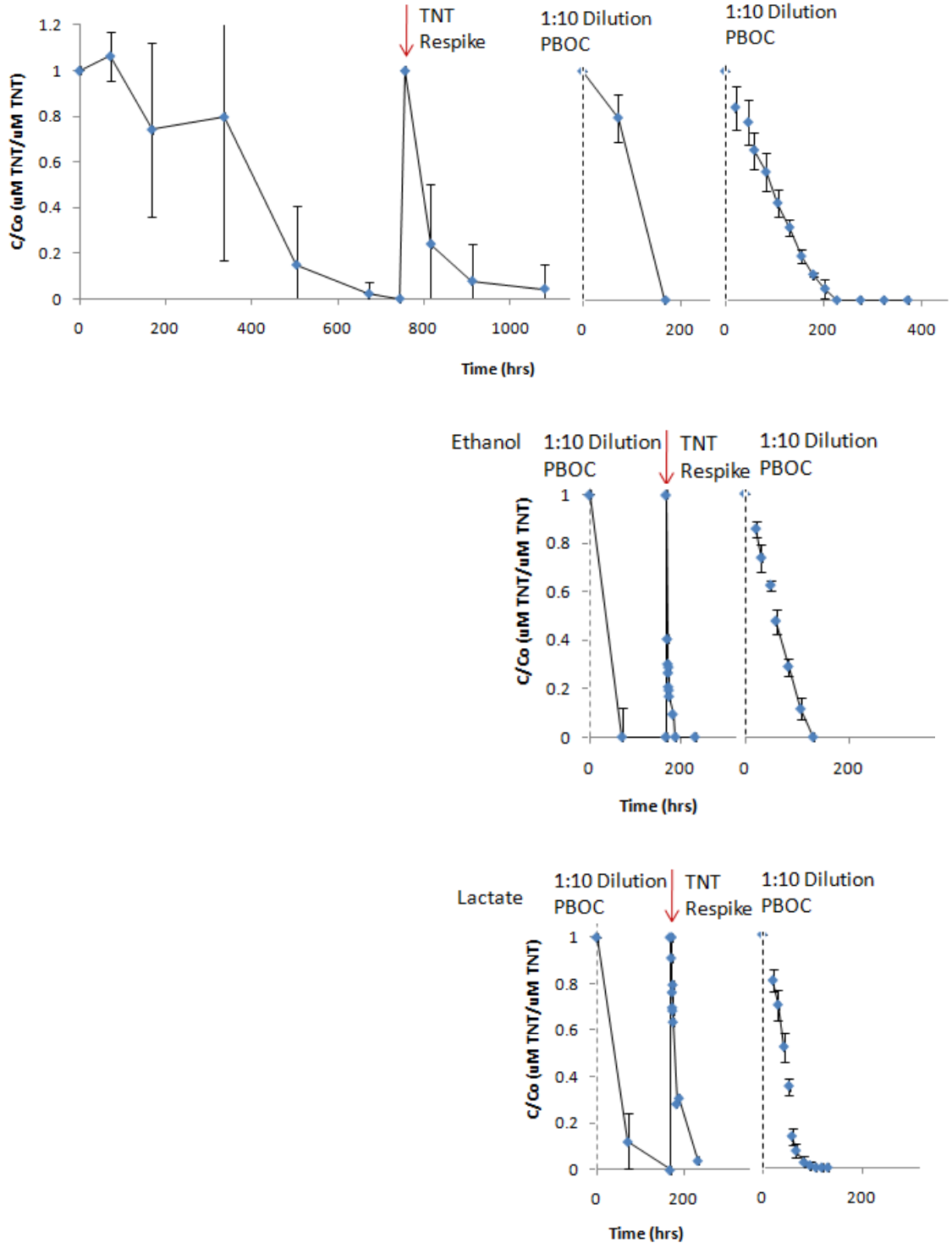

Figure C.1 Evidence of enrichment culture.

a. 

b. 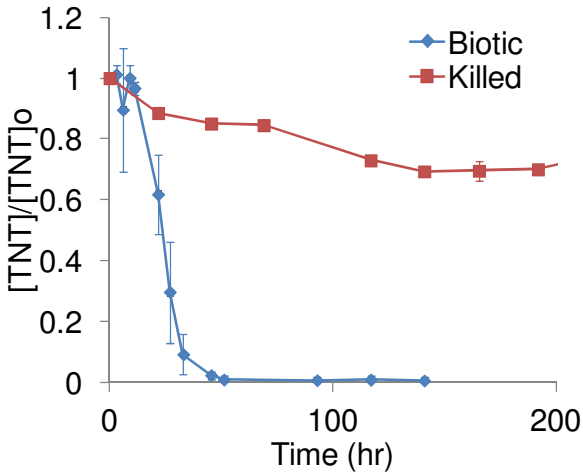

Figure C.2 Pseudomonas pure culture plate and TNT degradation

Table C.1 Rate constants and R^2 values corresponding to zero, first, and second order modeling of microcosms stimulated with different electron donors

		Zero Order[1]		*First Order*[2]		*Second Order*[3]	
Test condition	***Replicate ID***	k_0	R^2	k_1	R^2	k_2	R^2
Lactate	a	-1.3×10^{-1}	0.94	-4.3×10^{-2}	0.83	3.1×10^{-2}	0.53
	b	-1.5×10^{-1}	0.95	-3.4×10^{-2}	0.78	1.1×10^{-2}	0.58
	c	-1.5×10^{-1}	0.95	-4.8×10^{-2}	0.73	3.3×10^{-2}	0.45
	d	-1.2×10^{-1}	0.91	-3.6×10^{-2}	0.91	1.9×10^{-2}	0.72
Ethanol	a	-9.4×10^{-2}	0.98	-2.2×10^{-2}	0.90	7.0×10^{-3}	0.68
	b	-9.0×10^{-2}	0.98	-2.3×10^{-2}	0.88	9.1×10^{-3}	0.64
	c	-8.5×10^{-2}	0.98	-1.9×10^{-2}	0.94	5.3×10^{-3}	0.80
	d	-8.4×10^{-2}	0.99	-2.1×10^{-2}	0.90	6.9×10^{-3}	0.69
	e	-8.2×10^{-2}	0.98	-1.4×10^{-2}	0.89	3.1×10^{-3}	0.73
PBOC	a	-5.6×10^{-2}	0.99	-1.3×10^{-2}	0.93	3.9×10^{-3}	0.72
	b	-5.1×10^{-2}	0.98	-1.4×10^{-2}	0.91	5.9×10^{-3}	0.64
	c	-5.4×10^{-2}	0.95	-1.3×10^{-2}	0.94	4.6×10^{-3}	0.65
	d	-2.6×10^{-2}	0.89	-1.0×10^{-1}	0.75	4.8×10^{-3}	0.66
	e	-4.8×10^{-2}	0.98	-1.1×10^{-2}	0.92	3.7×10^{-3}	0.76

[1] k_0 is the slope found plotting Concentration of TNT versus time (hrs), [2] k_1 is found plotting ln(TNT concentration) versus time (hrs), [3] k_2 is the slope found by plotting 1/(TNT concentration) versus time.

APPENDIX D. Supplemental kinetic modeling results

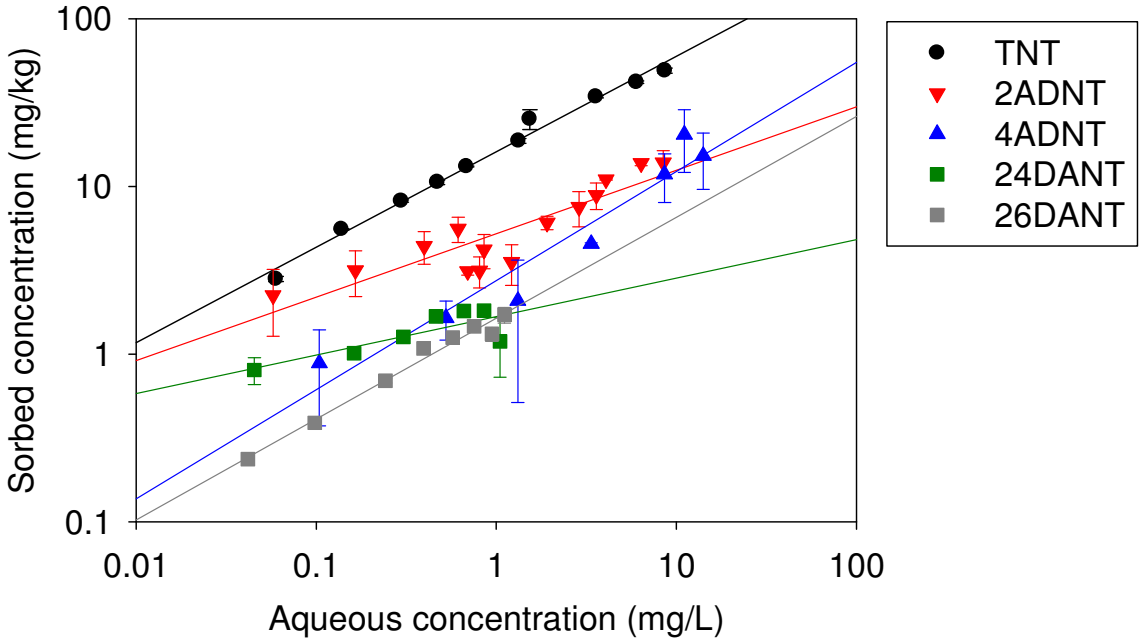

Figure D. 1 Freundlich sorption isotherms

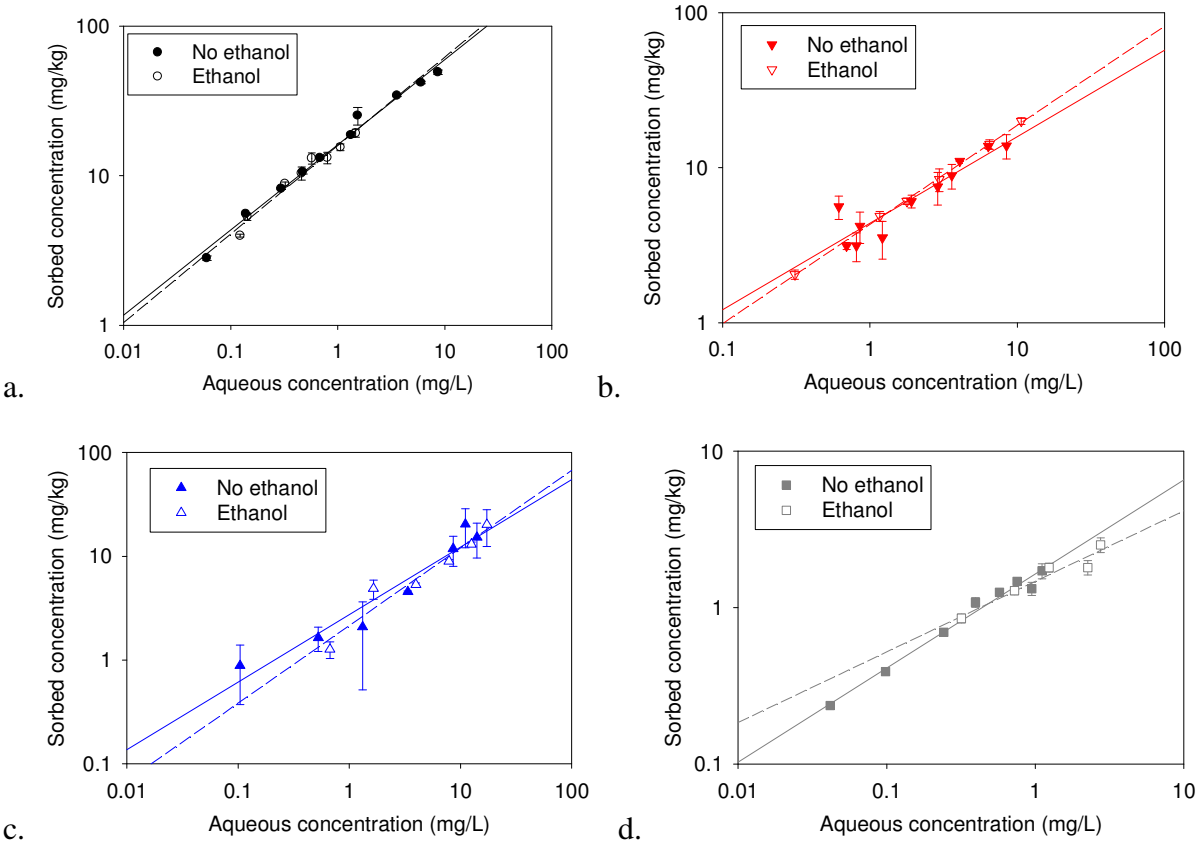

Figure D.2 Freundlich sorption isotherms spiked with ethanol for a. TNT, b. 2ADNT, c. 4ADNT, and d. 26DANT. Solid lines represent regression with no ethanol and dashed lines represent regression for samples with 0.08% ethanol.

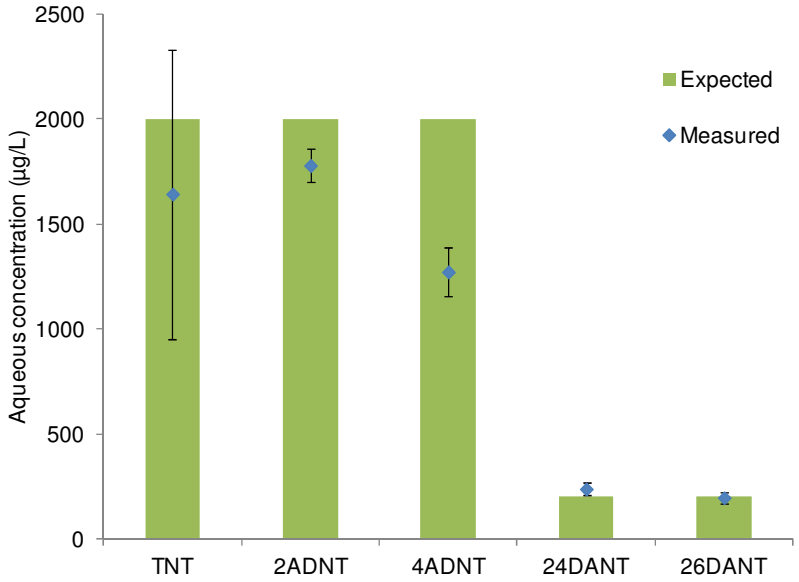

Figure D.3 Example matrix spike recovery

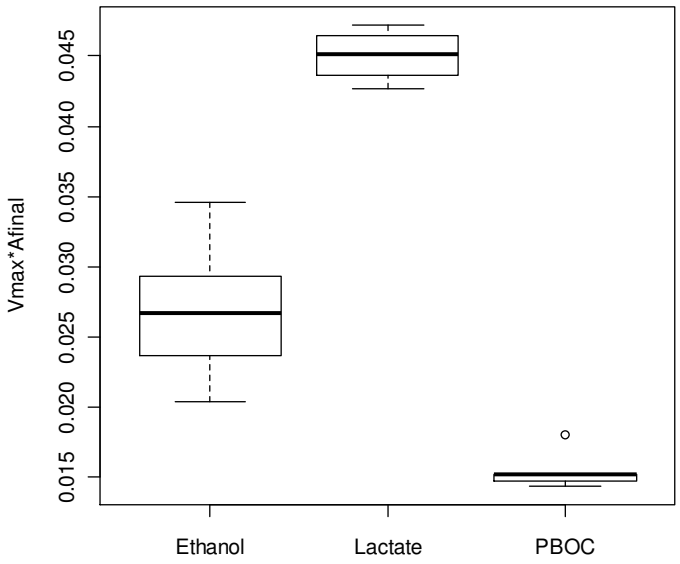

Figure D.4 Boxplot illustrating lumped degradation rate, the product of v_{max} and M_f, final biomass concentration, for replicates of each test condition.

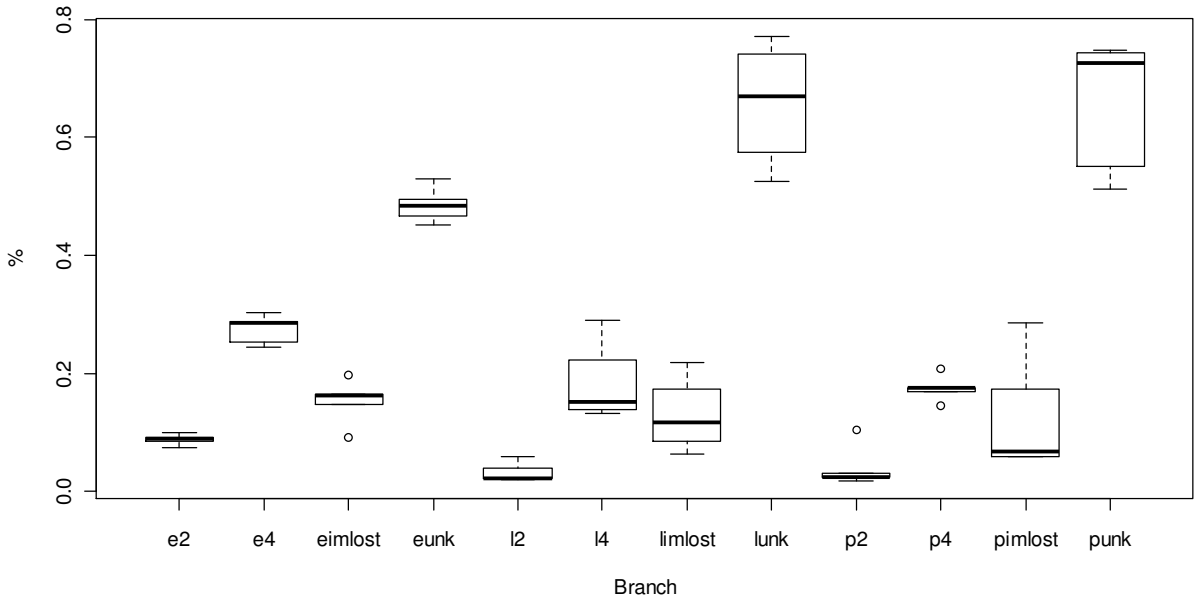

Figure D.5 Box plot comparing branching coefficients for ethanol (e), lactate (l), and PBOC (p), representing the 2 branch, 4 branch, initial bound (imlost) branch, and downstream bound (unk) branch.

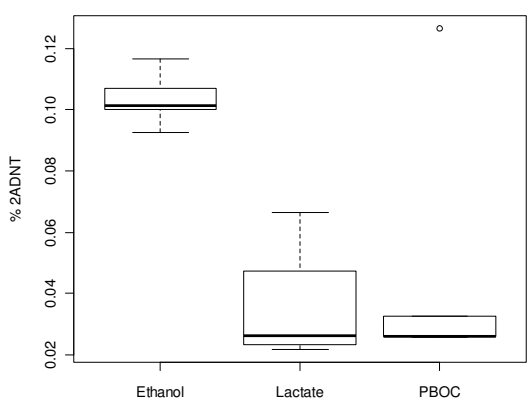

a.

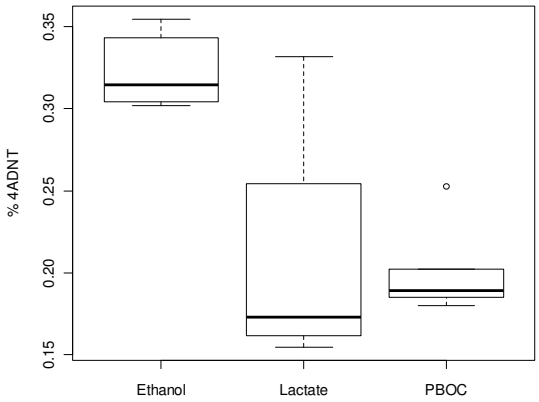

b.

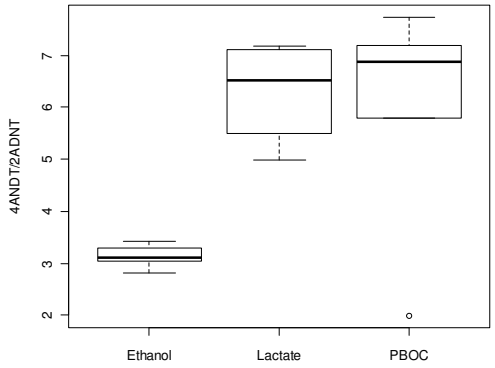

c.

Figure D.6 Box plots of branching coefficients for each test conditions comparing values determined for replicates for the a. 2 branch, b. 4 branch, and c. the 4:2 branch ratio.

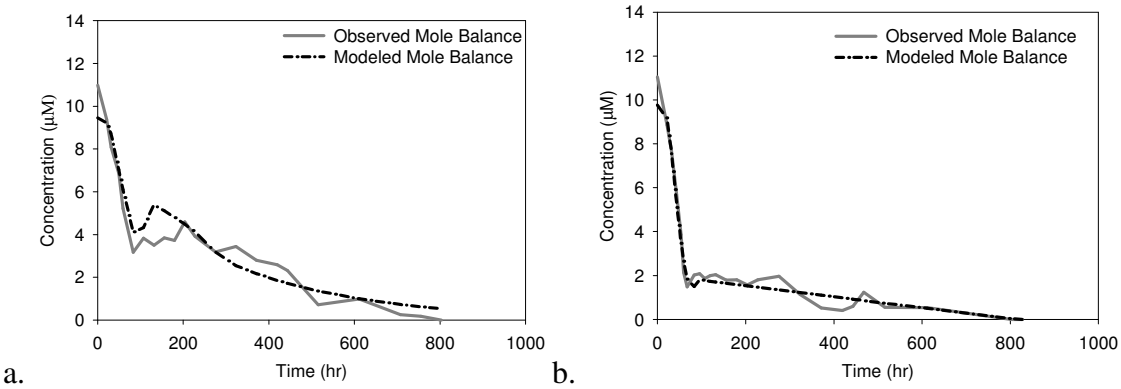

a. b.

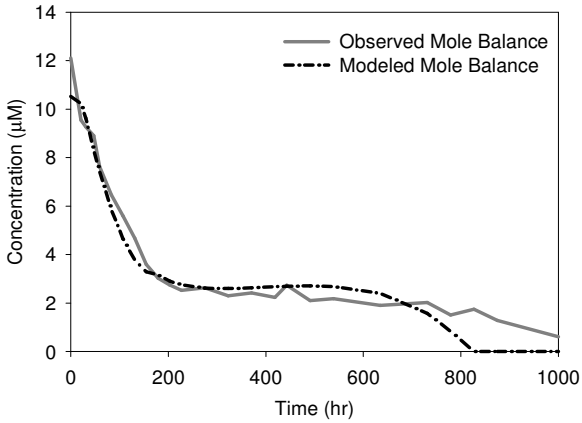

c.

Figure D.7 Total moles observed and model fit with time for a. ethanol, b. lactate, c. PBOC.

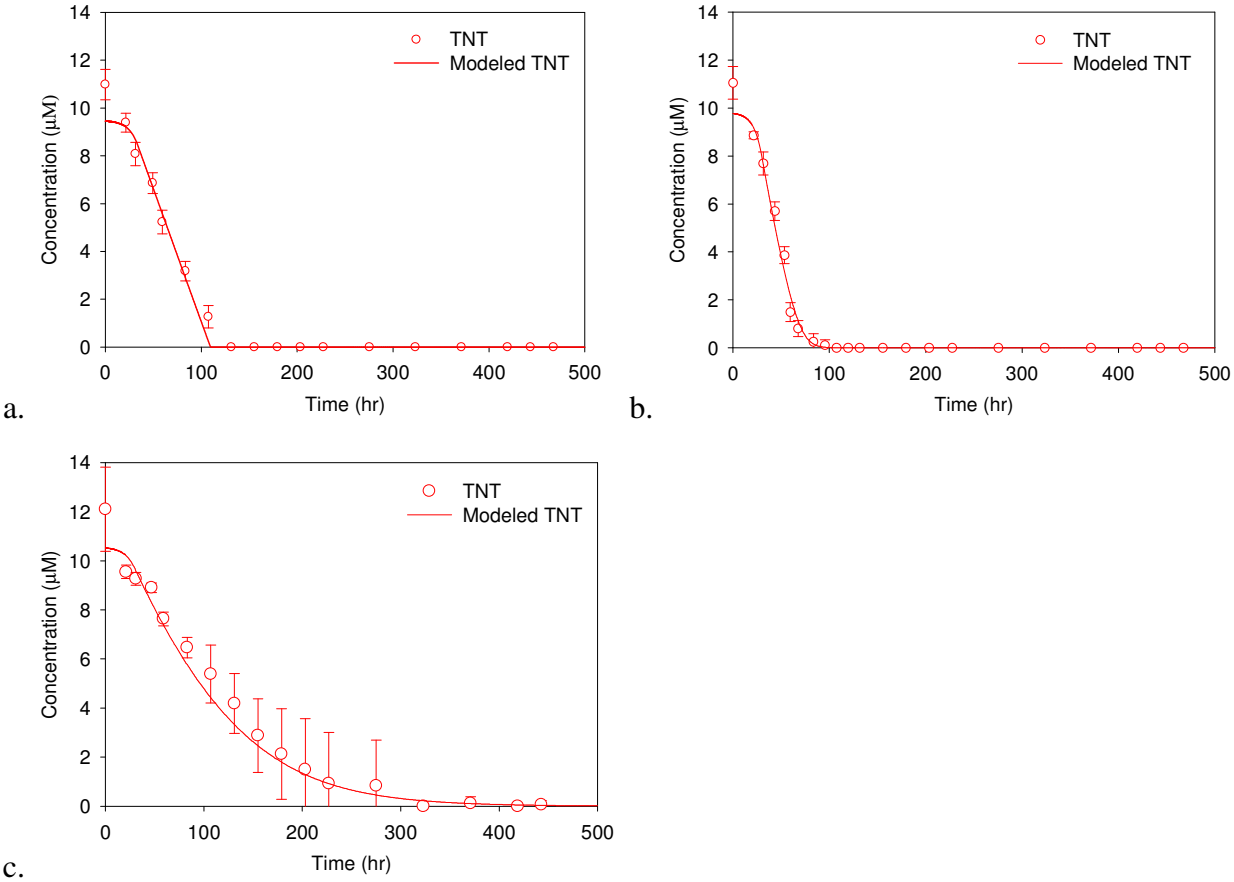

Figure D.8 TNT observed and model fit for a. ethanol, b. lactate, c. PBOC.

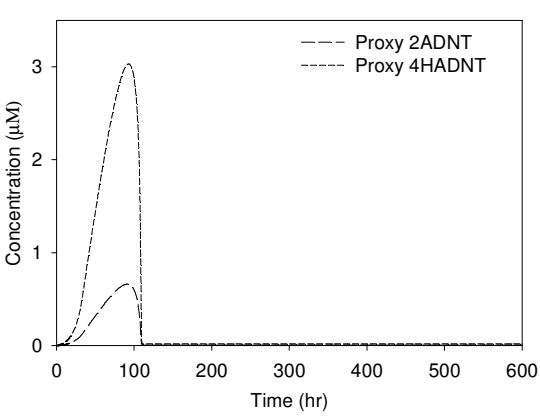

a.

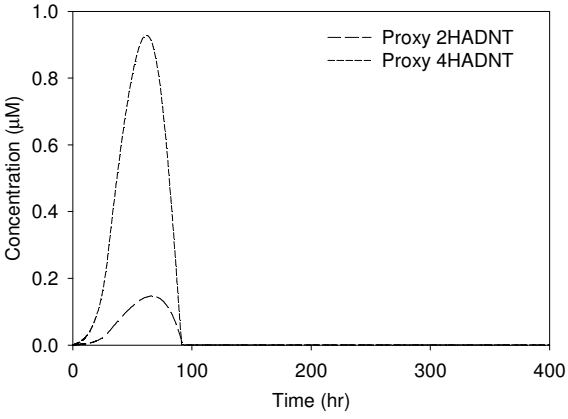

b.

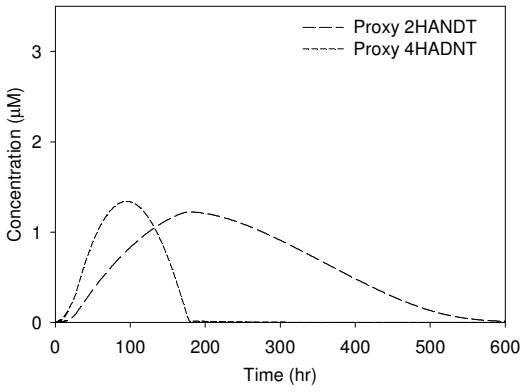

c.

Figure D.9 Proxy 2HADNT and 4HADNT generated to retard appearance of downstream products for a. ethanol, b. lactate, c. PBOC.

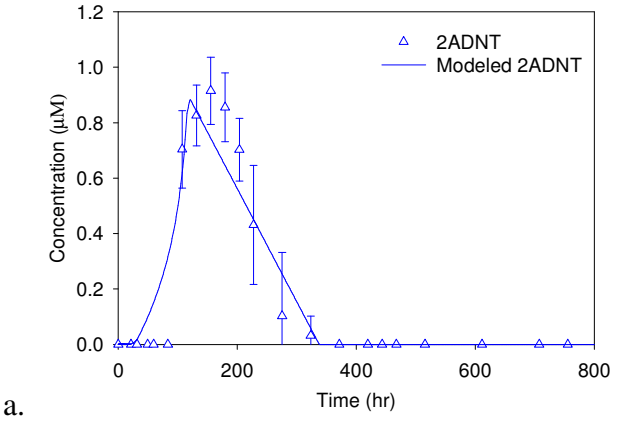

a.

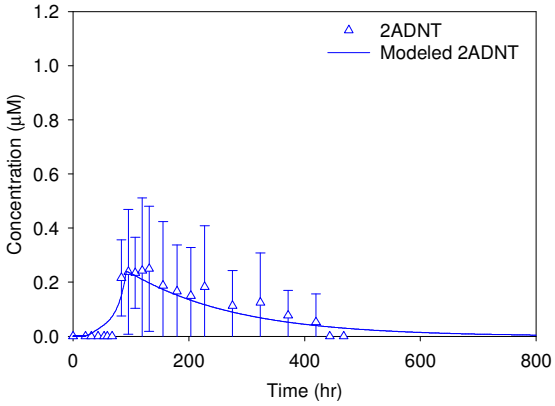

b.

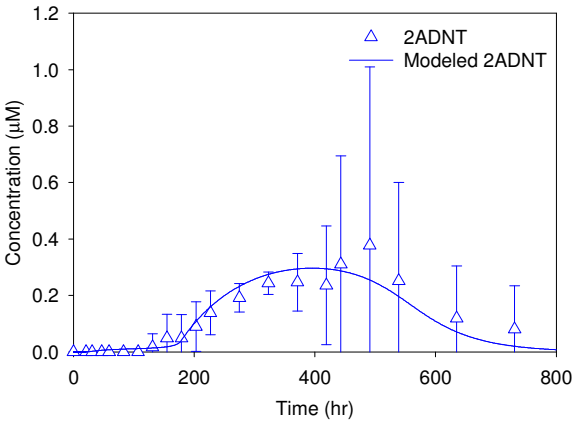

c.

Figure D.10 2ADNT observed and model fit for a. ethanol, b. lactate, c. PBOC.

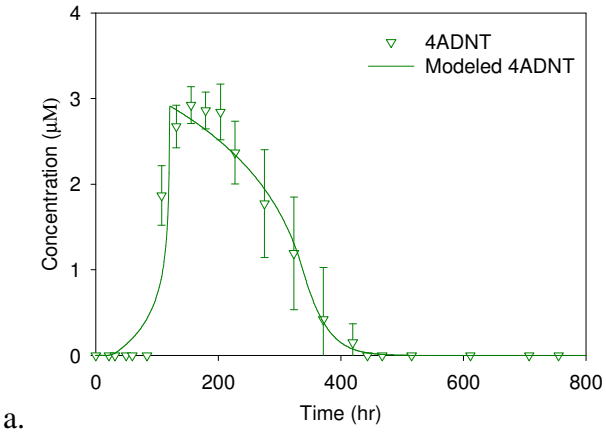

a.

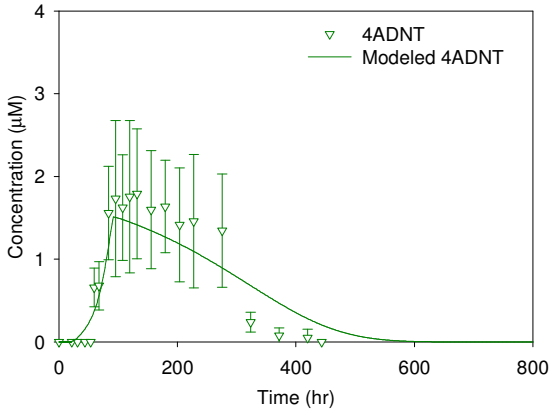

b.

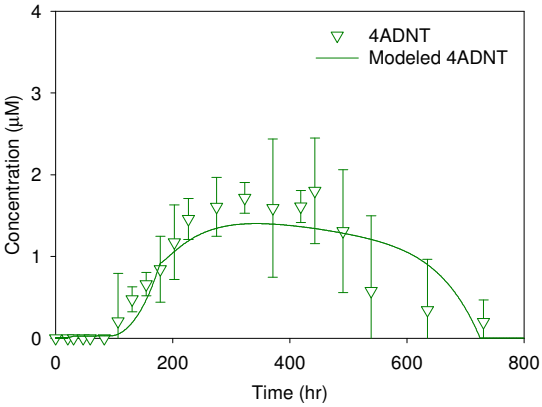

c.

Figure D.11 4ADNT observed and model fit for a. ethanol, b. lactate, c. PBOC.

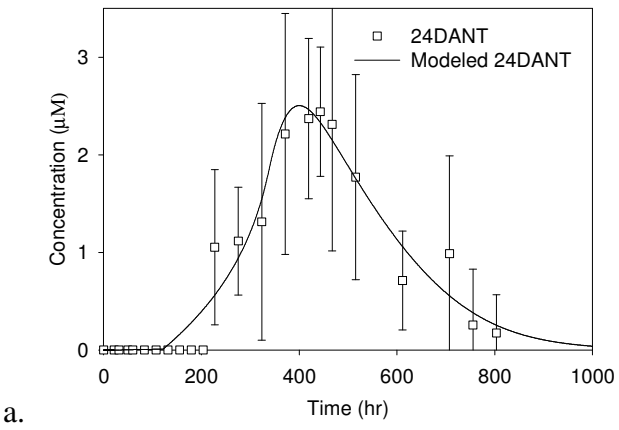

a.

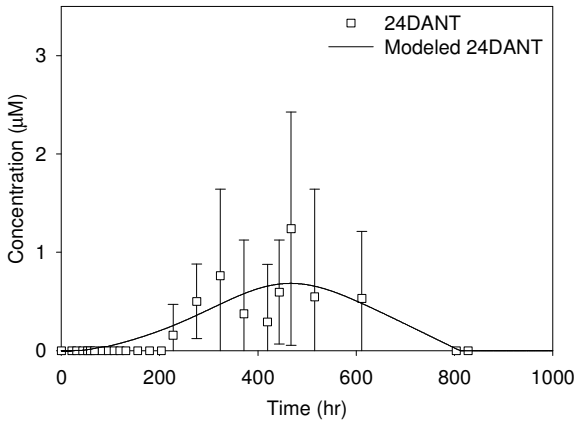

b.

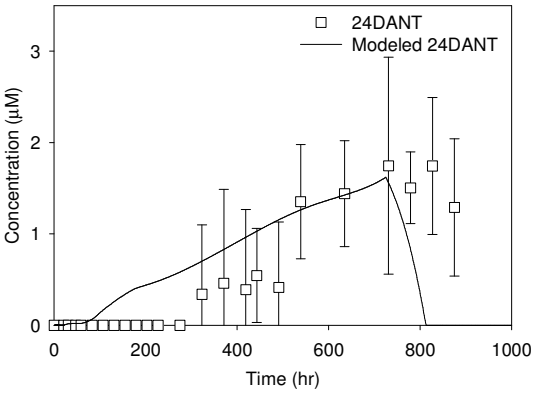

c.

Figure D.12 24DANT observed and model fit for a. ethanol, b. lactate, c. PBOC.

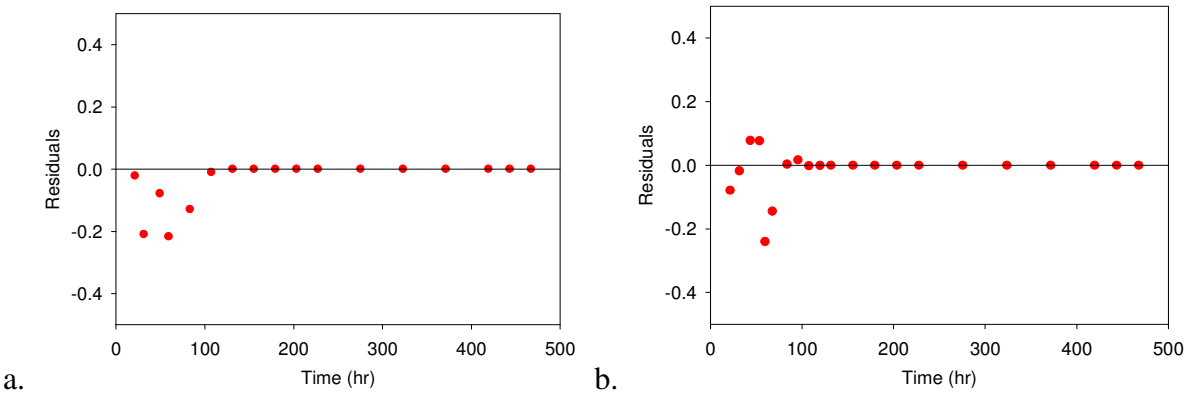

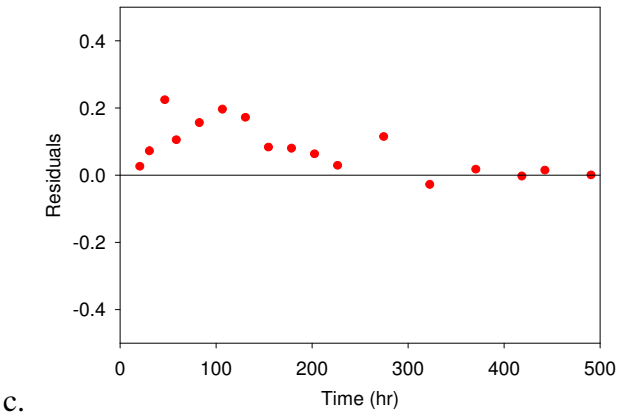

Figure D.13 Residuals for TNT modeling for a. ethanol, b. lactate, and c. PBOC.

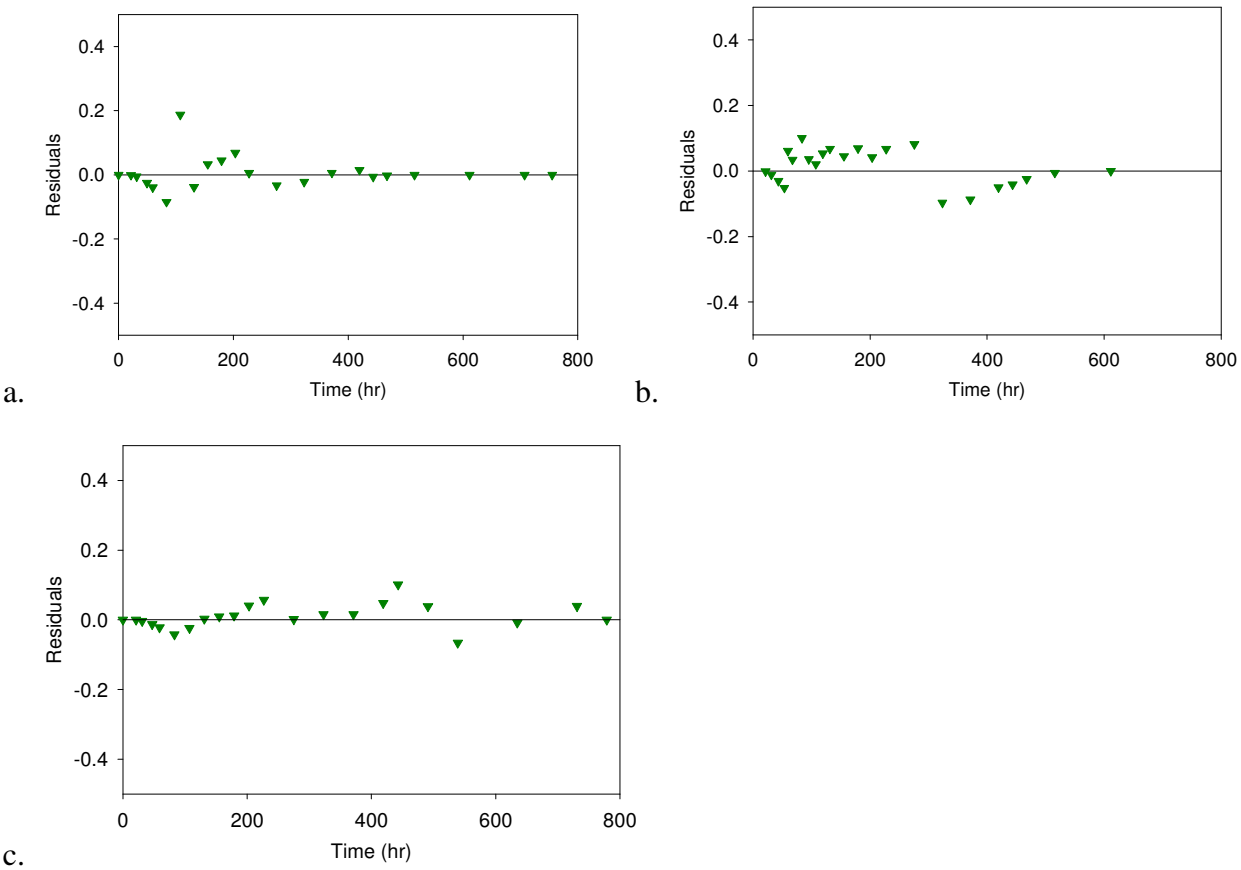

Figure D.14 Residuals for 2ADNT modeling for a. ethanol, b. lactate, and c. PBOC.

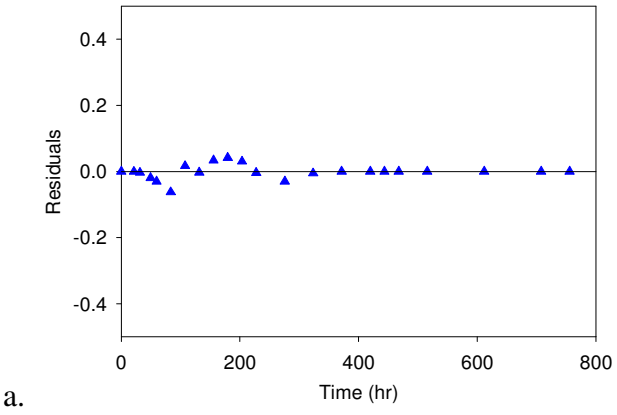

a.

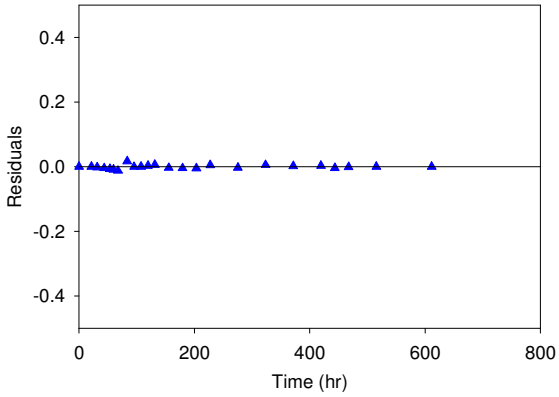

b.

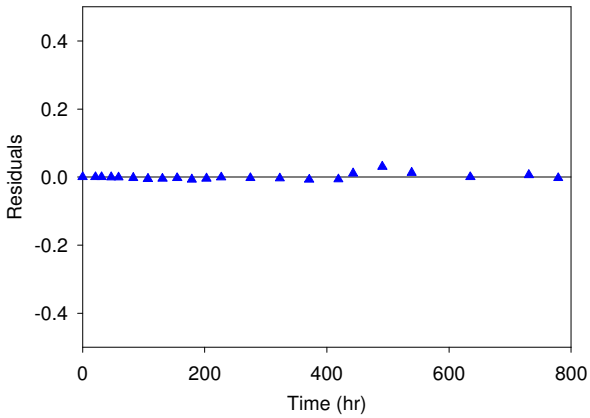

c.

Figure D.15 Residuals for 4ADNT modeling for a. ethanol, b. lactate, and c. PBOC.

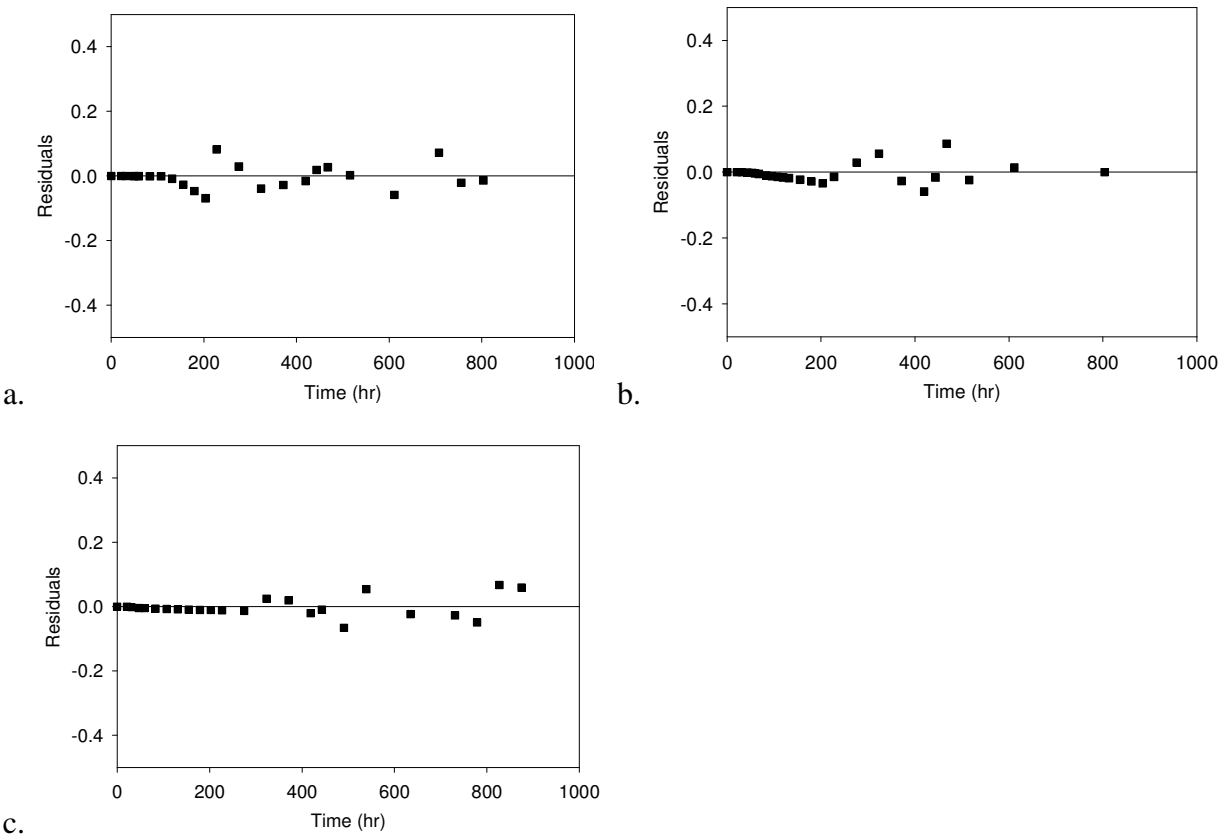

Figure D.16 Residuals for 24DANT modeling for a. ethanol, b. lactate, and c. PBOC.

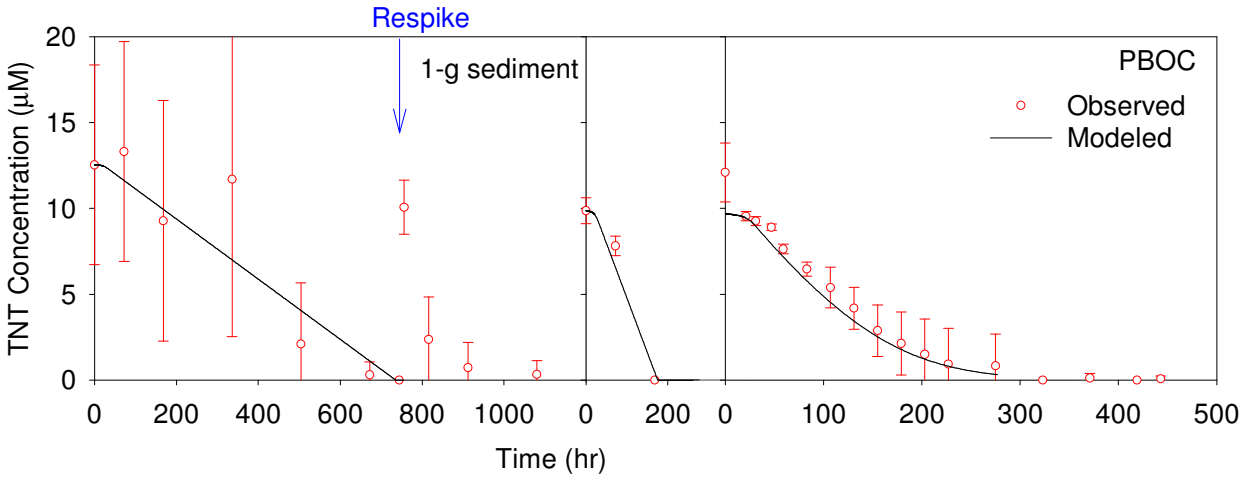

Figure D.17 Observed and modeled TNT concentrations for all generations of microcosms not receiving lactate or ethanol amendment.

Table D.1 Freundlich sorption parameters with and without ethanol

	No Ethanol			*With Ethanol*		
	K_f	n	R^2	K_f	n	R^2
TNT	16.1	0.57	0.99	15.9	0.59	0.97
2ADNT	5.2	0.38	0.80	4.3	0.63	0.99
4ADNT	2.7	0.65	0.93	2.1	0.75	0.94
24DANT	2.0	0.31	0.94			
26DANT	1.6	0.60	0.98	1.5	0.45	0.93

Table D.2 Nitroreductase gene primer sequences

Primer	***Forward***	***Reverse***	***Expected bp***	***Source***
pnrA	TCAAGACGAAGCACTCAAAGCC	GGCACGTACTGATCGATGCTGC	108 (64)	(van Dillewijn et al. 2008)
xlpA	GGTGGGGATGGAGGACTTC	CATGATGGGCAGTTTCGC	549	(Fuller and Steffan 2008)
nitA	ACTGCTCACTCCATGGGTCT	TTTCTTTCTTCGTCCGGGTA	165	(Kutty and Bennett 2005)
nitB	TCTGTTGTTGCTGCCGAAT	TGTGATTCATCAGCCGGATA	151	(Kutty and Bennett 2005)

D.1 References

Fuller ME, Steffan R (2008) Groundwater Chemistry and Microbial Ecology Effects on Explosives Biodegradation - Final Report. SERDP Project ER-1378. http://www.serdp.org/Program-Areas/Environmental-Restoration/Contaminants-on-Ranges/Characterizing-Fate-and-Transport/ER-1378. Accessed 5/1/2012

Kutty R, Bennett G (2005) Biochemical characterization of trinitrotoluene transforming oxygen-insensitive nitroreductases from Clostridium acetobutylicum; ATCC 824. Arch Microbiol 184 (3):158-167.

van Dillewijn P, Couselo JL, Corredoira E, Delgado A, Wittich R-M, Ballester A, Ramos JL (2008) Bioremediation of 2,4,6-trinitrotoluene by bacterial nitroreductase expressing transgenic aspen. Environ Sci Technol 42 (19):7405-7410.

(this page left intentionally blank)